SCATTERING FROM SINGULAR POTENTIALS

by

Sema Seymen

B.S., Physics Engineering, İTÜ, 2011

M.S., Physics, Boğaziçi University, 2015

Submitted to the Institute for Graduate Studies in
Science and Engineering in partial fulfillment of
the requirements for the degree of
Doctor of Philosophy

Graduate Program in Physics

Boğaziçi University

2022

ACKNOWLEDGEMENTS

Foremost, the completion of my thesis would not have been possible without my dear supervisor Prof. O. Teoman Turgut. I would like to thank him for introducing and teaching me the interesting topics of this thesis, sharing his boundless knowledge with me all the time and his wise guidance and limitless support during my journey in Boğaziçi University. I can not thank enough Prof. Turgut for being the most friendly, kind, helpful and considerate thesis advisor.

I would like to express my deepest gratitude to Prof. Ali Mostafazadeh for giving me the precious opportunity to be a part of his study group, sharing his wide knowledge on the subjects of this thesis and accepting me as a boursier in his TÜBİTAK projects with numbers $117F108$ and $120F061$ to support my phd studies.

I am extremely grateful to Assoc. Prof. Fatih Erman for sharing his intelligence generously with me and his patient, endless help during our studies.

Many thanks to Dr. Hai Viet Bui for his immense help and support during our joint work, his friendship and the scientific discussions.

I'm deeply indebted to my thesis committee, Assoc. Prof. Levent Akant, Prof. Savaş Arapoğlu, Assist. Prof. İlmar Gahramanov for their interest and comments.

Special thanks to my dearest friends from the department, Dr. Emine Ertuğrul and Kaya Güven Akbaş, the joyful time we spent to discuss physics and every other thing and giving me strength during my phd studies.

Last but not the least, I would like to thank my parents and my sisters for their unlimited support in my life.

ABSTRACT

SCATTERING FROM SINGULAR POTENTIALS

In this thesis, some well-known mathematical methods are applied to a new set of problems as some bound state and scattering properties of singular potentials are investigated quantum mechanically. Firstly, we work on the hybrid singular potential systems consisting of circular and spherical delta potentials with additional point-wise delta potentials which are outside of these circle and sphere in two and three dimensional spaces. We also investigate the cases when there is a small deformation in these shells in the normal direction. We apply the cut-off regularization method to regularize the ill-defined Hamiltonian and perform a convenient renormalization process for the singularity occurring in the self-interaction terms of the point defects. We show that the first order correction to the bound state energies has a simple geometric interpretation when the circle and the sphere that support the delta potentials are slightly deformed. Secondly, we give a detailed study of scattering from linear Dirac-delta potentials in two dimensions which are supported on infinitely long parallel lines normal to the scattering axis. We also explore how the presence of these lines affect the geometric scattering. We take the asymptotically flat Gaussian bump as a perturbation to the line defects system and we calculate the scattering amplitude. We give plots for one or two line defects and show that the presence of line defects, especially when the bump is located between the defects, amplifies the geometric scattering effects. We give a brief expression for the scattering amplitude for the case combining a finite size linear defect and a point defect. Lastly, we introduce a distributional direct method which is performed in momentum space to perform the bound and scattering state analysis of the spherical and circular delta potentials. The results are compatible with the standard partial wave approach.

ÖZET

TEKİL POTANSİYELLERDEN SAÇILMA

Bu tezde, bazı bilinen matematiksel yöntemler bir dizi yeni probleme uygulanmıştır ve kuantum mekaniği çerçevesinde, tekil potansiyeller için bağlı durum ve saçılmaların bazı özellikleri incelenmiştir. İlk olarak, iki ve üç boyutlu reel uzayda, çembersel ve küresel delta potansiyeller ile bu çember ve kürenin dışında bulunan birer noktasal delta potansiyelden oluşan hibrid yapıda potansiyellere bakılmıştır. Tekil potansiyellerle yazılan Hamiltonyenler eksik tanımlı olduğundan, kesme noktası regülarizasyonu kullanılmıştır. Ayrıca noktasal kusurların içsel etkileşim terimlerindeki tekilliklere uygun bir renormalizasyon da uygulanmıştır. Delta potansiyellerini ifade eden çemberde ve kürede küçük şekil bozuklukları olması durumunda, bağlı durum enerjilerindeki birinci mertebeden değişimin basit bir geometrik yorumunun olduğu gösterilmiştir. İkincil olarak, göreli olmayan bir skaler parçacığın, saçılma eksenine dik, çizgisel delta potansiyelleri ile ifade edilen sonsuz uzunlukta paralel çizgisel kusurların var olduğu durumda Gaussiyen bir tümsekten geometrik saçılma kavramı ayrıntılı bir biçimde incelenmiştir. Gauss tümseği bir tedirgeme olarak alınmış, saçılma genliği hesapları yapılmıştır. Bir ve iki tane çizgisel kusurun grafikleri çizdirilmiştir ve çizgisel kusurların, özellikle de tümsek iki çizginin ortasındayken, geometrik saçılma etkilerini arttırdığı gösterilmiştir. Sonlu boyda bir çizgisel kusurla noktasal kusuru birleştiren durum için bir saçılma genliği ifadesi yazılmıştır. Son olarak, yine çember ve küresel delta potansiyeller için bağlı durumlar ve düşük enerjili saçılmaları çözmek üzere, genellestirilmis fonksiyonların ve momentum uzayının kullanıldığı doğrudan bir yöntem geliştirilmiştir. Bulunan sonuçlar, bilinen kısmi dalga analizi sonuçları ile uyumludur.

TABLE OF CONTENTS

LIST OF FIGURES

LIST OF SYMBOLS

$\mathbf{a}$	Position of the point singular potential
$A(S^2)$	Surface area of the sphere
A_{mn}	Matrix to solve Lippmann-Schwinger equation
ci	Cosine integral function
f_i	State vector of the singular potential
F	Matrix of f_i's
$\mathcal{F}(f)$	Fourier transform of f function
$\mathfrak{g}$	Metric tensor
$\mathfrak{g}_0$	Eucledean metric tensor
$G(x)$	Green's function
$H(\theta, R)$	Mean curvature of the sphere
H_ϵ	Regularized Hamiltonian
H_0	Homogeneous Hamiltonian
$H_n^{(m)}(x)$	n^{th} order Hankel function of the m^{th} kind
$I_n(x)$	Modified Bessel function of the first kind
$j_n(x)$	n^{th} order spherical Bessel function
$J_n(x)$	n^{th} order Bessel function
$\mathbf{k}$	Wave vector
K	Gaussian curvature
$K_t(x, y)$	Heat kernel
$K_n(x)$	Modified Bessel function of the second kind
$L^2(\mathbb{R}^2)$	Hilbert space
$L(S^1)$	Length of the circle
$\mathcal{L}_{\mathbf{x}}$	Differential operator including the geometric potential
M	Mean curvature
$N(\theta, \phi)$	Normal vector field
$R(E)$	Resolvent operator
$\mathbb{R}^d$	Real number space in d-dimension

$\mathrm{pv}(f)$	Principle value of f
S^n	Surface of the sphere in n dimension
$\mathrm{sgn}(x)$	Sign function
si	Sine integral function
Y_{lm}	Spherical harmonics
γ	Euler's constant
$\gamma(\theta)$	Parametrization function of the circle
$\tilde{\gamma}(s)$	Deformation of a curve along normal direction
Γ	Position of the circular singular potential
δ	Height of Gaussian bump
δ_{S^n}	Dirac-delta function supported on the n-dimensional sphere
ϵ	Small deformation parameter
ζ	Perturbation parameter
$\theta(x)$	Step function
λ	Strength of the interaction between the particle and potential
$\lambda_{1,2}$	Real coefficients of the curvatures
μ	Renormalization parameter
ν_*	Zeroes of the eigenvalues of the principal matrix
ξ	Coupling constant or strength of the interaction
σ	Width of Gaussian bump
$\sigma(\Omega)$	Differential cross section
$\sigma(\theta, \phi)$	Location of the circular singular potential in two dimensions
$\tilde{\sigma}(\theta, \phi)$	Surface deformation of a sphere along the normal direction
Σ	Position of the spherical singular potential
Φ_{ij}	Principal matrix
$\psi(x)$	Wave function in position space
ω_i	Eigenvalues of Φ matrix
Ω	Solid angle

1. INTRODUCTION

Owing to works of great many scientists, 20th century had started with a crucial improvement of our understanding of nature. Starting from the end of the 1900's, as physicists became more and more interested in essence of light and the dynamics of smaller constituents of matter such as atoms, molecules (and even subatomic structures) as well as peculiar inter-connections between all these. At the same time, there were many recent experimental results and observations that could not be explained by the existing theories. Both these newly observed phenomena and evolving theoretical suggestions gave birth to the quantum theory. As a result of this, a natural division of the problems in physics as classical and quantum mechanical appeared. Hertz's observation of the photoelectric effect and Einstein's theoretical interpretations of this occurrence led to the ideas about the quantization of the energy of the electromagnetic radiation. This work coincided with Planck's famous formula of black body radiation when he introduced Planck's constant, which could be considered as a signature of quantum phenomena, for the first time. Thus by the beginning of 20th century, the nature of light was identified very differently than before as it displayed essentially the particle characteristics in place of the wave characteristics within the frame of a new physical concept, called photon. The discovery of the nucleus, in other words, Rutherford's experiment in 1907 with $\alpha-$ particles sent to a thin gold foil resulted in the detection of unexpected scattering angles of the $\alpha-$ particles and brought a much clearer picture of the atomic model. Compton, who was one of the first scientists who used the term photon, discovered that the wavelength of a photon scattered from a charged particle such as an electron was increased, in the same way, the energy of the photon was reduced. This discovery was another validation of the quantum mechanical interpretation of light which claims that there are discrete energy levels of light and also led to the wave-particle duality. Meanwhile, Bohr's examination of the discrete photon energy ideas of Planck and Einstein, gave rise to Bohr atom model which explained in some sense the stability of the atom and relation between the energy of the electrons and their orbital radius.

Mathematical progress in physics in the beginning of the 1900s also supported the construction of the quantum theory. In 1923, de Broglie argued that if light quanta is a good explanation to recent observations, could a subatomic particle also be considered as a wave? de Broglie's suggestion is confirmed with Davisson-Germer experiment, which is the observation of the diffraction of electrons by scattering from crystals. This suggestion was an introduction to the wave mechanics. Schrödinger contributed the wave mechanics by writing the famous Schrödinger equation to establish the relation between the behaviour of the wave function which describes the particle and the physical quantities such as the potential and Hamiltonian that describe the mechanical properties of the system. A wave function is not an observable quantity and Heisenberg argued that a theory should be conceivable in terms of observable entities. Heisenberg's studies on the relation between the energy states of the atom and the frequency of the atomic radiation led to one of the most important perceptions in quantum mechanics: uncertainty relation. He found out that some pairs of physical properties of the subatomic nature can not be observed simultaneously, unlike in classical mechanics. Born confirmed that Heisenberg's formulae about observables can be recast into the matrix formulation and using this idea Jordan and Born built up the matrix mechanics accordingly. Additionally, Dirac depicted an abstract formulation combining the matrix and wave mechanics. His advantageous bra-ket notation made the upcoming challenging calculations of quantum mechanics more clear and extendable [1].

Understanding the nature of the quantum mechanical object is essentially based on the results obtained from its spectroscopic analysis. This is inherently the main reason why the scattering concept is a very important tool of quantum mechanics. Spectroscopic data is basically obtained from the collision of two objects. The target particles enter the analytic calculations as potentials and an energy spectrum that can be used to describe both parties is observed from this collision [2]. However, the word "scattering" is more convenient to use instead of "collision" since the solutions of the dynamic equations of the scattered substance have a different characteristic than in the classical case. Differing from a classical collision, in quantum scattering, there are two cases, which are the bound and the scattering states, depending on whether the

scattered particle's energy is greater or smaller than height of the scattering potential respectively. In addition to spectroscopy as an experimental scattering application, the high energy colliders are important facilities which are built up with the principles of scattering and very useful sources of information to verify the answers reached in nuclear and particle physics.

Theoretical aspects of the physical process of scattering is mathematically well-developed and today is usually referred to as scattering theory. To obtain a physically meaningful scattering solution, the scattering potential should have some mathematical properties. For example, a spherically symmetric potential $V(\mathbf{r})$ should go to zero as r goes to infinity and this convergence must be faster than the order of r^{-3} [3]. On the other hand, the potentials which go to infinity faster than the order of $r^{-3/2}$ as r goes to zero are typically called singular potentials [3]. These potentials are the main concern of this thesis. There are several mathematical concepts used by physicists while dealing with scattering such as the spectral theory of operators. As the solution of the scattering problem is usually decomposed into incoming and outgoing waves, any incoming wave in a particular state leads to a superposition of all possible outgoing states multiplied with some coefficients. This transformation to the outgoing states define the $S-$matrix [1]. $S-$matrix can be considered as an important instrument to describe and solve many scattering problems. Green's operator, better known as 'resolvent' in mathematical literature [3], is another essential tool adopted to solve scattering examples especially with singularities [1, 4] and construct perturbative solutions for some cases. The fundamental information about the scattering is contained in the $T-$matrix which basically describes the transition of the scattered particle between two states. It also can be portrayed as an operator. Combining $T-$matrix with the resolvent for singular cases is one way to reach to the Lippmann-Schwinger equation [3, 5].

Scattering theory of quantum mechanics has a wide area of mathematical applications. As one of the primary collections on scattering theory, authors give a broad range of these applications especially for low velocities in [5] and led physicists to write other various important books [6–10] after many remarkable mathematical de-

velopments. Scattering theory is also adopted in applied mathematics. For an early example, being mathematicians, authors of [11] give the representation theory formulation of scattering.

In this thesis, we work on the elastic scattering properties of non-relativistic scalar particles. We mainly discuss the mathematical framework of the process. We produce the energy spectrum for the bound and scattering states for each case and calculate the wave function solutions and scattering amplitudes in two or three dimensions. As mentioned before, a target in the scattering process enters the Hamiltonian of the system as the potential term and it is sometimes called "scatterer". The scatterers in this thesis are described as Dirac-delta functions. Dirac-delta functions can also be called as singular potentials and they are used to represent the point interactions between particles. Point interactions are considered as exactly solvable models in quantum mechanics and reader can find a comprehensive analysis of the spectral properties and analytic structure of the exact solutions of such potentials in [12, 13]. Singular potentials are also implemented to demonstrate the inhomogeneities in the molecular structure of the materials such as impurities or dislocations. Therefore, the Dirac-delta potentials are also called as "defects" in some parts of this thesis.

Working with Hamiltonians described for a curved space is another important field for many physicists such as [14–18]. Therefore, quantum scattering from singular potentials in a curved space is another important application of scattering theory. This application leads to studies on some models about the quantum theory of gravity which is a very interesting subject for recent decades [19–25]. Also the recent interest towards the superfluidity and superconductivity technologies gave rise to condensed matter studies which chase the dynamics of electrons in an effectively curved surface. In [26], the curvature in the geometry acts as a scattering potential. There is a wide formulation of the geometric scattering of a scalar particle which moves on an asymptotically flat curved surface in [27]. Since the electron gas considered in such a problem could have some impurities in it, the combination of the geometric scattering and singular potential scattering is a valuable issue to look at. In reference [28], the authors investigate

how the presence of several point defects would affect the scattering amplitude of the geometric scattering.

As an elementary example of the special geometries of the singular potentials, spherical delta potentials and their various applications are covered in many quantum mechanics books [29–31]. One can find an explicit construction of the mathematics of the delta shell potentials in reference [32]. When the support of the delta potential is codimension two or three, the problem needs a renormalization. In [33, 34], reader can find the discussions on the renormalization of Hamiltonians consisting of delta potentials. Authors of [32] also discuss the case of the presence of a point-wise delta potential placed at the center of the spherical shell for $l = 0$ case, in other words, where the angular momentum is zero. Later on, these results are extended to more general cases where the delta potential supports are taken as curves or surfaces [35–38]. The generalizations to delta functions supported on curves and surfaces embedded in manifolds are presented in the works [39, 40]. Such circular/spherical singular interactions, considered to be models for circular/spherical quantum billiards are studied analytically and numerically recently [41, 42]. The solutions for delta shell interactions in higher dimensions are also developed in [43] by implementing the partial wave analysis method. Small deformations in the geometry of the support of the delta potential, which are also considered as perturbations, is also an interesting problem to look at [44], since the area of the deformed part can affect the energy eigenvalues. Another aspect of deformations in the singular potentials is studied in [45] for a planar potential which is locally deformed.

Although, in general not easier, there are some cases when it is more efficient to study the quantum mechanics in momentum space. In [46], authors give a solution to scattering problem from singular potentials in momentum space. Both in this work and [47], wave function solutions are found by a distributional approach.

The organization of this thesis is as follows. In chapter 2, we give the brief introductory calculation of our published papers. We provide the derivations of some

results used throughout the thesis.

Chapter 3 is based on our recent work [48] that combines two chosen geometries of singular potentials. We describe the singular interactions in the Hamiltonian as rank one perturbations on Hilbert space. We solve the Schrödinger equations and construct their bound state and scattering spectrum for the following interaction scenarios: A circular and a point-wise delta potential outside of this circle, a spherical and a point-wise delta potential outside of this sphere, a small deformation of the circular delta potential in the normal direction, a small deformation of the spherical delta potential in the normal direction. We give the geometric interpretation of the change in the bound state energies because of this perturbation in the shells. Then in 3.5 and 3.6, we combine the deformed shells with point-wise delta potentials and look for the perturbative change in the bound state energies, which are not included in a published work.

In chapter 4, we give the calculations and demonstrations accomplished in [49]. In this work, we search for the effect of a collection of parallel line defects on the geometric scattering amplitude. The scattering calculations of a non-relativistic scalar particle are grounded on the Lippmann-Schwinger equation. The first part of the problem is considered on a plane and the potential is taken as a collection of parallel linear delta functions. Next, we examine the scattering problem on an asymptotically flat surface that is embedded in a three dimensional manifold and has a curvature which is considered as a perturbation. We take the space curved locally as a Gaussian bump and give the plots for the scattering cross section. In Appendix A, we give the details of some of the necessary mathematical results. We also give a calculation of the scattering amplitude of a system combining a point-wise defect and a short line defect which is not yet published.

Finally, in chapter 5, the content of our work [50] is shared. We proposed a direct method, which we do not analytically solve the differential equations, but solve the states directly in momentum space, for the calculations of the bound states and scat-

tering from circular and spherical delta shell potentials at low energies. Different from the common way of putting the boundary conditions in integrals implicitly, i.e. $\pm i\epsilon$ prescription, we use the outgoing boundary conditions explicitly. To reach the scattering solutions, wave functions in momentum space are interpreted as distributional functions.

2. A BRIEF SUMMARY OF THE PRELIMINARY CALCULATIONS

To demonstrate the simplest case in quantum mechanics, the goal is to get the complete wave function $\psi(x)$ with energy eigenvalue E for some particular time-independent potential $V(x)$ in one dimension. To achieve this, we basically solve the Schrödinger equation:

$$-\frac{\partial^2}{\partial x^2}\psi(x) + V(x)\psi(x) = E\psi(x) \ . \tag{2.0.1}$$

Here and throughout this thesis, we use units when $\hbar = 2m = 1$. If we want to write the general scattering solution satisfying the outgoing boundary condition, or also called Sommerfeld radiation condition [31, 51, 52], we have

$$\psi(\mathbf{r}, \mathbf{k}) = N\left(e^{i\mathbf{k}\cdot\mathbf{r}} + f(k,\theta)\frac{e^{ikr}}{r^{\frac{n-1}{2}}} + o\left(\frac{1}{r^{\frac{n-1}{2}}}\right)\right) \ , \tag{2.0.2}$$

for $r \to \infty$, where $f(k,\theta)$ is the scattering amplitude, N is a normalization constant and $n = 2, 3$ is the dimension of space.

When the potential V is a singular function of x, we need some new techniques to obtain the wave function. The concern of this thesis is Dirac-delta type singularities for the potentials. Dirac-delta functions satisfy the equation $\delta(x-a)f(x) = \delta(x-a)f(a)$ for any function $f(x)$. Below, we will give a brief derivation of the mathematical techniques used in this thesis to solve Schrödinger equations with such Dirac-delta potentials.

2.1. Lippmann-Schwinger Equation and Green's Operator

An important tool for solution of the scattering problem for a singular potential is the use of Lippmann-Schwinger equation. To derive the expression for this equation, we start by writing the Schrödinger equation for a general potential $V(\mathbf{r})$ and we define

the linear differential operator L as

$$\underbrace{(-\nabla^2 + E)}_{L}\ \psi(\mathbf{r}) = V(\mathbf{r})\ \psi(\mathbf{r})\ . \tag{2.1.1}$$

For an E value which is away from the spectrum L^{-1} exists. Acting L^{-1} operator from left on both sides of the equation (2.1.1):

$$\psi(\mathbf{r}) = L^{-1}V(\mathbf{r})\ \psi(\mathbf{r})\ . \tag{2.1.2}$$

The integral kernel is denoted by $G_0(\mathbf{r}, \mathbf{r}'|E)$, which satisfies:

$$\langle \mathbf{r}|\ L\ L^{-1}\ |\mathbf{r}'\rangle = (-\nabla^2 + E)\ G_0(\mathbf{r}, \mathbf{r}'|E) = \delta(\mathbf{r} - \mathbf{r}') \tag{2.1.3}$$

and L^{-1} is the Green's function of this L. The sub index zero here indicates the free Green's function. Also, Green's function is widely known as resolvent in the mathematical literature. When the potential is zero, $V(\mathbf{r}) = 0$, Schrödinger equation is also called as Helmholtz equation and the solution of this equation is called as a homogeneous solution:

$$L\ \psi_{\text{hom}}(\mathbf{r}) = 0\ . \tag{2.1.4}$$

It is known that solutions of Schrödinger equation are additive (in Euclidean space). Hence, we get the expression below

$$\psi(\mathbf{r}) = \psi_{\text{hom}}(\mathbf{r}) + \int G_0(\mathbf{r}, \mathbf{r}'|E)\ V(\mathbf{r}')\ \psi(\mathbf{r}')d^3r' \tag{2.1.5}$$

which is the integral form of the Lippmann-Schwinger equation. We will use this equation substantially throughout this thesis. This expression obviously gives a series solution for the wave function. To see this, one can insert the right hand side to replace $\psi(\mathbf{r})$ in the integral:

$$\begin{aligned}\psi(\mathbf{r}) =& \psi_{\text{hom}}(\mathbf{r}) + \int G_0(\mathbf{r}, \mathbf{r}'|E)V(\mathbf{r}')\psi_{\text{hom}}(\mathbf{r}')d^3r' \\ &+ \int\int G_0(\mathbf{r}, \mathbf{r}'|E)\ V(\mathbf{r}')\ G_0(\mathbf{r}', \mathbf{r}''|E)\ V(\mathbf{r}'')\psi_{\text{hom}}(\mathbf{r}'')d^3r'd^3r'' + \cdots\end{aligned}$$

The result of this iteration is called the Born series. In Lippmann-Schwinger equation, we take only the first term of this series which is known as the first Born approxima-

tion. As another useful form of it, the Lippmann-Schwinger equation can be written abstractly as [53]

$$|\psi\rangle = |\phi\rangle + G_0(E)\ V\ \ |\psi\rangle \tag{2.1.6}$$

in ket notation, where ϕ is the homogeneous part of the solution.

2.2. Krein's Formula and the Principal Matrix

Throughout this thesis, we use another mathematical approach to find the Green's operator exactly. From now on it will be called as the resolvent operator of the Dirac-delta type singular interactions in terms of the free resolvent operator. This method is known as Krein's formula in literature [12, 13, 38]. Here, we state briefly this formula in the form that is used in this thesis.

Let H_0 be a free Hamiltonian operator in Hilbert space, $\mathcal{H}$. The resolvent of this operator is $R_0(E) = (H_0 - E)^{-1}$ where the energy value E is away from the spectrum. If we add a potential term to this free Hamiltonian, being $H = H_0 - V$, we solve the inhomogenous Shrödinger equation below

$$(H - E)\,|\psi\rangle = |\rho\rangle \tag{2.2.1}$$

for a function $\rho(\mathbf{r}) = \langle \mathbf{r}|\rho\rangle \in \mathcal{H}$, to find $R(E)^{-1}$. Resolvent operator of this Hamiltonian, $R(E)$, is simply $(H - E)^{-1}$. We can rewrite (2.2.1) as

$$\begin{aligned}
(H_0 - V - E)\,|\psi\rangle &= |\rho\rangle \\
(H_0 - E)\,|\psi\rangle - V\,|\psi\rangle &= |\rho\rangle \\
(H_0 - E)^{-1}(H_0 - E)\,|\psi\rangle &= (H_0 - E)^{-1}\,|\rho\rangle + (H_0 - E)^{-1}V\,|\psi\rangle \\
\Rightarrow |\psi\rangle &= R_0(E)\,|\rho\rangle + R_0(E)V\,|\psi\rangle
\end{aligned} \tag{2.2.2}$$

Let us now specialize to delta type potentials. For this purpose we first introduce a regularized form expressed as finite rank perturbation which means defining the potential as a projection operator that that has a well-defined action on the vectors on the Hilbert space. We can express the singular potential consisting of N Dirac-delta

potentials as

$$V = \sum_{j=1}^{N} |\tilde{f}_j\rangle \langle \tilde{f}_j| \tag{2.2.3}$$

where λ_j being the positive and real interaction strength, $|\tilde{f}_j\rangle = \sqrt{\lambda_j}\,|f_j\rangle$ and $|f_j\rangle$ is an integrable function which goes to delta functions in the short distance limit. Hence they describe the regularized form of the defects. Rewriting equation (2.2.2),

$$|\psi\rangle = R_0(E)\,|\rho\rangle + R_0(E) \sum_{j=1}^{N} |\tilde{f}_j\rangle \langle \tilde{f}_j|\psi\rangle \tag{2.2.4}$$

we end up with this expression. We need to project this equation onto $\langle \tilde{f}_i|$ to obtain a self-consistent equation

$$\langle \tilde{f}_i|\psi\rangle = \langle \tilde{f}_i|\, R_0(E)\,|\rho\rangle + \sum_{j=1}^{N} \langle \tilde{f}_i|\, R_0(E)\,|\tilde{f}_j\rangle \langle \tilde{f}_j|\psi\rangle \tag{2.2.5}$$

and we separate the $i = j$ term since this term may lead to a divergence in the final answer:

$$\Big(1 - \langle \tilde{f}_i|\, R_0(E)\,|\tilde{f}_i\rangle\Big) \langle \tilde{f}_i|\psi\rangle - \sum_{i\neq j=1}^{N} \langle \tilde{f}_i|\, R_0(E)\,|\tilde{f}_j\rangle \langle \tilde{f}_j|\psi\rangle = \langle \tilde{f}_i|\, R_0(E)\,|\rho\rangle \tag{2.2.6}$$

At this point, introduce the principal matrix, $\tilde{\Phi}$ as

$$\tilde{\Phi}_{ij}(E) = \begin{cases} 1 - \langle \tilde{f}_i|\, R_0(E)\,|\tilde{f}_i\rangle & i = j\ , \\ - \langle \tilde{f}_i|\, R_0(E)\,|\tilde{f}_j\rangle & i \neq j\ . \end{cases} \tag{2.2.7}$$

With the help of this operator, we can write equation (2.2.2) in a more compact form as:

$$\sum_{j=1}^{N} \tilde{\Phi}_{ij}(E) \langle \tilde{f}_j|\psi\rangle = \langle \tilde{f}_i|R_0(E)|\rho\rangle\ . \tag{2.2.8}$$

Here, we assume that we are able to render the possible divergences of some of the elements to well-defined expressions in principal matrix (in the proceeding section, we will clarify this matter in detail) and the operator is invertible. Therefore, we write

the solution in terms of this inverted operator as:

$$|\psi\rangle = R_0(E)\,|\rho\rangle + R_0(E)\sum_{i,j=1}^{N} |\tilde{f}_j\rangle \left(\tilde{\Phi}^{-1}(E)\right)_{ij} \langle\tilde{f}_j|R_0(E)|\rho\rangle \tag{2.2.9}$$

Now we put $|\psi\rangle$ expression in equation (2.2.1) in terms of the general resolvent operator back in the equation (2.2.9),

$$|\psi\rangle = (H-E)^{-1}\,|\rho\rangle = R_0(E)\,|\rho\rangle + R_0(E)\sum_{i,j=1}^{N} |\tilde{f}_i\rangle \left(\tilde{\Phi}^{-1}(E)\right)_{ij} \langle\tilde{f}_j|R_0(E)|\rho\rangle \tag{2.2.10}$$

and finally ρ being an arbitrary element in Hilbert space, we obtain

$$R(E) = R_0(E) + R_0(E)\sum_{i,j=1}^{N} |\tilde{f}_i\rangle \left(\tilde{\Phi}^{-1}(E)\right)_{ij} \langle\tilde{f}_j|\,R_0(E)\ . \tag{2.2.11}$$

To go back and see the explicit dependence of this expression on the interaction strength, we basically write the second term of the right hand side of the equation (2.2.11) in terms of the trace of a matrix with operator entries as

$$\sum_{i,j=1}^{N} |\tilde{f}_i\rangle \left(\tilde{\Phi}^{-1}(E)\right)_{ij} \langle\tilde{f}_j| = \mathrm{Tr}\Big(\tilde{F}\tilde{\Phi}^{-1}\Big) \tag{2.2.12}$$

where the $\tilde{F}$ matrix is taken as $\tilde{F}_{ij} = |\tilde{f}_i\rangle\langle\tilde{f}_j|$. Now we define a diagonal matrix as $D_{ij} = \sqrt{\lambda_i}\ \delta_{ij}$ to make the decomposition $\tilde{F} = DFD$. For example, for $N = 2$,

$$\begin{aligned}
&\begin{pmatrix} \lambda_1\,|f_1\rangle\langle f_1| & \sqrt{\lambda_1\lambda_2}\,|f_1\rangle\langle f_2| \\ \sqrt{\lambda_1\lambda_2}\,|f_2\rangle\langle f_1| & \lambda_2\,|f_2\rangle\langle f_2| \end{pmatrix} \\
&= \begin{pmatrix} \sqrt{\lambda_1} & 0 \\ 0 & \sqrt{\lambda_2} \end{pmatrix} \begin{pmatrix} |f_1\rangle\langle f_1| & |f_1\rangle\langle f_2| \\ |f_2\rangle\langle f_1| & |f_2\rangle\langle f_2| \end{pmatrix} \begin{pmatrix} \sqrt{\lambda_1} & 0 \\ 0 & \sqrt{\lambda_2} \end{pmatrix}
\end{aligned} \tag{2.2.13}$$

we reach to the regular form of the matrix $F_{ij} = |f_i\rangle\langle f_j|$, i.e., in a form which is independent of the interaction strength. Now we can apply this relation to the matrix form of the inverse of the principal matrix as $D\tilde{\Phi}^{-1}D = \Phi^{-1}$ and multiplying both sides with proper inverse operators we get $\tilde{\Phi}^{-1} = D^{-1}\Phi^{-1}D^{-1}$. Then we can write $\mathrm{Tr}(\tilde{F}\tilde{\Phi}^{-1}) = \mathrm{Tr}(DF\underbrace{DD^{-1}}_{1}\Phi^{-1}D^{-1})$. As we can always change the order of the matrices under trace operation, we reach to the equity $\mathrm{Tr}(\tilde{F}\tilde{\Phi}^{-1}) = \mathrm{Tr}(F\Phi^{-1})$. So we

can isolate the F-matrix from the interaction strengths and import it in the relation between the forms of the principal matrix as $\tilde{\Phi}_{ij} = \sqrt{\lambda_i \lambda_j}\Phi_{ij}$. Finally, we write the Φ matrix in terms of the interaction strengths explicitly as

$$\Phi_{ij}(E) = \begin{cases} \frac{1}{\lambda_i} - \langle f_i|R_0(E)|f_i\rangle & i = j \\ -\langle f_i|R_0(E)|f_j\rangle & i \neq j \end{cases} \tag{2.2.14}$$

and obtain the final form of the equation (2.2.11) as below

$$R(E) = R_0(E) + R_0(E) \sum_{i,j=1}^{N} |f_j\rangle \left(\Phi^{-1}(E)\right)_{ij} \langle f_j| \, R_0(E) \ . \tag{2.2.15}$$

Following these, in equation (2.2.9) taking $R_0(E)\,|\rho\rangle = |\phi\rangle$, a general wave function can be written as

$$|\psi\rangle = |\phi\rangle + R_0(E) \sum_{i,j=1}^{N} |f_j\rangle \left(\Phi^{-1}(E)\right)_{ij} \langle f_j|\phi\rangle \ . \tag{2.2.16}$$

These are two expressions that we use repeatedly in our applications henceforward.

It is well-known in scattering theory that the essential information is contained in the $T-$matrix and it satisfies the following exact equation [3]

$$R = R_0 \ + \ R_0 \, T \, R_0 \ . \tag{2.2.17}$$

Comparing the well-known scattering solution in (2.0.2) with the Lippmann-Schwinger equation above, we see that the scattering amplitude can also be written in terms of $T(E)$, in two dimensions as

$$f(\mathbf{k}', \mathbf{k}) = -\frac{1}{4}\sqrt{\frac{2}{\pi k}} \langle \mathbf{k}'|T(E)|\mathbf{k}\rangle \ , \tag{2.2.18}$$

where $|k\rangle$ is the wave vector. Here, we exclude $\sqrt{i}$ factor, since the plane wave expansion in two dimensions brings the phase factor $e^{i\pi/4}$ also [54]. $T(E)$ relates to the principal matrix as below

$$T(E) = -\sum_{i,j=1}^{N} |f_i\rangle \Big[\Phi^{-1}(E)\Big]_{ij} \langle f_j| \ . \tag{2.2.19}$$

2.3. Regularization of the Hamiltonians and Renormalization

The interactions defined by the singular potentials make the Hamiltonian ill-defined since the resulting states after interaction will not remain in the Hilbert space of the free Hamiltonian. Additionally, it is well-known in literature that renormalization is needed (see e.g., [33, 34] for the point interactions in two and three dimensions) if the support of the interaction is codimension two or three. Therefore, as the principal matrix assumed to be invertible, we need to regularize and possibly renormalize the Hamiltonian when we are dealing with singular interactions. One method to regularize these types of ill-defined Hamiltonians is considered in our recent work [48]. In this approach, the interaction potentials are defined as finite rank projections onto Hilbert space first. Then, one can write the regularized resolvent operators associated with these regularized Hamiltonians. After that, considering the strong limit of these regularized resolvents, i.e. the $\epsilon \to 0$ limit, where ϵ is the regularization parameter, one can then remove the regularization parameter. In this work, regularization does not guarantee the self-adjointness, so we also show the self-adjointness of the resolvent operator corresponding to these limits. If there is also a singularity codimension two or three, to renormalize the divergent elements of the principal matrix, we need to choose the interaction strengths as functions of the regularization parameter such that the limit converges. This choice is called renormalization in that case.

Here, we give another regularization method, the cut-off regularization construction used in our paper [49] briefly. Since the derivations for the other cases are essentially similar, only the structure of the regularization and renormalization of the circular and point-point term of the principal matrix is derived in detail.

Let us consider the case when there is only one point defect at position $\mathbf{a}$ in the system, i.e., the singular term of the principal matrix in two dimensions. The divergent

part of the first diagonal term of the principal matrix is [3]

$$\begin{aligned}\langle \mathbf{a}|R_0(E)|\mathbf{a}\rangle &= \int\int \langle \mathbf{a}|\mathbf{p}\rangle \langle \mathbf{p}|R_0^+(E)|\mathbf{p}'\rangle \langle \mathbf{p}'|\mathbf{a}\rangle \, d^2p \; d^2p' \\ &= \int\int \frac{e^{i\mathbf{a}\cdot(\mathbf{p}-\mathbf{p}')}}{(2\pi)^2} \langle \mathbf{p}|R_0^+(E)|\mathbf{p}'\rangle \, d^2p \; d^2p' \\ &= \int\int \frac{e^{i\mathbf{a}\cdot(\mathbf{p}-\mathbf{p}')}}{(2\pi)^2} \frac{\delta(\mathbf{p}-\mathbf{p}')}{p^2-E+i\epsilon} d^2p \; d^2p' \\ &= \int \frac{d^2p}{(2\pi)^2} \frac{1}{p^2-k^2+i\epsilon} \end{aligned} \tag{2.3.1}$$

where ϵ here is not the regularization parameter, but the outgoing boundary condition parameter that is inserted by hand at this stage and $k^2 = E$. Upper index + of the resolvent also indicates that the outgoing resolvent operator is in subject. In two dimensions

$$R_0^+(\mathbf{r},\mathbf{r}'|E) = \langle \mathbf{r}|R_0^+(E)|\mathbf{r}'\rangle = -\frac{i}{4} H_0^{(1)}(k|\mathbf{r}-\mathbf{r}'|) \tag{2.3.2}$$

where $H_0^{(1)}$ is the zeroth order Hankel function of the first kind. To regularize the integral given in (2.3.1), we calculate it with a cut-off parameter Λ as,

$$\langle \mathbf{a}|R_0^+(E)|\mathbf{a}\rangle = \frac{1}{2\pi}\int_0^\Lambda \frac{pdp}{p^2-k^2+i\epsilon} = \frac{1}{4\pi}\ln\left(p^2-k^2+i\epsilon\right)\Big|_0^\Lambda \tag{2.3.3}$$

where we make the transformation $p^2-k^2+i\epsilon = x^2$ and used $\int \frac{dx}{x} = \ln x$. Placing the integral limits and writing $-k^2 = e^{-i\pi}k^2$, we get

$$\langle \mathbf{a}|R_0^+(E)|\mathbf{a}\rangle = \frac{1}{4\pi}\ln\left(\frac{\Lambda^2-k^2+i\epsilon}{-k^2+i\epsilon}\right) = \frac{1}{4\pi}\ln\left(\frac{\Lambda^2-k^2+i\epsilon}{e^{-i\pi}k^2+i\epsilon}\right). \tag{2.3.4}$$

For large Λ limit, we can simply ignore k^2 in the numerator and ϵ already goes to zero. Using the relation $\ln(ab) = \ln a + \ln b$, we have

$$\langle \mathbf{a}|R_0^+(E)|\mathbf{a}\rangle = \frac{1}{2\pi}\ln\left(\frac{\Lambda}{e^{-\frac{i\pi}{2}}k}\right) = \frac{1}{2\pi}\left[\ln\left(\frac{\Lambda}{k}\right)+\frac{i\pi}{2}\right] = \frac{1}{2\pi}\ln\left(\frac{\Lambda}{k}\right)+\frac{i}{4}\,. \tag{2.3.5}$$

We could calculate the integral, however, the result we have for Φ_{11} term is divergent in the limit $\Lambda \to \infty$. To renormalize this result, we pick an abstract momentum such as μ, in other words a renormalization constant, and we shift this divergence into the

interaction strength that we can choose freely:

$$\underbrace{\frac{1}{\lambda}-\frac{1}{2\pi}\ln\left(\frac{\Lambda}{\mu}\right)}_{\text{we need to keep finite}}+\underbrace{\frac{1}{2\pi}\ln\left(\frac{k}{\mu}\right)-\frac{i}{4}}_{\text{already finite}} \tag{2.3.6}$$

Here, we call $\frac{1}{\lambda}-\frac{1}{2\pi}\ln\left(\frac{\Lambda}{\mu}\right)=\frac{1}{\lambda_R}$ where R sub-index indicates that the interaction strength is renormalized and finally obtain the renormalized principal matrix element as

$$\Phi_{11}(E)=\frac{1}{\lambda_R}+\frac{1}{2\pi}\ln\left(\frac{k}{\mu}\right)-\frac{i}{4}\,. \tag{2.3.7}$$

For the case when there are more then one point defects, the only thing in this calculation that changes is the point defect state and the renormalization constant take index n for the nth defect.

3. HYBRID GEOMETRIES OF DELTA POTENTIALS AND THEIR DEFORMATIONS

In this chapter, we give the spectrum of the bound state energy and scattering state analysis via the calculation of the differential cross sections for systems of a circle defect plus a point defect and a spherical shell defect plus a point defect. Additionally, we study how some small deformations in the normal directions of the supports of the delta potentials change the bound state energies in the first order of the deformation parameter. Our observation here is remarkable: the change noted in the bound state energy in the first order of the deformation is equal to the change in the bound state energies in the first order of the deformation parameter when the radius of the circle is increased by the amount of the average of the deformation over the support of the defect. This method of calculation of the change in the bound state energies under deformation in principle can be applied also to delta potentials supported by curves and surfaces in general.

The organization of this chapter is follows. In Section 3.1, our concern is a system of Dirac-delta potentials supported by a circle centered at the origin and a point outside of this circle. We discuss the bound state analysis and the scattering properties for this case in brief. In section 3.2, the concern is a Dirac-delta potential supported by a sphere centered at the origin and a point outside of this shell. Similarly we deal with the bound state spectrum and scattering states. After that, in 3.3 and 3.4, we look for how the small deformations of the circle and sphere in the normal directions change the bound state spectrum and scattering results. Finally, in sections 3.5 and 3.6, we combine the deformed defects with the outer point defect and check the change in the bound and scattering states similarly.

Now, let us give some expressions used in upcoming calculations. Dirac delta function supported by a point $\mathbf{a}$ is defined on the test functions ψ by $\langle \delta_{\mathbf{a}} | \psi \rangle = \langle \mathbf{a} | \psi \rangle := \psi(\mathbf{a})$. Similarly, the Dirac delta function δ_Γ supported by the curve Γ and the Dirac

delta function δ_Σ supported by the surface Σ are defined by their action on ψ [56] as

$$\langle \delta_\Gamma | \psi \rangle = \langle \Gamma | \psi \rangle \;\; := \;\; \frac{1}{L(\Gamma)} \int_\Gamma \psi \; ds \; , \tag{3.0.1}$$

$$\langle \delta_\Sigma | \psi \rangle = \langle \Sigma | \psi \rangle \;\; := \;\; \frac{1}{A(\Sigma)} \int_\Sigma \psi \; dA \; , \tag{3.0.2}$$

where L is the length of the curve, A is the area of the surface, ds is the integration element over the curve Γ and dA is the integration element over the surface Σ. For the circle $\Gamma = S^1$, $ds = Rd\theta$ and $L(\Gamma) = 2\pi R$. For the sphere $\Sigma = S^2$, $dA = R^2 \sin\theta d\theta d\phi$ and $A(\Sigma) = 4\pi R^2$, where both circle and sphere are considered to have radius R.

3.1. Delta Potential Supported by a Circle and a Point in 2D

The Hamiltonian for a setup consisting a circular and a point-wise defect can be written as

$$H = H_0 - \lambda_1 |\mathbf{a}\rangle\langle\mathbf{a}| - \lambda_2 |\Gamma\rangle\langle\Gamma| \; , \tag{3.1.1}$$

where H_0 is the free Hamiltonian, λ_1 and λ_2 are the interaction strengths for the circle and spherical shell defects respectively, $\mathbf{a}$ represents the point-wise defect at location a and Γ represent the circular defect centered at the origin with radius R with the parametrization function $\Gamma \to \gamma(s) = R\mathbf{n}(\theta)$. We already have the renormalized term

$$\begin{aligned} \Phi_{11}(E) &= \frac{1}{\lambda_R} + \frac{1}{2\pi} \ln\left(\frac{i\nu}{\mu}\right) - \frac{i}{4} = \frac{1}{\lambda_R} + \frac{1}{2\pi} \ln\left(\frac{e^{i\frac{\pi}{2}}\nu}{\mu}\right) - \frac{i}{4} \\ &= \frac{1}{\lambda_R} + \frac{1}{2\pi} \ln\left(\frac{\nu}{\mu}\right) \end{aligned} \tag{3.1.2}$$

where the energy is chosen to be in the negative part of the spectrum here, $E = k^2 = -\nu^2$, $\nu > 0$ as initially we are looking for the bound state solutions. We have the definition

$$\langle \mathbf{p} | \Gamma \rangle = \frac{1}{L(\Gamma)} \int_0^L e^{-i\mathbf{p}\cdot\gamma(s)} |\gamma'(s)| \; ds \tag{3.1.3}$$

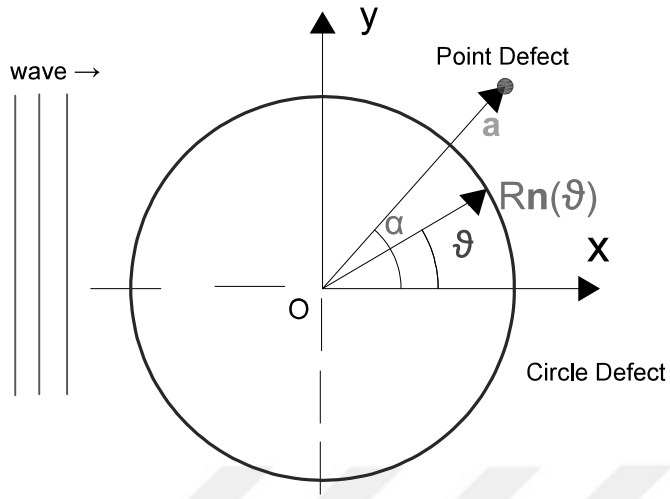

Figure 3.1. Circle and point defects in 2D setup where $R\mathbf{n}(\theta)$ and $\mathbf{a}$ are the position vectors of the defects respectively

where $|\gamma'(s)| = 1$. Therefore, the second term of the principal matrix that we need to construct can be written as

$$\begin{aligned}
\Phi_{12}(-\nu^2) = \Phi_{21}(-\nu^2) &= -\langle \mathbf{a}|R_0(-\nu^2)|\Gamma\rangle = -\int \langle \mathbf{a}|\mathbf{p}\rangle \langle \mathbf{p}|R_0(-\nu^2)|\Gamma\rangle \, d^2p \\
&= -\int \frac{e^{i\mathbf{a}\cdot\mathbf{p}}}{(2\pi)^2} \frac{1}{p^2+\nu^2} \left(\frac{1}{2\pi R} \int_0^{2\pi} e^{-i\mathbf{p}\cdot\gamma(s)} R d\theta \right) d^2p \\
&= -\frac{1}{(2\pi)^2} \int_0^{\infty} \int_0^{2\pi} e^{iap\cos\alpha} \frac{J_0(pR)}{p^2+\nu^2} \, pdp \, d\alpha \\
&= -\frac{1}{2\pi} \int_0^{\infty} J_0(ap) \frac{J_0(pR)}{p^2+\nu^2} \, pdp \\
&= -\frac{1}{2\pi} K_0(a\nu) \, I_0(R\nu) \qquad (3.1.4)
\end{aligned}$$

where $J_n(z)$ is the nth order Bessel function of the first kind. Zeroth order Bessel function of the first kind has the integral representation below:

$$J_0(z) = \frac{1}{2\pi} \int_0^{2\pi} e^{-iz\cos\theta} d\theta \ . \qquad (3.1.5)$$

On the other hand, $K_n(z)$ and $I_n(z)$ are nth order modified Bessel functions. Here, we used the integral relation between these functions that can be found in [61],

$$\int_0^\infty J_n(ax)J_n(bx)\,\frac{x}{x^2+c^2}\,dx = \begin{cases} K_n(ac)I_n(bc) & 0<b<a \\ K_n(bc)I_n(ac) & 0<a<b \end{cases}, \tag{3.1.6}$$

for $\mathrm{Re}(n) > -1$, assuming $a > R$.

Finally, for the second diagonal term of the principal matrix, we do not need renormalization. We do the similar calculations and obtain

$$\begin{aligned} \Phi_{22}(-\nu^2) &= \frac{1}{\lambda_2} - \langle\Gamma|R_0(-\nu^2)|\Gamma\rangle = \frac{1}{\lambda_2} - \int_{\mathbb{R}^2} \frac{\langle\mathbf{p}|\Gamma\rangle\langle\Gamma|\mathbf{p}\rangle}{p^2+\nu^2}\frac{d^2p}{(2\pi)^2} \\ &= \frac{1}{\lambda_2} - -\frac{1}{2\pi} I_0(\nu R)K_0(\nu R)\,. \end{aligned} \tag{3.1.7}$$

Hence, the principal matrix $\Phi(-\nu^2)$, looks like

$$\Phi(-\nu^2) := \begin{pmatrix} \frac{1}{\lambda_R} + \frac{1}{2\pi}\ln\left(\frac{\nu}{\mu}\right) & -\frac{1}{2\pi}K_0\left(\nu a\right)I_0\left(\nu R\right) \\ \\ -\frac{1}{2\pi}K_0\left(\nu a\right)I_0\left(\nu R\right) & \frac{1}{\lambda_2} - \frac{1}{2\pi}K_0(\nu R)I_0(\nu R) \end{pmatrix} \tag{3.1.8}$$

for this case. Recalling the resolvent operator, (2.2.15),

$$R(E) = R_0(E) + R_0(E)\sum_{i,j=1}^{2} |f_i\rangle \left(\Phi^{-1}(E)\right)_{ij} \langle f_j|R_0(E)\,, \tag{3.1.9}$$

for $E = -\nu^2$. For the time being, we assume $\det\Phi(E) \neq 0$. Again, here $|f_1\rangle = |\mathbf{a}\rangle$ and $|f_2\rangle = |\Gamma\rangle$.

Now we reach to the point that we can project the expression given in (2.2.16) onto the position space. In terms of energy, k^2, we obtain the wave function below which includes integrals that we need to deal with

$$\psi(\mathbf{r}) = \phi(\mathbf{r}) + \sum_{i,j=1}^{2} \langle\mathbf{r}|R_0(k^2)|f_i\rangle \left[\Phi^{-1}(k^2)\right]_{ij} \langle f_j|\phi\rangle\,, \tag{3.1.10}$$

where

$$\langle \mathbf{a}|\phi\rangle = \phi(\mathbf{a}) \qquad \text{and} \qquad \langle \Gamma|\phi\rangle = \frac{1}{L(\Gamma)}\int_{S^1}\phi(\gamma(s))\,ds\ . \tag{3.1.11}$$

Giving the other terms as

$$\langle \mathbf{r}|R_0(k^2)|f_1\rangle = \langle \mathbf{r}|R_0(k^2)|\mathbf{a}\rangle = \int_{\mathbb{R}^2}\frac{e^{i\mathbf{p}\cdot(\mathbf{r}-\mathbf{a})}}{p^2-k^2+i\epsilon}\,\frac{d^2p}{(2\pi)^2} = \frac{i}{4}H_0^{(1)}(k|\mathbf{r}-\mathbf{a}|)\ , \tag{3.1.12}$$

where $H_0^{(1)}$ is the zeroth order Hankel function of the first kind. We also have

$$\begin{aligned}\langle \mathbf{r}|R_0(k^2)|f_2\rangle = \langle \mathbf{r}|R_0(k^2)|\Gamma\rangle &= \int_{\mathbb{R}^2}\frac{e^{i\mathbf{p}\cdot\mathbf{r}}}{p^2-k^2+i\epsilon}\,J_0(pR)\frac{d^2p}{(2\pi)^2}\\ &= \int_0^\infty \frac{pJ_0(pr)J_0(pR)}{p^2-k^2+i\epsilon}\frac{dp}{(2\pi)}\\ &= \frac{i}{4}\left(H_0^{(1)}(kr)J_0(kR)\theta(R-r)+H_0^{(1)}(kR)J_0(kr)\theta(r-R)\right)\end{aligned} \tag{3.1.13}$$

where $\theta(x)$ is the step function here. We have evaluated the last integral by the analytic continuation of the result (3.1.6) which means taking ν to $-ik$. We also use the relations between Bessel functions

$$K_0(z) = \frac{i\pi}{2}H_0^{(1)}(e^{i\pi/2}z) \qquad \text{and} \qquad I_0(z) = e^{-i\pi/2}J_0(e^{i\pi/2}z) \tag{3.1.14}$$

for $-\pi < arg(z) < \pi/2$, which can be found in [62]. Hence, we obtain set of wave functions

$$\begin{aligned}\psi(\mathbf{r}) =&\phi(\mathbf{r}) + \frac{i}{4}H_0^{(1)}(k|\mathbf{r}-\mathbf{a}|)\\ &\times\left(\left[\Phi^{-1}(k^2)\right]_{11}\phi(\mathbf{a}) + \left[\Phi^{-1}(k^2)\right]_{12}\left(\frac{1}{L}\int_{S^1}\phi(\gamma(s))\,ds\right)\right)\\ &+\ \frac{i}{4}\left(H_0^{(1)}(kr)J_0(kR)\theta(R-r)+H_0^{(1)}(kR)J_0(kr)\theta(r-R)\right)\\ &\times\left(\left[\Phi^{-1}(k^2)\right]_{21}\phi(\mathbf{a}) + \left[\Phi^{-1}(k^2)\right]_{22}\left(\frac{1}{L}\int_{S^1}\phi(\gamma(s))\,ds\right)\right)\end{aligned} \tag{3.1.15}$$

for the positive energy values. The details of this discussion can be found in our article [48].

3.1.1. Bound State Analysis

For the bound state spectrum of this problem, we look at to the values $E = -\nu^2 < 0$. The poles of the resolvent operator $R(-\nu^2)$ given by (3.1.9) provide the bound state spectrum of the problem and the poles of this operator can only appear if the matrix $\Phi(-\nu^2)$ is singular, that is, if

$$\det[\Phi(-\nu^2)] = 0\ . \tag{3.1.16}$$

This equation is not easy to solve. Therefore, at this point, we assume that we have a bound state solution at $\nu = \nu_*$. So we can write the eigenvalue equation below

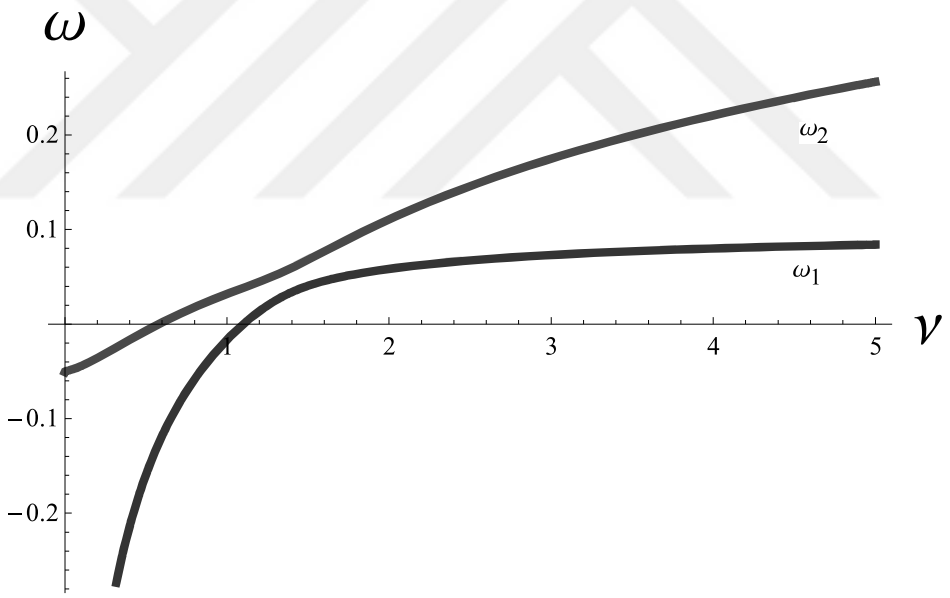

Figure 3.2. Plot of the eigenvalues of the principal matrix Φ, ω versus ν for a cirle and point defect with $\lambda_2 = 10$, $\mu = 1$, $R = 1$, $a = 2$ settings.

$$\sum_{j=1}^{2} \Phi_{ij}(-\nu_*^2) A_j = 0\ , \tag{3.1.17}$$

where A_j is an eigenvector of the matrix $\Phi(-\nu_*^2)$ with a zero eigenvalue. In our paper, [48], we show that these normalized eigenvectors are unique. However, we will not go

into details of that derivation here. Now we can write the eigenvalue and eigenfunction equation with the eigenvalue ω as,

$$\Phi A = \omega A \, . \tag{3.1.18}$$

The eigenvalues can be explicitly calculated as

$$\begin{aligned}\omega_1(\nu) = &\frac{1}{2\lambda_R} - \frac{1}{4\pi} I_0(\nu R) K_0(\nu R) + \frac{1}{2\lambda_2} + \frac{1}{4\pi} \ln\left(\frac{\nu}{\mu}\right) \\ &+ \left[\left(\frac{1}{2\pi} \ln\left(\frac{\nu}{\mu}\right) + \frac{1}{\lambda_R} \right) \left(\frac{1}{2\pi} K_0(\nu R) I_0(\nu R) - \frac{1}{\lambda_2} \right) - \frac{1}{4\pi^2} K_0^2(\nu R) I_0^2(\nu R) \right]^{1/2}\end{aligned} \tag{3.1.19}$$

and

$$\begin{aligned}\omega_2(\nu) = &\frac{1}{2\lambda_R} - \frac{1}{4\pi} I_0(\nu R) K_0(\nu R) + \frac{1}{2\lambda_2} + \frac{1}{4\pi} \ln\left(\frac{\nu}{\mu}\right) \\ &- \left[\left(\frac{1}{2\pi} \ln\left(\frac{\nu}{\mu}\right) + \frac{1}{\lambda_R} \right) \left(\frac{1}{2\pi} K_0(\nu R) I_0(\nu R) - \frac{1}{\lambda_2} \right) - \frac{1}{4\pi^2} K_0^2(\nu R) I_0^2(\nu R) \right]^{1/2} .\end{aligned} \tag{3.1.20}$$

Finding zeroes of the determinant of the matrix Φ is equivalent to finding the zeroes of its eigenvalues, ω's. Still, it is not easy to solve analytically. Therefore, we will look at the behaviour of these eigenvalues with respect to ν. We suppose that the eigenvectors are normalized for simplicity. Then we can determine how the eigenvalues change with respect to ν according to the Feynman-Hellman theorem [65] which can be stated as

$$\frac{\partial \omega}{\partial \nu} = A^{*T} \frac{\partial \Phi}{\partial \nu} A \, , \tag{3.1.21}$$

where the symbols $*$ and T denote the complex conjugation and transpose, respectively. Here, we take the derivative of each element of Φ matrix as below,

$$\frac{\partial \Phi_{11}}{\partial \nu} = \frac{1}{2\pi\nu}$$

$$\frac{\partial \Phi_{12}}{\partial \nu} = \frac{\partial \Phi_{21}}{\partial \nu} = (2\nu) \int_{\mathbb{R}^2} \frac{e^{i\mathbf{p}\cdot\mathbf{a}}}{(p^2+\nu^2)^2} J_0(pR) \frac{d^2p}{(2\pi)^2} \, , \tag{3.1.22}$$

$$\frac{\partial \Phi_{22}}{\partial \nu} = (2\nu) \int_{\mathbb{R}^2} \frac{J_0^2(pR)}{(p^2+\nu^2)^2} \frac{d^2p}{(2\pi)^2} \ . \tag{3.1.23}$$

So placing these into (3.1.21) we get

$$\begin{aligned} \frac{\partial \omega_{1,2}}{\partial \nu} = A_1^{*T} \frac{1}{2\pi\nu} A_1 &+ A_1^{*T}(2\nu) \int_{\mathbb{R}^2} \frac{e^{i\mathbf{p}\cdot\mathbf{a}}}{(p^2+\nu^2)^2} J_0(pR) \frac{d^2p}{(2\pi)^2} A_2 \\ &+ A_2^{*T}(2\nu) \int_{\mathbb{R}^2} \frac{e^{i\mathbf{p}\cdot\mathbf{a}}}{(p^2+\nu^2)^2} J_0(pR) \frac{d^2p}{(2\pi)^2} A_1 \\ &+ A_2^{*T}(2\nu) \int_{\mathbb{R}^2} \frac{J_0^2(pR)}{(p^2+\nu^2)^2} \frac{d^2p}{(2\pi)^2} A_2 \ . \end{aligned} \tag{3.1.24}$$

We can write the right hand side of (3.1.24) in a more compact form and we can show that

$$\frac{\partial \omega_{1,2}}{\partial \nu} = (2\nu) \int_{\mathbb{R}^2} \left| A_1 e^{i\mathbf{p}\cdot\mathbf{a}} + A_2 J_0(pR) \right|^2 \frac{1}{(p^2+\nu^2)^2} \frac{d^2p}{(2\pi)^2} > 0 \ , \tag{3.1.25}$$

for all $\nu > 0$. We used the identity $\int_0^\infty \frac{pdp}{(p^2+\nu^2)^2} = \frac{1}{2\nu^2}$ here. This positivity condition means that all the eigenvalues of the principal matrix Φ are strictly increasing functions of ν. Figure 3.2 shows how the eigenvalues behave with respect to ν for the fixed values of the other parameters and it is taken from our paper [48] which has a slightly different Φ_{11} (there is an extra $1/\lambda_R$ term) element since the regularization method used is different. However, this difference does not change the behaviour of the eigenvalues. Therefore, we directly use the graphs given in [48] in the rest of this chapter. The positivity condition (3.1.25) implies that there are at most two bound state energies since both ω_1 and ω_2 can cross the ν axis only once. In Figure 3.2, the zero of the eigenvalue ω_1, in other words where the blue line crosses the ν axis, corresponds to the ground state energy since $E = -\nu^2$. This bound state always exists for all values of the other parameters of the problem since $\lim_{\nu\to 0^+} \omega_1 = -\infty$ and it is an increasing function of ν and positive for sufficiently large values of ν. However, the second eigenvalue ω_2 may not have any zeroes if it is not negative around $\nu = 0$, in other words, it never crosses the ν axis if $\lim_{\nu\to 0^-} \omega_2 < 0$ is not satisfied. We also numerically calculate the bound state energies and plot them as a function of a and R, i.e. taking ω_1 (ground state) and ω_2 (excited state) equal to zero and then releasing a and R values, for the fixed given values of the parameters, as shown in Figure 3.3, 3.4, and Figure 3.5, 3.6 respectively.

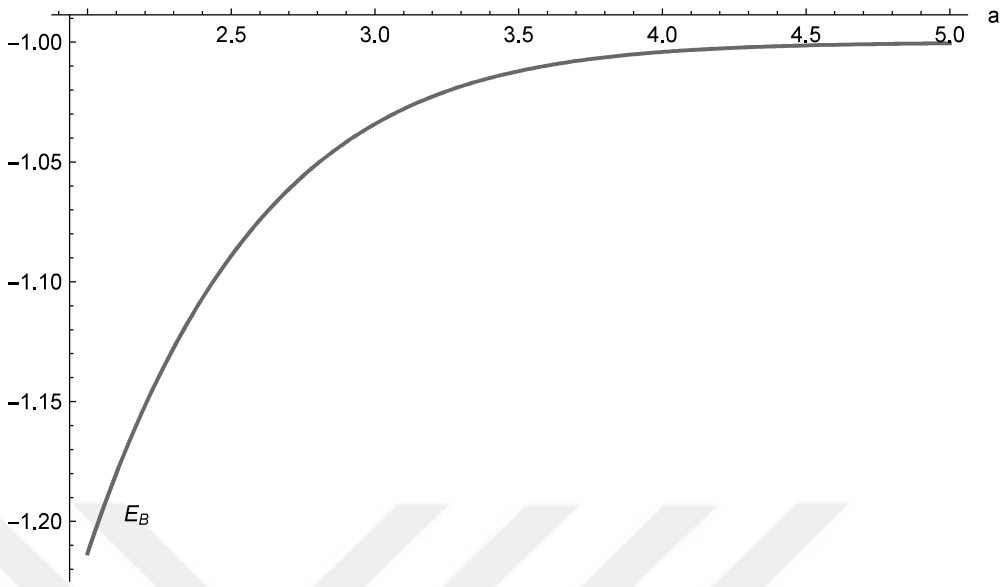

Figure 3.3. Ground state energy versus a, where $\lambda = 10$, $R = 1$, $\mu = 1$.

3.1.2. Stationary Scattering Problem

Stationary scattering problem for such singular potentials is well-defined and many examples are known in literature. As we built the principal matrix, now we can study the scattering amplitudes and related physically measurable quantities (e.g., cross section). For this reason, we use the operator $T(E)$ which is the operator form of the $T-$matrix. The relation between the resolvent and the $T-$matrix is given by [3]

$$R(E) = R_0(E) - R_0(E)T(E)R_0(E) \; . \tag{3.1.26}$$

Since we have the explicit expression for the resolvent (3.1.9), we can read off the matrix $T(E)$ as:

$$T(E) = -\sum_{i,j=1}^{2} |f_i\rangle \Big[\Phi^{-1}(E)\Big]_{ij} \langle f_j| \; . \tag{3.1.27}$$

The scattering amplitude denoted by f and the matrix $T(E)$ in two dimensions are related by

$$f(\mathbf{k} \to \mathbf{k}') = -\frac{1}{4}\sqrt{\frac{2}{\pi k}}\langle \mathbf{k}'|T(E)|\mathbf{k}\rangle \; , \tag{3.1.28}$$

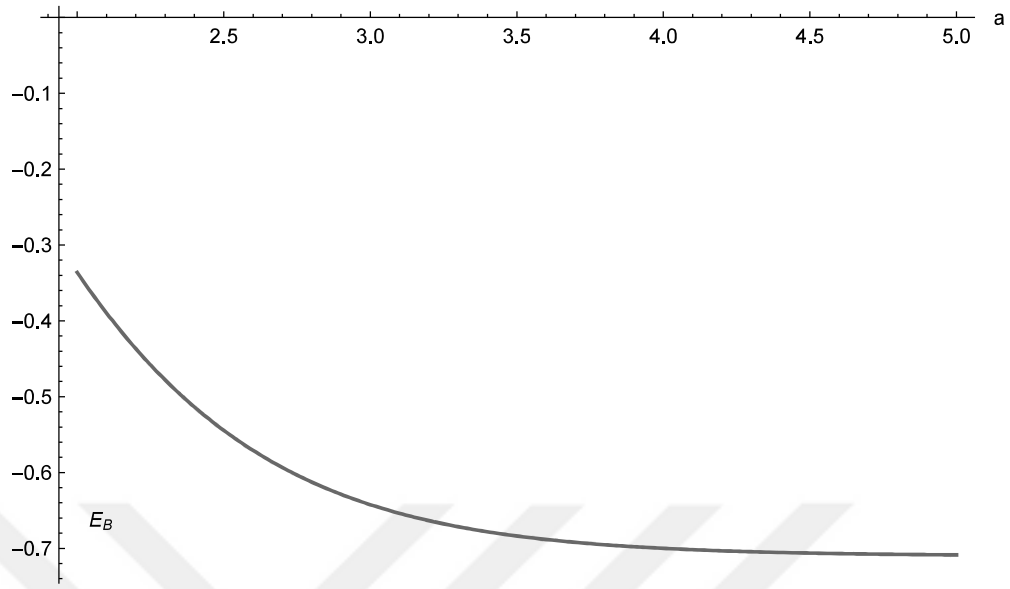

Figure 3.4. Excited state energy versus a, where $\lambda = 10$, $R = 1$, $\mu = 1$.

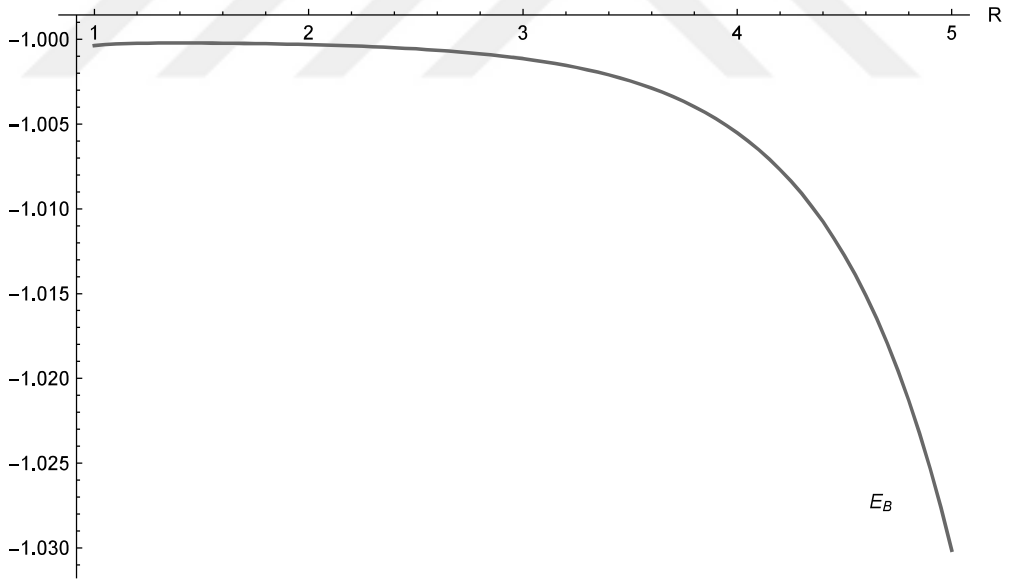

Figure 3.5. Ground state energy versus R, where $\lambda = 10$, $a = 5.1$, $\mu = 1$.

where $|\mathbf{k}\rangle$ is the wave vector and $|\mathbf{k}'| = |\mathbf{k}|$. Substituting the result (3.1.27) into (3.1.28) we get

$$\langle \mathbf{k}'|T(E)|\mathbf{k}\rangle = \int_{\mathbb{R}^2}\int_{\mathbb{R}^2} e^{i\mathbf{k}\cdot\mathbf{x}-i\mathbf{k}'\cdot\mathbf{x}'}\langle \mathbf{x}'|T(E)|\mathbf{x}\rangle \, d^2x \, d^2x' \tag{3.1.29}$$

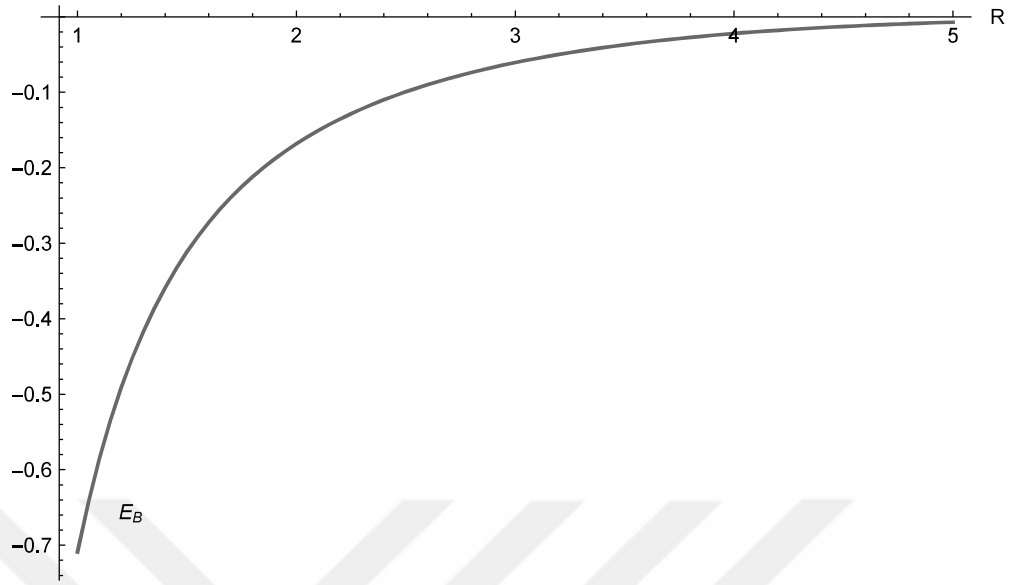

Figure 3.6. Excited state energy versus R, where $\lambda = 10$, $a = 5.1$, $\mu = 1$.

where $\mathbf{x}$ is the position vector in two dimensions. Using the integral representation of the Bessel function $J_0(x)$ given in (3.1.5) we find

$$\begin{aligned}\langle \mathbf{k}'|T(E)|\mathbf{k}\rangle =& e^{i(\mathbf{k}-\mathbf{k}')\cdot\mathbf{a}}\left(\Phi^{-1}(E)\right)_{11} + J_0(kR)\left(e^{-i\mathbf{k}'\cdot\mathbf{a}} + e^{i\mathbf{k}\cdot\mathbf{a}}\right)\left(\Phi^{-1}(E)\right)_{12} \\ &+ J_0^2(kR)\left(\Phi^{-1}(E)\right)_{22}\ , \end{aligned} \tag{3.1.30}$$

where $\left(\Phi^{-1}(E)\right)_{ij}$ is the ijth element of the inverse of the matrix $\Phi(E)$ given in equation (3.1.8) with $-\nu^2 = k^2$. So at this point, we can claim that the differential cross section for the delta potential supported by a circle of radius R centered at the origin and by the point at $\mathbf{a}$ outside of the circle is given by

$$\begin{aligned}\frac{d\sigma}{d\theta} &= |f(\mathbf{k}\to\mathbf{k}')|^2 \\ &= \frac{1}{8\pi k}\Big| e^{i(\mathbf{k}-\mathbf{k}')\cdot\mathbf{a}}\left(\Phi^{-1}(E_k)\right)_{11} \\ &\quad + J_0(kR)\left(e^{-i\mathbf{k}'\cdot\mathbf{a}} + e^{i\mathbf{k}\cdot\mathbf{a}}\right)\left(\Phi^{-1}(E_k)\right)_{12} + J_0^2(kR)\left(\Phi^{-1}(E_k)\right)_{22}\Big|^2 . \end{aligned} \tag{3.1.31}$$

The graph that demonstrates the behaviour of the differential cross section as a function of θ is in Figure 3.7. Here we assume that θ is the angle between $\mathbf{k}'$ and $\mathbf{k}$. Also, the

incoming wave is chosen to be along the positive x axis. We have also the plots of the

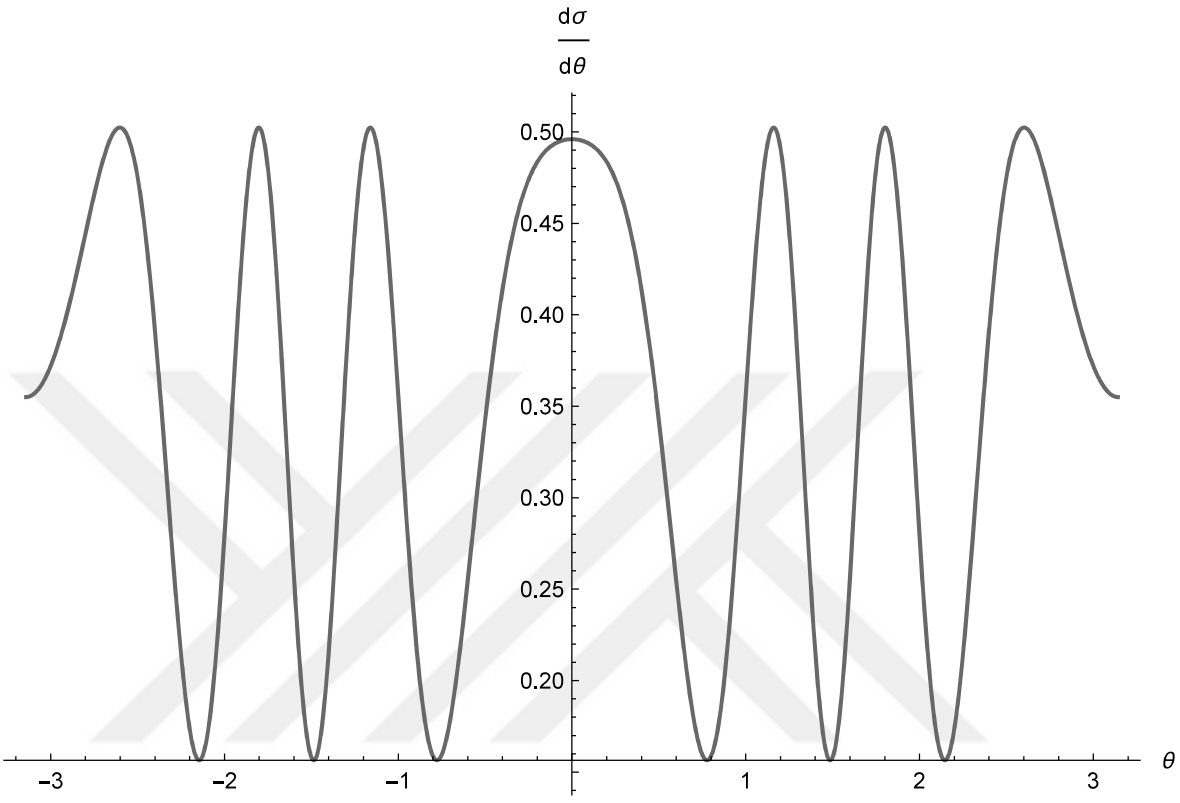

Figure 3.7. Differential Cross Section versus θ, where $k = 2$, $\lambda_2 = 20$, $a = 5$, $R = 1$, $\mu = 1$.

differential cross section as a function of k for different choice of parameters, as shown in Figure 3.8 and Figure 3.9. These two graphs shows us that the behaviour of the differential cross section near $k = 0$, in other words for the waves with low energies, is consistent with the fact that the differential cross section for two dimensional low energy scatterings blows up with decreasing energy, as emphasized in [106]. Also, in these plots we see that as far as we place the point defect from the circular defect, we see more fluctuation in the energy of the incoming wave.

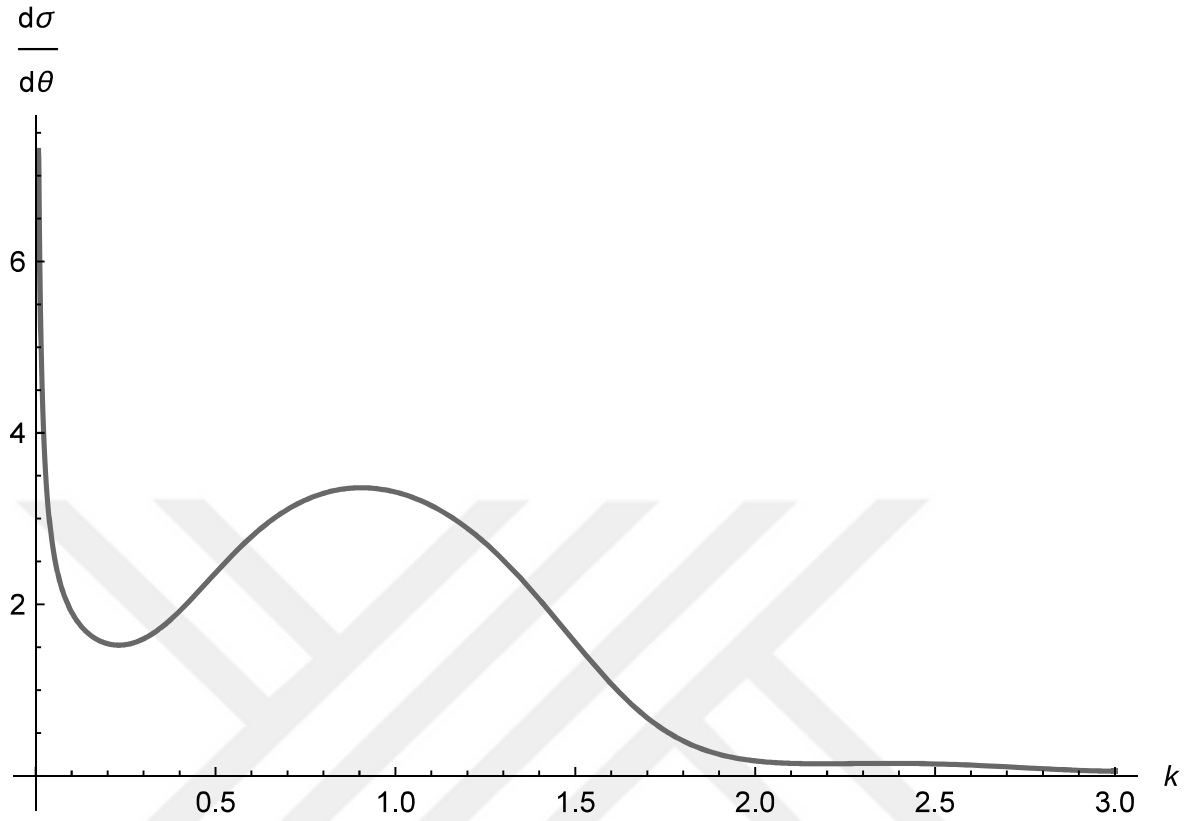

Figure 3.8. Differential Cross Section versus k,where $\theta = 0$, $\lambda_2 = 20$, $a = 2$, $R = 1$, $\mu = 10$.

3.2. Delta Potential Supported by a Sphere and a Point in 3D

In this section, we will consider the case that includes a spherical shell delta potential and a point like delta potential outside of this shell in three dimensions. The setup is demonstrated in Figure 3.10. Since all the techniques and results are similar to the case discussed in the previous section, we will summarize some results without giving detailed proofs. The regularized Hamiltonian for this model is given by

$$H = H_0 - \lambda_1 |\mathbf{a}\rangle\langle\mathbf{a}| - \lambda_2 |\Sigma\rangle\langle\Sigma| \ , \tag{3.2.1}$$

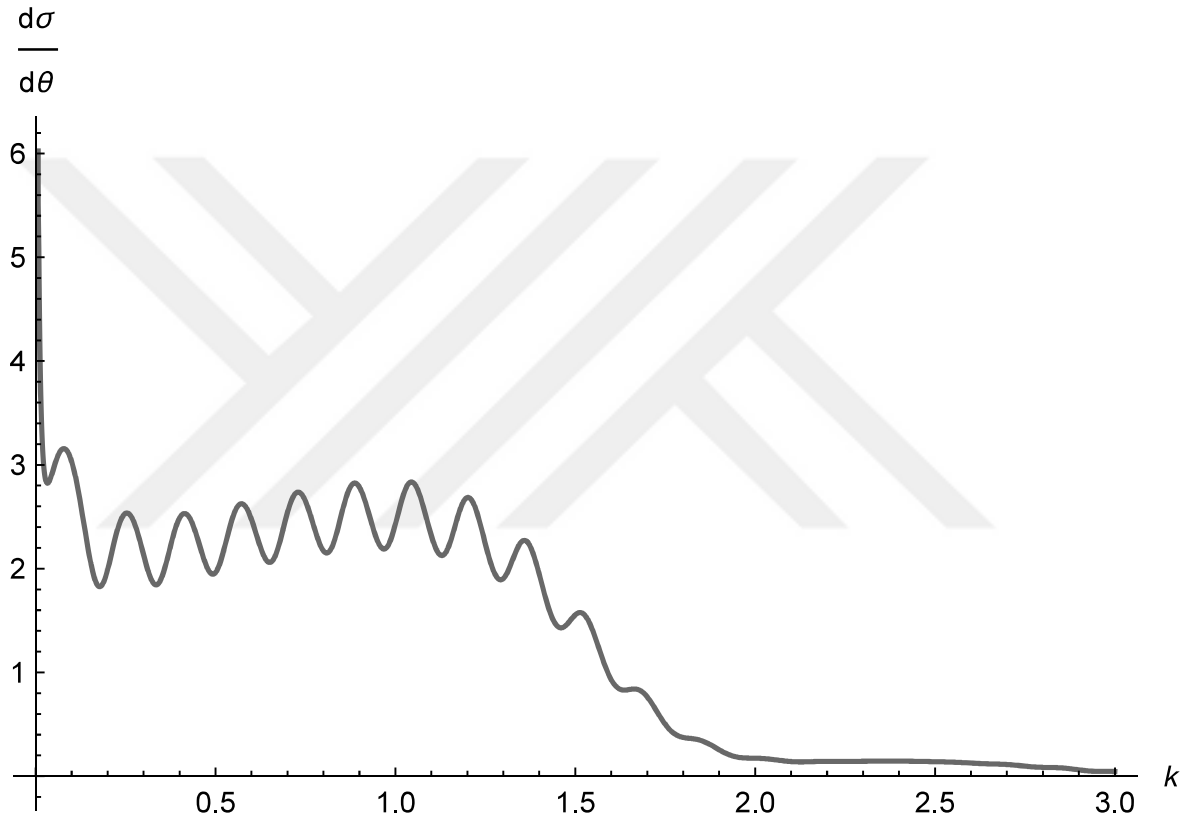

Figure 3.9. Differential Cross Section versus k,where $\theta = 0$, $\lambda_2 = 20$, $a = 20$, $R = 1$, $\mu = 10$.

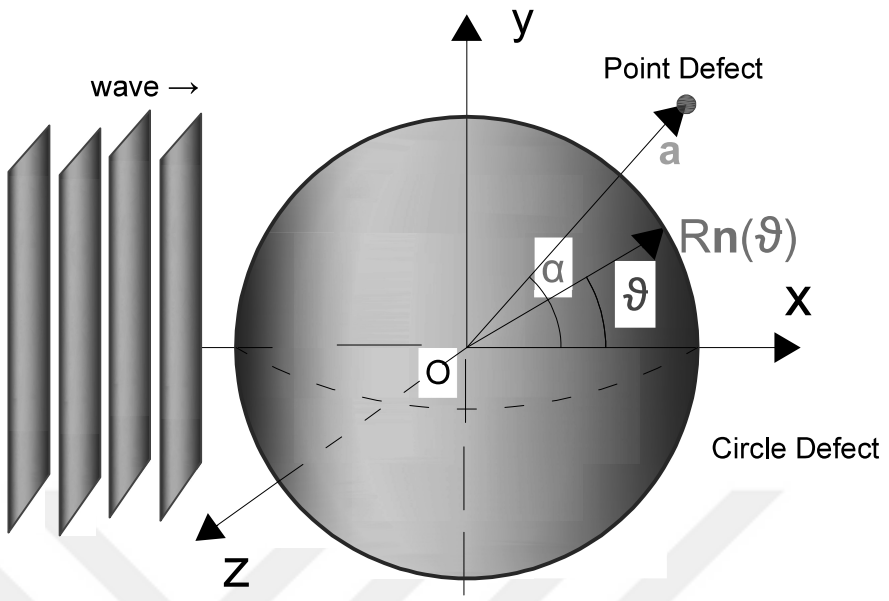

Figure 3.10. Spherical shell and point defects setup where $R\mathbf{n}(\theta)$ and $\mathbf{a}$ are the position vectors of the defects respectively.

where Σ is the sphere centered at the origin with radius R. Here $\sigma : (0, 2\pi) \times (0, \pi) \to S^2$ is the local parametrization given by

$$\sigma(\theta, \phi) := (R\sin\theta\cos\phi,\ R\sin\theta\sin\phi,\ R\cos\theta)\ . \tag{3.2.2}$$

And we have the expressions

$$\langle \mathbf{a}|\phi\rangle = \phi(\mathbf{a}) \quad \text{and} \qquad \langle \Gamma|\phi\rangle = \frac{1}{A(\Sigma)}\int \phi(\sigma(s))ds \tag{3.2.3}$$

where $A(\Sigma)$ is the area of the spherical shell. We follow the analogous calculations to the two dimensional case and we obtain the resolvent operator in a similar sense. In this case, the first diagonal element of the matrix Φ for $E = -\nu^2$, $\nu > 0$ can be calculated similarly:

$$\begin{aligned}
\Phi_{11}(-\nu^2) &= \frac{1}{\lambda_1} - \langle \mathbf{a}|R_0(E)|\mathbf{a}\rangle = \frac{1}{\lambda_1} - \int\int \langle \mathbf{a}|\mathbf{p}\rangle \langle \mathbf{p}|R_0^+(E)|\mathbf{p}'\rangle \langle \mathbf{p}'|\mathbf{a}\rangle \, d^3p \, d^3p' \\
&= \frac{1}{\lambda_1} - \int\int \frac{e^{i\mathbf{a}\cdot(\mathbf{p}-\mathbf{p}')}}{(2\pi)^6} \langle \mathbf{p}|R_0^+(E)|\mathbf{p}'\rangle \, d^3p \, d^3p' \\
&= \frac{1}{\lambda_1} - \int \frac{d^3p}{(2\pi)^3}\frac{1}{p^2+\nu^2}\ .
\end{aligned} \tag{3.2.4}$$

Using a cut-off Λ as an integral limit, we get

$$\Phi_{11}(-\nu^2) = \frac{1}{\lambda_1} - \frac{\Lambda}{2\pi^2} + \frac{\nu}{2\pi^2} \arctan\left(\frac{\Lambda}{\nu}\right) \tag{3.2.5}$$

Now, taking the limit $\Lambda \to \infty$, the last term above converges as

$$\lim_{x\to\infty} \arctan x = \frac{\pi}{2} \ . \tag{3.2.6}$$

However, we need to adjust $\frac{1}{\lambda_1}$ accordingly to get rid of the divergence in the second term. We make the choice of some renormalization parameter μ as

$$\frac{1}{\lambda_1} - \frac{\Lambda}{2\pi^2} = -\frac{\mu}{4\pi} \tag{3.2.7}$$

where minus sign and the 4π in the denominator are just for simplicity. With this, we arrive at

$$\Phi_{11}(-\nu^2) = \frac{1}{4\pi}(\nu - \mu) \ . \tag{3.2.8}$$

To find the off-diagonal matrix elements of Φ, we calculate the integral below by choosing the position of the point defect along the z axis:

$$\begin{aligned} \Phi_{12}(-\nu^2) = \Phi_{21}(-\nu^2) &= -\langle \mathbf{a}|R_0(-\nu^2)|\Sigma\rangle = -\int_{\mathbb{R}^3} \frac{e^{i\mathbf{p}\cdot\mathbf{a}}}{(p^2+\nu^2)} \frac{\sin(pR)}{pR} \frac{d^3p}{(2\pi)^3} \\ &= -\frac{1}{4\pi\nu a R}\, e^{-\nu a} \sinh(\nu R) \ , \end{aligned} \tag{3.2.9}$$

where we have used

$$\begin{aligned} \langle \mathbf{p}|\Sigma\rangle &= \frac{1}{A(\Sigma)} \int e^{-i\mathbf{p}\cdot\sigma(s)} d^3x = \frac{1}{4\pi R^2} \int_0^{2\pi} \int_0^{\pi} e^{-ipR\cos\theta} R^2 \sin\theta \ d\theta \ d\phi \\ &= \frac{\sin(pR)}{pR} \end{aligned} \tag{3.2.10}$$

and

$$\int_0^{\pi} e^{-ix\cos\theta} \sin\theta \ d\theta = 2 \ \frac{\sin x}{x} \ . \tag{3.2.11}$$

Similarly, the second diagonal term of Φ is

$$\begin{aligned}\Phi_{22}(-\nu^2) &= \frac{1}{\lambda_2} - \langle\Sigma|R_0(-\nu^2)|\Sigma\rangle = \frac{1}{\lambda_2} - \int_{\mathbb{R}^3} \frac{1}{p^2+\nu^2}\frac{\sin^2(pR)}{(pR)^2}\frac{d^3p}{(2\pi)^3}\,, \\ &= \frac{1}{\lambda_2} - \frac{1}{4\pi\nu R^2}e^{-\nu R}\sinh(\nu R)\,. \end{aligned} \tag{3.2.12}$$

The matrix Φ can be defined on the complex plane by an analytic continuation, implying $\nu = ik$, again. To make the principal matrix look more similar to its two dimensional analogy, we express the elements in terms of the Bessel functions using the transformation relations $I_{1/2}(z) = \sqrt{\frac{2}{\pi z}}\sinh z$ and $K_{1/2}(z) = \sqrt{\frac{\pi}{2z}}e^{-z}$ and we obtain the final form as:

$$\Phi(-\nu^2) = \begin{pmatrix} \frac{1}{4\pi}(\nu-\mu) & -\frac{1}{4\pi\sqrt{aR}}\,K_{1/2}(\nu a)\,I_{1/2}(\nu R) \\ -\frac{1}{4\pi\sqrt{aR}}\,K_{1/2}(\nu a)\,I_{1/2}(\nu R) & \frac{1}{\lambda_2} - \frac{1}{4\pi R}K_{1/2}(\nu R)\,I_{1/2}(\nu R) \end{pmatrix} \tag{3.2.13}$$

3.2.1. Bound State Problem

Bound state of this case is similar to the circle+point analysis. As we look at the derivative of the principal matrix with respect to ν, we see that positivity of the flow of eigenvalues still holds in this case. There are at most two bound states and at least one bound state of the system with a sphere and a point defect also.

Again, we have the plots of the behaviour of the eigenvalues of the principal matrix with fixed parameters of the problem. Figure 3.11 and 3.12 show that the strength of the spherical interaction has an important effect on the bound state energy. As we look at these graphs, we notice that there is only one bound state, if we choose the same values of the parameters including λ_2 for the circular defect perturbed by a point defect case. The reason for this may be based on the fact that the particle has more freedom to escape from the spherical defect compared to the circular defect. When we increase the strength of the spherical defect potential, λ_2, from 10 to 20, we see that ω_2 also crosses the ν axis which marks another bound state of this problem. We also have the plots of the bound state energies changing with respect to the parameters

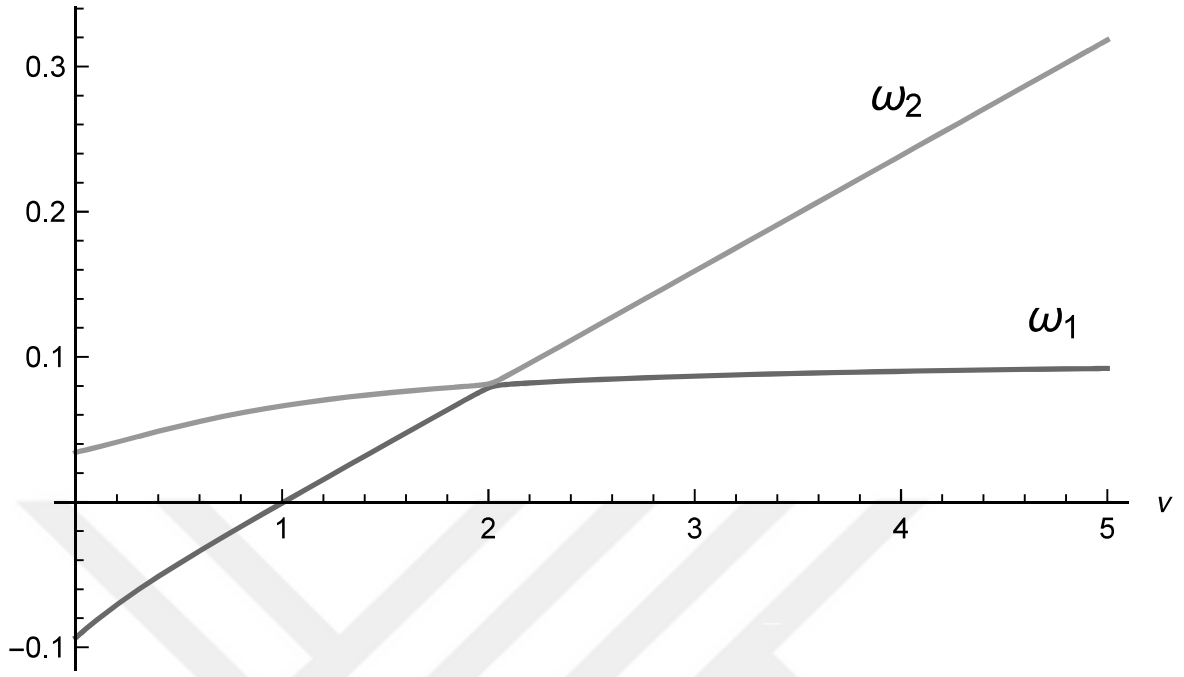

Figure 3.11. Eigenvalues of the principal matrix Φ versus ν, where $\lambda_2 = 10$, $a = 2$, $R = 1$, and $\mu = 1$.

R and a by numerically solving the zeroes of the eigenvalues ω_1 and ω_2 and these plots are given in Figure 3.13, 3.14 and Figure 3.15, 3.16.

3.2.2. Stationary Scattering Problem

Scattering state analysis of this case is investigated similarly with using the analytical continuation of Φ-matrix

$$\Phi(E) = \begin{pmatrix} \frac{1}{4\pi}(-ik-\mu) & -\frac{1}{4\pi aRk}e^{ika}\ \sin(kR) \\ -\frac{1}{4\pi aRk}e^{ika}\ \sin(kR) & \frac{1}{\lambda_2} - \frac{e^{ikR}}{4\pi R^2 k}\sin(kR) \end{pmatrix}, \qquad (3.2.14)$$

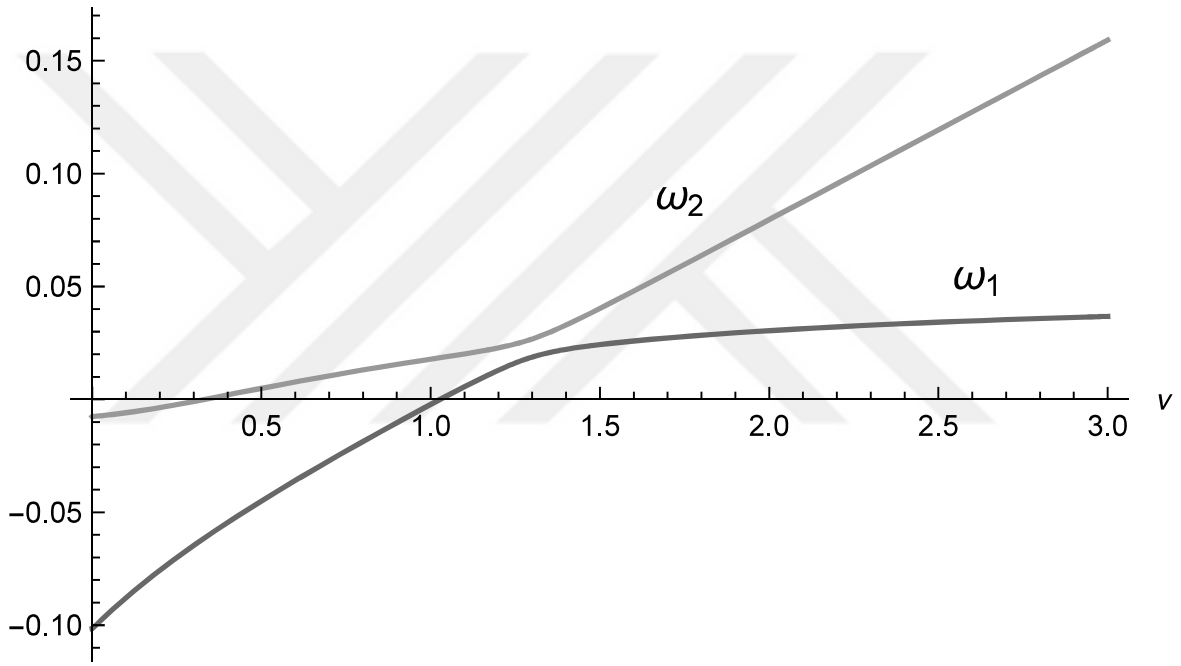

Figure 3.12. Eigenvalues of the principal matrix Φ versus ν, where $\lambda_2 = 20$, $a = 2$, $R = 1$, and $\mu = 1$.

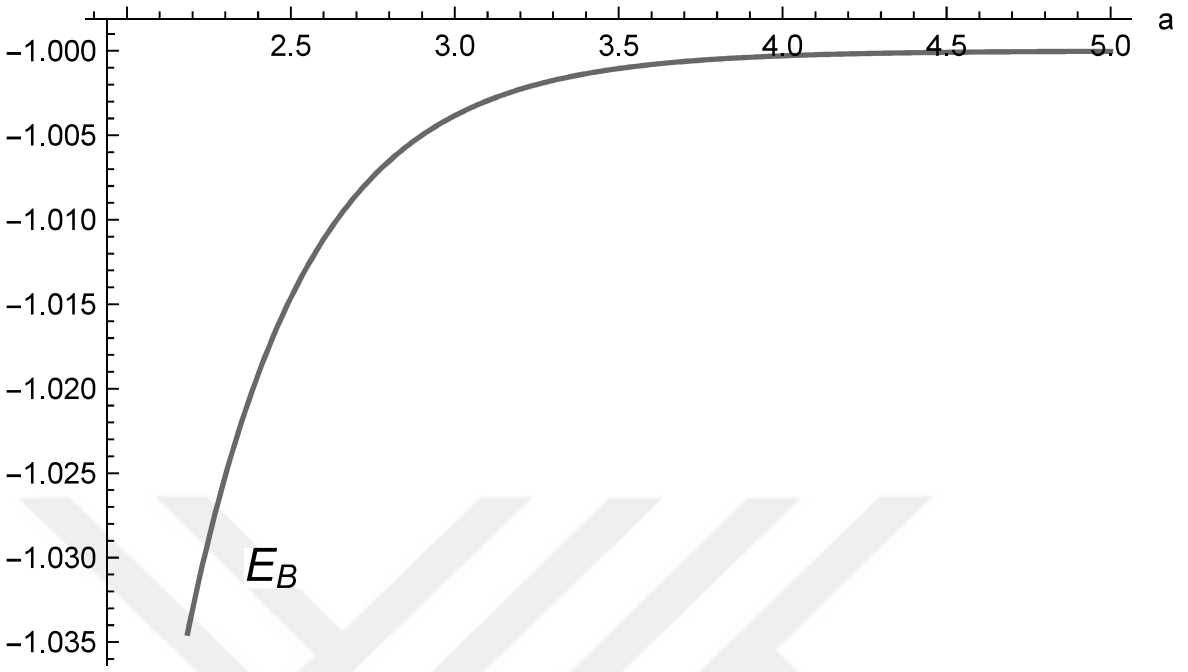

Figure 3.13. Ground state energy versus a, where $\lambda_2 = 20$, $R = 1$, $\mu = 1$.

and writing the T-matrix element as below

$$\langle \mathbf{k}'|T(E)|\mathbf{k}\rangle = -\sum_{i,j=1}^{2} \langle \mathbf{k}'|f_i\rangle \left(\Phi^{-1}(E)\right)_{ij} \langle f_j|\mathbf{k}\rangle = -\Bigg(e^{i(\mathbf{k}-\mathbf{k}')\cdot\mathbf{a}} \left(\Phi^{-1}(E)\right)_{11} + \frac{\left(e^{-i\mathbf{k}'\cdot\mathbf{a}} + e^{i\mathbf{k}\cdot\mathbf{a}}\right)\sin(kR)}{kR} \left(\Phi^{-1}(E)\right)_{12} + \frac{\sin^2(kR)}{k^2R^2} \left(\Phi^{-1}(E)\right)_{22} \Bigg) . \tag{3.2.15}$$

So we have the scattering amplitude expression from the formula

$$f(\mathbf{k} \to \mathbf{k}') = -\frac{1}{4\pi}\langle \mathbf{k}'|T(E)|\mathbf{k}\rangle \tag{3.2.16}$$

and the graph of the differential cross section $\frac{d\sigma}{d\Omega} = |f(\mathbf{k} \to \mathbf{k}')|^2$ as a function of θ which is given in Figure 3.17. In Figures 3.18 and 3.19, we have the plot of the differential cross section as a function of k for some fixed parameters except the strength of the spherical interaction. It can be seen in these graphs that the energy of the scattered wave gets more fluctuated as we increase the strength of the spherical interaction.

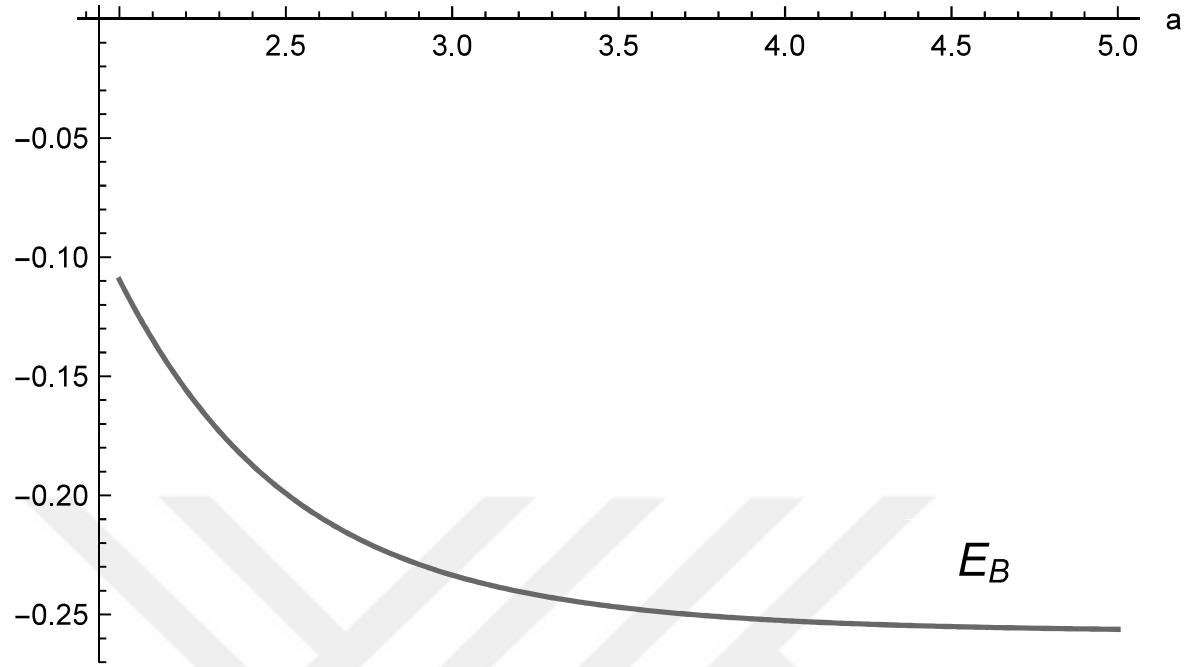

Figure 3.14. Excited state energy versus a, where $\lambda_2 = 20$, $R = 1$, $\mu = 1$.

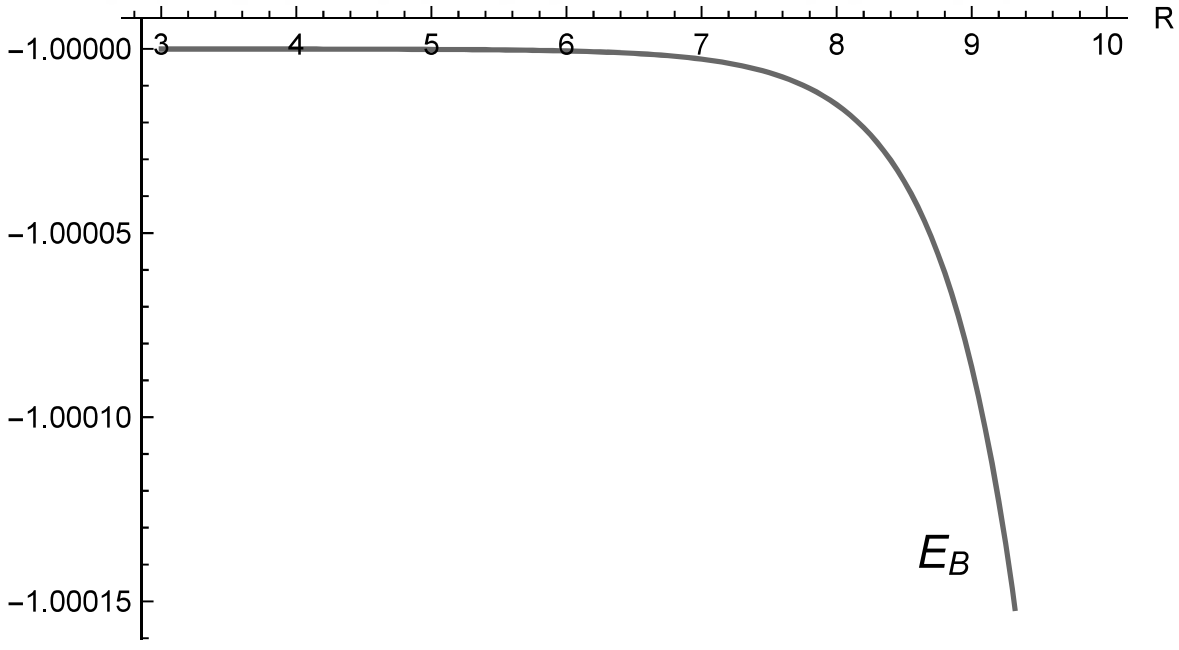

Figure 3.15. Ground state energy versus R, where $\lambda_2 = 150$, $a = 10.1$, $\mu = 1$.

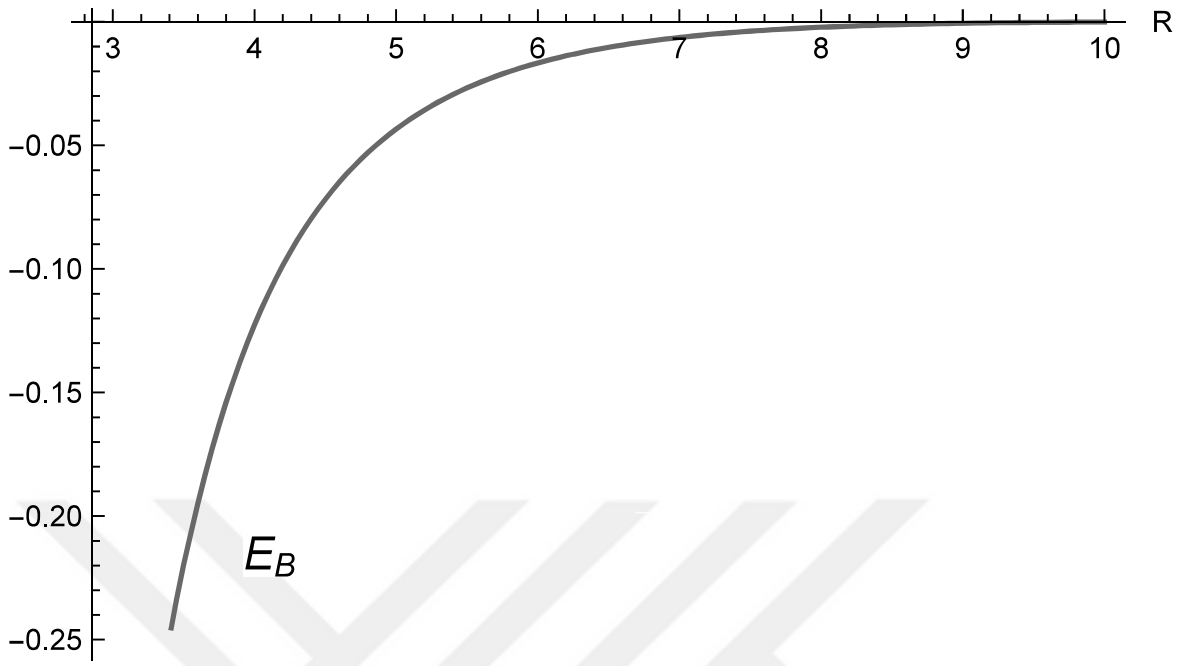

Figure 3.16. Excited state energy versus R, where $\lambda_2 = 150$, $a = 10.1$, $\mu = 1$.

3.3. Small Deformations of a Circle

In this section, we give the answer of the question how would bound state spectrum and scattering properties of such singular potentials change under small deformations of the support of these potentials. We will investigate the case of a deformed circle as demonstrated in Figure 3.20.

First, we define the normal deformations of a general curve in two dimensions. We consider a regular planar curve Γ parametrized with its arc length s which is finite. The Serret-Frenet equations that give the curvature properties for this curve, are given by

$$\frac{d\gamma}{ds} = \mathbf{t} \ , \qquad \frac{d\mathbf{t}}{ds} = \kappa \mathbf{n} \ , \qquad \text{and} \qquad \frac{d\mathbf{n}}{ds} = -\kappa \mathbf{t} \tag{3.3.1}$$

where $\mathbf{t}$ is the tangent vector to the curve Γ, $\mathbf{n}$ is the normal vector, and κ is the curvature of the curve [68]. The small deformation along a normal direction to Γ is

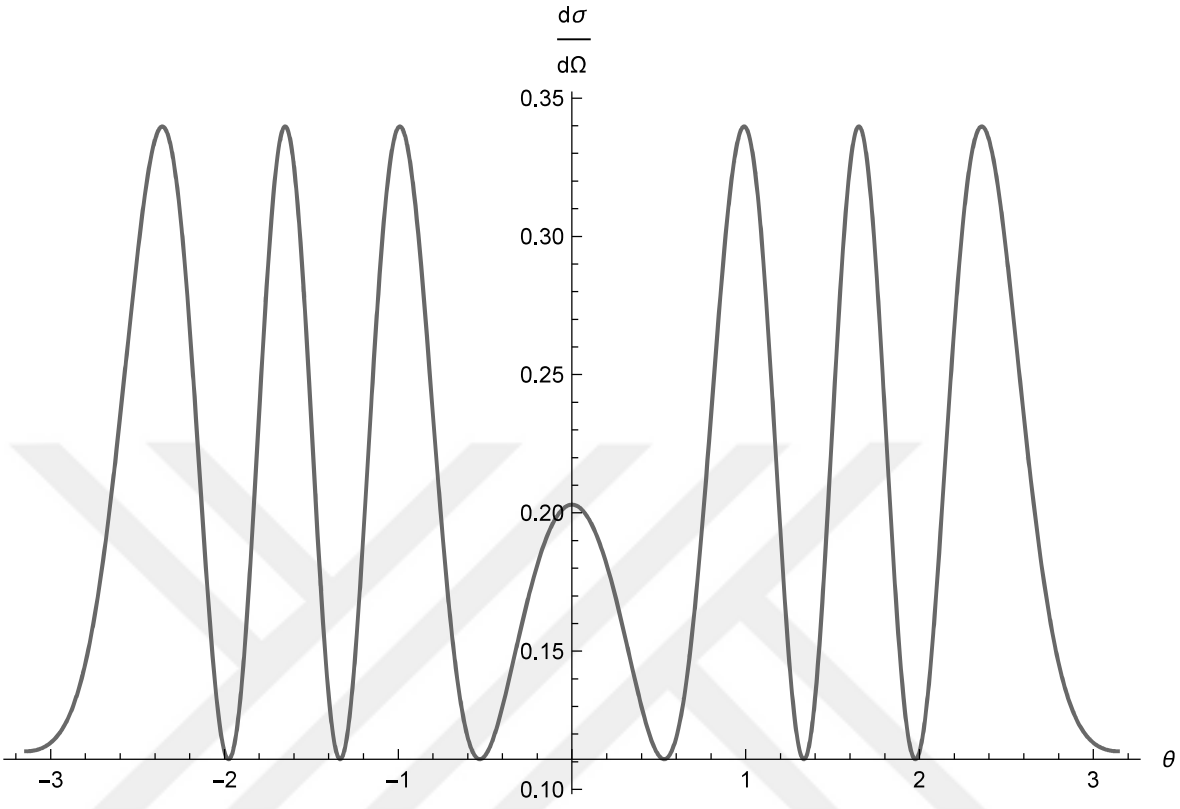

Figure 3.17. Differential cross section versus θ, where $k = 2$, $\lambda_2 = 10$, $a = 5$, $R = 1$, $\mu = 1$.

defined by

$$\tilde{\gamma}(s) = \gamma(s) + \epsilon h(s)\mathbf{n}(s) \,, \tag{3.3.2}$$

where h is assumed to be a smooth function of s. We note that ϵ here is a small deformation parameter, not the regularization parameter or the boundary condition

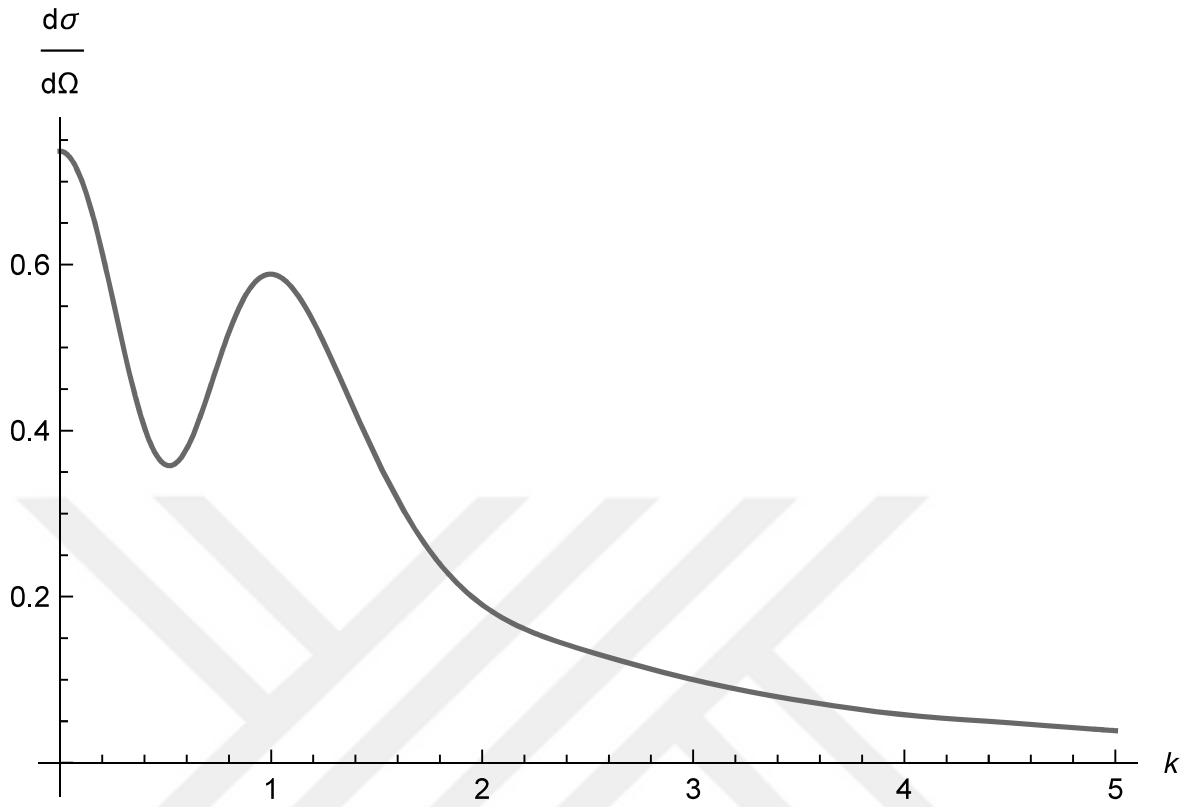

Figure 3.18. Differential cross section versus k, where $\theta = 0$, $\lambda_2 = 5$, $a = 2$, $R = 1$, $\mu = 1$.

used earlier in the text. The length of the deformed curve $\tilde{\Gamma}$ up to order ϵ is given by

$$\begin{aligned} L(\tilde{\Gamma}) &= \int_0^L \frac{d\tilde{s}}{ds}\, ds = \int_0^L \left(\frac{d\tilde{\gamma}}{ds} \cdot \frac{d\tilde{\gamma}}{ds}\right)^{1/2} ds \\ &= \int_0^L \left(\left(1 - \epsilon\kappa(s)\psi(s)\right)^2 + \epsilon^2 \left(\frac{dh(s)}{ds}\right)^2 \right)^{1/2} ds \\ &= \int_0^L \left(\left(1 - 2\epsilon\kappa(s)h(s)\right)^{1/2} + O(\epsilon^2) \right)\, ds \\ &= \int_0^L \left(1 - \epsilon\kappa(s)h(s) + O(\epsilon^2)\right)\, ds \\ &= L(\Gamma) - \epsilon \int_0^L \kappa(s)h(s)ds + O(\epsilon^2). \end{aligned} \tag{3.3.3}$$

If Γ is a circle of radius R, curvature of this circle is $\kappa = 1/R$. So the deformation can

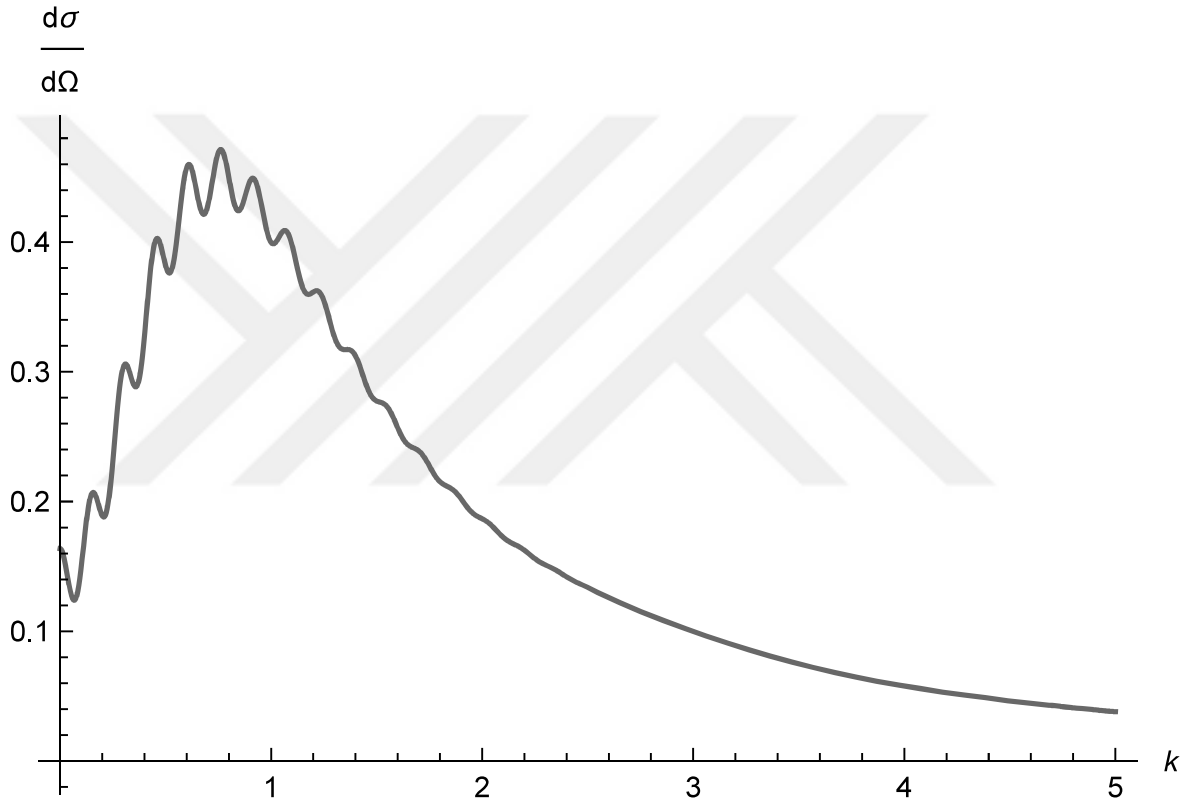

Figure 3.19. Differential cross section versus k, where $\theta = 0$, $\lambda_2 = 20$, $a = 2$, $R = 1$, $\mu = 1$.

be written as

$$L(\tilde{\Gamma}) = 2\pi R - \frac{\epsilon}{R}\int_0^L h(s)ds + O(\epsilon^2) \ . \tag{3.3.4}$$

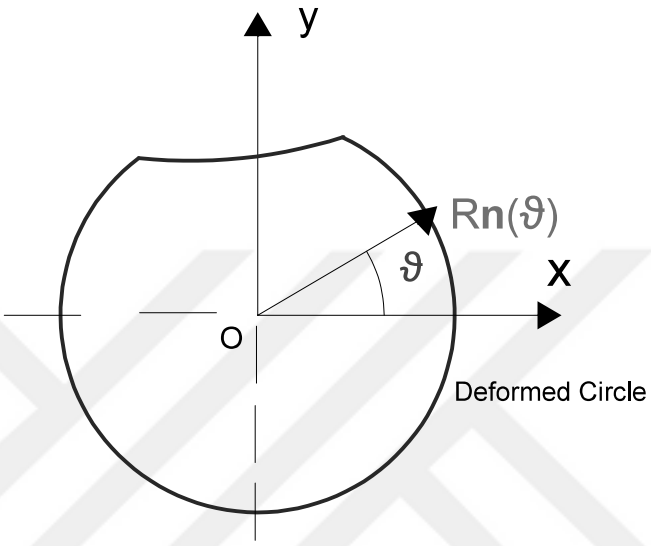

Figure 3.20. The deformed circle setup where $R\mathbf{n}(\theta)$ is the position vector of the circle defect.

3.3.1. Perturbative First Order Calculation of the Bound State Energy

Now we consider only a small deformation in the normal direction which indicates that the deformation function is a function of the angle only, i.e., $h(s) \to h(\theta)$. We will follow the earlier arguments about the resolvent operator. However, in this case, the Φ-matrix has only one term since there is only one singular potential. We can write the general resolvent operator of a deformed circular defect as

$$R(E) = R_0(E) + R_0(E)|\tilde{\Gamma}\rangle\frac{1}{\tilde{\Phi}(E)}\langle\tilde{\Gamma}|R_0(E) \ , \tag{3.3.5}$$

where we denote the deformation of the circle by $\tilde{\Gamma}$. For finding the bound state, we need to calculate

$$\tilde{\Phi}(-\nu^2) = \frac{1}{\lambda} - \langle\tilde{\Gamma}|R_0(-\nu^2)|\tilde{\Gamma}\rangle = \frac{1}{\lambda} - \int_{\mathbb{R}^2}\frac{\langle\tilde{\Gamma}|\mathbf{p}\rangle\langle\mathbf{p}|\tilde{\Gamma}\rangle}{p^2+\nu^2}\,\frac{d^2p}{(2\pi)^2} \tag{3.3.6}$$

where λ is the interaction strength of the deformed circle and we have used

$$\langle\tilde{\Gamma}|\mathbf{p}\rangle = \frac{1}{L(\tilde{\Gamma})}\int_0^L e^{i\mathbf{p}\cdot\tilde{\gamma}(s)}\,|\tilde{\gamma}^{'}(s)|\,ds\;, \tag{3.3.7}$$

[70], and

$$\tilde{\gamma}'(s) = \frac{d}{ds}\tilde{\gamma}(s) = \frac{d}{ds}\gamma(s) + \epsilon\frac{d}{ds}[h(s)\mathbf{n}(s)]\;. \tag{3.3.8}$$

Using (3.3.1), we can write

$$\left|\tilde{\gamma}'(s)\right| = \left|\mathbf{t} + \epsilon\frac{d}{ds}h(s)\mathbf{n} - \epsilon h(s)\mathbf{t}\right| = 1 - \frac{\epsilon}{R}h(s) + O(\epsilon^2) \tag{3.3.9}$$

where $\kappa = \frac{1}{R}$ and $\mathbf{t}\cdot\mathbf{n} = 0$, and we have also used the identity

$$e^{i\epsilon h(s)\mathbf{p}\cdot\mathbf{n}(s)} = 1 + i\epsilon h(s)\mathbf{p}\cdot\mathbf{n}(s)\;. \tag{3.3.10}$$

We obtain a result for $\langle\tilde{\Gamma}|\mathbf{p}\rangle$ by placing (3.3.8), (3.3.9) and (3.3.10) in (3.3.7). Putting this result in (3.3.6), taking $\gamma(s) \equiv \gamma(\theta)$ since the curve is a circle in our case and and after some algebra, we have the following expression for Φ:

$$\begin{aligned}\tilde{\Phi}(-\nu^2) =& \frac{1}{\lambda} - \frac{1}{(2\pi)^2}\left(1 + \frac{\epsilon}{\pi R}\int_0^{2\pi} h(\theta)d\theta\right)\left[\int_{\mathbb{R}^2}\left(\int_0^{2\pi}\int_0^{2\pi}\frac{e^{i\mathbf{p}\cdot(\gamma(\theta_1)-\gamma(\theta_2))}}{p^2+\nu^2}\right.\right.\\ &\times\left(1 - \frac{\epsilon}{R}(h(\theta_1)+h(\theta_2)) + i\epsilon((\mathbf{p}\cdot\mathbf{n}(\theta_1))h(\theta_1) - (\mathbf{p}'\cdot\mathbf{n}(\theta_2))h(\theta_2))\right)\\ &\left.\left.\times\, d\theta_1 d\theta_2\right)\right]\frac{d^2p}{(2\pi)^2} + O(\epsilon^2)\end{aligned} \tag{3.3.11}$$

where $\gamma(\theta)$ is the position vector of the circle defect. Next we calculate the first integral in the square bracket:

$$\int_{\mathbb{R}^2}\left(\int_0^{2\pi}\int_0^{2\pi}\frac{e^{i\mathbf{p}\cdot(\gamma(\theta_1)-\gamma(\theta_2))}}{p^2+\nu^2}d\theta_1 d\theta_2\right)\frac{d^2p}{(2\pi)^2}\;. \tag{3.3.12}$$

We can separately take the angular integrals

$$\int_0^{2\pi} e^{i\mathbf{p}\cdot\gamma(\theta_1)}d\theta_1 = 2\pi J_0(pR) \tag{3.3.13}$$

and we are left with the integration over the variable p only:

$$2\pi \int_0^\infty \frac{J_0^2(pR)}{p^2+\nu^2}\, p\, dp\ , \tag{3.3.14}$$

Thanks to the integral representation that can be found in [61]

$$\int_0^\infty \frac{x}{x^2+a^2} J_0^2(x)dx = I_0(a)K_0(a)\ , \tag{3.3.15}$$

we find

$$\int_{\mathbb{R}^2} \left(\int_0^{2\pi}\int_0^{2\pi} \frac{e^{i\mathbf{p}\cdot(\gamma(\theta_1)-\gamma(\theta_2))}}{p^2+\nu^2} d\theta_1 d\theta_2 \right) \frac{d^2p}{(2\pi)^2} = (2\pi) I_0(\nu R)K_0(\nu R) \tag{3.3.16}$$

for the first term of the bracket. For the second integral in equation (3.3.11), it is sufficient to consider the first term (the term with $h(\theta_1)$)

$$\int_{\mathbb{R}^2} \left(\int_0^{2\pi}\int_0^{2\pi} \frac{e^{i\mathbf{p}\cdot(\gamma(\theta_1)-\gamma(\theta_2))}}{p^2+\nu^2} h(\theta_1) d\theta_1 d\theta_2 \right) \frac{d^2p}{(2\pi)^2}\ . \tag{3.3.17}$$

This part a bit tricky and we need to be very careful with the angles. We should note that the angle between $\mathbf{p}$ and $\gamma(\theta_1)$ is not θ_1, let us call it ϕ. Since there is no θ_2 dependence of the deformation function h, θ_2 integral results as the Bessel function, $J_0(pR)$. Lastly, we need to calculate also the angle dependence in d^2p since the interaction between $\mathbf{p}$ and $\gamma(\theta_1)$ is not symmetric anymore, the wave sees an angle dependent deformation. Therefore, we need to write d^2p as $pdpd\phi$ and the ϕ integral brings another Bessel function, $J_0(pR)$. Writing these integrals more clearly we get

$$\begin{aligned}\int_0^\infty \left(\underbrace{\int_0^{2\pi} e^{i\mathbf{p}\cdot\gamma(\theta_1)} d\phi}_{2\pi J_0(pR)} \int_0^{2\pi} h(\theta_1) d\theta_1 \underbrace{\int_0^{2\pi} e^{-i\mathbf{p}\cdot\gamma(\theta_2)} d\theta_2}_{2\pi J_0(pR)} \right) \frac{1}{p^2+\nu^2}\frac{pdp}{(2\pi)^2} \\ = \int_0^\infty \frac{J_0^2(pR)}{p^2+\nu^2} pdp \int_0^{2\pi} h(\theta) d\theta\ .\end{aligned} \tag{3.3.18}$$

With the help of (3.3.15), the above integral becomes

$$I_0(\nu R)K_0(\nu R) \left(\int_{S^1} h(\theta) d\theta \right) \tag{3.3.19}$$

and this result is exactly the same for the term which is multiplied by $h(\theta_2)$ instead of $h(\theta_1)$ in equation (3.3.11).

Finally, last integral in (3.3.11) can be computed similarly. We will calculate the first term which includes $h(\theta_1)$. We first rewrite the exponential term as

$$i\mathbf{p}\cdot\mathbf{n}(\theta)e^{i\mathbf{p}\cdot\gamma(\theta)} = \frac{\partial}{\partial R}e^{i\mathbf{p}\cdot\gamma(\theta)} \ . \tag{3.3.20}$$

Since there is no other R dependence in the integral, we can take the derivative out and obtain

$$\int_{\mathbb{R}^2}\int_0^{2\pi} e^{-i\mathbf{p}\cdot\gamma(\theta_2)}\ d\theta_2\ \frac{\partial}{\partial R}\int_0^{2\pi}\frac{e^{i\mathbf{p}\cdot\gamma(\theta_1)}}{p^2+\nu^2}h(\theta_1)d\theta_1\frac{d^2p}{(2\pi)^2}\ . \tag{3.3.21}$$

The same arguments which mention that the angle between $\mathbf{p}$ and $\gamma(\theta_1)$ is not θ_1 are still valid for the angle variables in (3.3.21). We use the derivative relation between Bessel functions

$$\frac{dJ_0(x)}{dx} = -J_1(x) \tag{3.3.22}$$

and find the p integral as

$$\int_{\mathbb{R}^2}\int_0^{2\pi} e^{-i\mathbf{p}\cdot\gamma(\theta_2)}\ d\theta_2\ \frac{\partial}{\partial R}\int_0^{2\pi}\frac{e^{i\mathbf{p}\cdot\gamma(\theta_1)}}{p^2+\nu^2}h(\theta_1)d\theta_1\frac{d^2p}{(2\pi)^2} = -\int_0^\infty J_0(pR)J_1(pR)\,\frac{p^2}{p^2+\nu^2}\ dp\ . \tag{3.3.23}$$

Now, we rewrite the term

$$\frac{p^2}{p^2+\nu^2} \quad \text{as} \quad 1-\frac{\nu^2}{p^2+\nu^2}\ , \tag{3.3.24}$$

and using the formula (6.512) in [61] that is

$$\int_0^\infty J_\nu(\alpha x)J_{\nu-1}(\alpha x)dx = \frac{1}{2\alpha}\ , \tag{3.3.25}$$

and the formula (6.577) in [61] which is

$$\int_0^\infty \frac{J_0(pR)J_1(pR)}{p^2+\nu^2}dp = \frac{1}{\nu}I_1(\nu R)K_0(\nu R)\ , \tag{3.3.26}$$

we find:

$$\int_{\mathbb{R}^2}\left(\int_0^{2\pi}\int_0^{2\pi}\frac{e^{i\mathbf{p}\cdot(\gamma(\theta_1)-\gamma(\theta_2))}}{p^2+\nu^2}\,i\,(\mathbf{p}\cdot\mathbf{n}(\theta_1))h(\theta_1)d\theta_1 d\theta_2\right)\frac{d^2p}{(2\pi)^2}$$
$$=-\left(\frac{1}{2R}-\nu I_1(\nu R)K_0(\nu R)\right)\left(\int_0^{2\pi}h(\theta)d\theta\right)\ . \tag{3.3.27}$$

Combining (3.3.16), (3.3.19), and (3.3.27), we finally obtain

$$\tilde{\Phi}(-\nu^2)=\frac{1}{\lambda}-\frac{1}{2\pi}I_0(\nu R)K_0(\nu R)$$
$$+\frac{\epsilon}{2\pi^2}\left(-\frac{1}{2R}+\nu I_0(\nu R)K_1(\nu R)\right)\left(\int_0^{2\pi}h(\theta)d\theta\right)+O(\epsilon^2)\ , \tag{3.3.28}$$

where we have used the Wronskian relation of the modified Bessel fuctions:

$$I_1(x)K_0(x)+I_0(x)K_1(x)=\frac{1}{x}\ . \tag{3.3.29}$$

When there is no deformation ($\epsilon=0$), to find the bound state energy we simply take $\Phi=0$ and see that we have only one bound state. This can be shown by simply expressing the second term $I_0(\nu R)K_0(\nu R)$ using its integral representation (3.3.15):

$$\frac{1}{\lambda}=\frac{1}{2\pi}I_0(\nu R)K_0(\nu R)=\frac{1}{2\pi}\int_0^\infty\frac{x}{x^2+\nu^2R^2}J_0^2(x)dx\ . \tag{3.3.30}$$

and then by taking the derivative of the right hand side with respect to ν under the integral sign. We see that the integrand and Φ itself is a decreasing function of ν for given parameters λ and R. Therefore, we can say that there is a unique solution of the equation (3.3.28), let us say ν_*.

At this point, it is remarkable that small deformations satisfying the symmetry $\int_0^{2\pi}h(\theta)d\theta=0$ do not change the bound state energies up to first order in ϵ.

In [60, 69] a general formula for perturbations of eigenvalues for small perturbations of the principal matrix Φ was derived, here we have a one-dimensional version of this formula. Let $\nu=\nu_*+\epsilon\nu_1+O(\epsilon^2)$, where ν_* denotes the bound state energy of

the original unperturbed circle case. Then, we see that the bound state energy

$$E_B = -(\nu_* + \epsilon\nu_1)^2 = -\nu_*^2 - 2\epsilon\nu_*\nu_1 \tag{3.3.31}$$

for the deformed circular defect can be found by the zeroes of the perturbed principal matrix, $\tilde{\Phi}$. We basically replace ν with perturbed bound state energy, E_B and keep the terms up to order ϵ

$$\begin{aligned}&\frac{1}{\lambda} - \frac{1}{2\pi} I_0((\nu_* + \epsilon\nu_1)R) K_0((\nu_* + \epsilon\nu_1)R) \\ &- \frac{\epsilon}{2\pi^2}\left(\frac{1}{2R} - (\nu_* + \epsilon\nu_1) I_0((\nu_* + \epsilon\nu_1)R) K_1((\nu_* + \epsilon\nu_1)R)\right)\left(\int_0^{2\pi} h(\theta)d\theta\right) = 0\ .\end{aligned} \tag{3.3.32}$$

We Taylor expand this expression around $\epsilon\nu_1 R$. We see that there is no contribution coming from the term with the derivative of the $K_1(\nu_* R)$ since it is of order of ϵ and then we get

$$\begin{aligned}&\left[I_0(\nu_* R) + \epsilon\nu_1 R\ I_0'(\nu_* R)\right]\ \left[K_0(\nu_* R) + \epsilon\nu_1 R\ K_0'(\nu_* R)\right] = \\ &I_0(\nu_* R) K_0(\nu_* R) - \epsilon\nu_1 R\ I_0(\nu_* R) K_1(\nu_* R) + \epsilon\nu_1 R I_1(\nu_* R) K_0(\nu_* R)\end{aligned} \tag{3.3.33}$$

where we have used $I_0'(z) = I_1(z)$ and $K_0'(z) = -K_1(z)$. Putting (3.3.33) back into (3.3.32), we find

$$\begin{aligned}&\frac{1}{\lambda} - \frac{1}{2\pi} I_0(\nu_* R) K_0(\nu_* R) + \frac{\epsilon\nu_1 R}{2\pi}\ I_0(\nu_* R) K_1(\nu_* R) - \frac{\epsilon\nu_1 R}{2\pi} I_1(\nu_* R) K_0(\nu_* R) \\ &- \frac{\epsilon}{2\pi^2}\left(\frac{1}{2R} - \nu_* I_0(\nu_* R) K_1(\nu_* R)\right)\left(\int_0^{2\pi} h(\theta)d\theta\right) = 0\ .\end{aligned} \tag{3.3.34}$$

Here, we see that the zeroth order term in ϵ cancels out $\frac{1}{\lambda}$. We extract ν_1 from this equation, replace it in E_B, and obtain

$$E_B = -\nu_*^2 - \epsilon\,\frac{2\nu_*}{\pi R}\frac{\left(\frac{1}{2R} - \nu_* I_0(\nu_* R) K_1(\nu_* R)\right)}{I_1(\nu_* R) K_0(\nu_* R) - I_0(\nu_* R) K_1(\nu_* R)}\left(\int_0^{2\pi} h(\theta)d\theta\right) + O(\epsilon^2)\ , \tag{3.3.35}$$

which can be further simplified into

$$E_B = -\nu_*^2 - \epsilon \frac{\nu_*^2}{\pi R} \left(\int_0^{2\pi} h(\theta) d\theta \right) + O(\epsilon^2) \ . \tag{3.3.36}$$

The correction to the bound state energy in the first order of ϵ seems very important and gives a clue about the geometric interpretation of this problem: Let us suppose that we consider a circle with radius $R - \epsilon R_1$ instead of the original circle with radius R. Let the perturbation to the radius be defined as

$$\epsilon R_1 = \frac{1}{2\pi R} \int_0^{2\pi} \epsilon \ h(\theta) R d\theta \tag{3.3.37}$$

where the normal vector that appears in the curvature in our parametrization is inward. We replace ν with $\nu_* + \epsilon R_1$ and R with $R - \epsilon R_1$ in equation (3.3.30) and get

$$\frac{1}{\lambda} - \frac{1}{2\pi} I_0((\nu_* + \epsilon\nu_1)(R - \epsilon R_1)) K_0((\nu_* + \epsilon\nu_1)(R - \epsilon R_1)) = 0 \ . \tag{3.3.38}$$

We find the relation $R\nu_1 = \nu_* R_1$ when we expand all the terms to the first order of ϵ. On the other hand, if we use the equation

$$E_B = -(\nu_* + \epsilon\nu_1)^2 = -\nu_*^2 - 2\epsilon\nu_*\nu_1 \ , \tag{3.3.39}$$

we obtain exactly the same result. Subsequently, we state this observation as following: A small deformation in the normal direction of a given circle, which supports an attractive delta function, leads to a perturbation of the original bound state energy. This perturbative change of the energy can be obtained up to first order in the perturbation parameter as follows: increase the initial radius by an amount equal to the average of the deformation over the given circle, then compute the first order perturbation of the bound state energy corresponding to this new circle with the same coupling constant. So we conclude that, in the case of a small deformation, we can consider the problem as a delta function supported on the original circle plus a series of perturbations.

It would be interesting to take these analysis to the second order in ϵ and see if there is any geometric interpretation of the result. At the moment the calculations seem to be rather lengthy.

We can numerically plot the bound state energy E_B of the deformed circular defect as a function of R with fixed values of λ for a particular deformation. We choose the deformation function to be as $h(\theta) = \sin^2\theta$ which is an easily integrable function. With this deformation, we can plot how the bound state energy E_B changes with respect to R numerically with the help of Mathematica, as shown in Figure 3.21. The principal matrix of the deformed circle, $\tilde{\Phi}$, demonstrates a decreasing function of

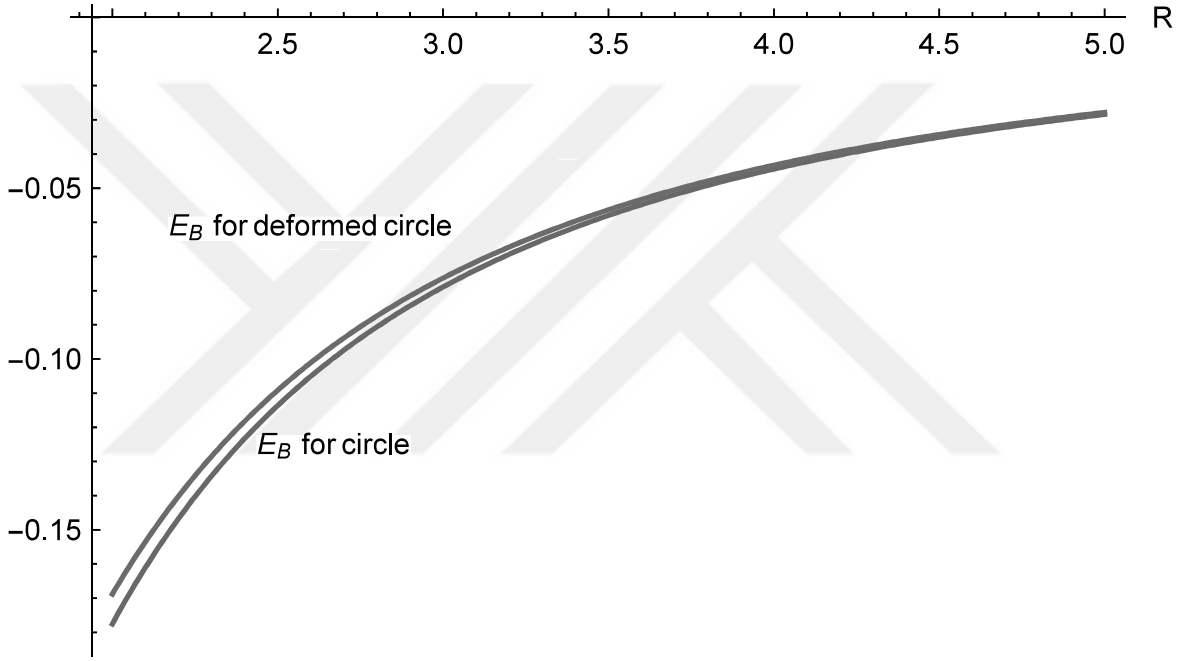

Figure 3.21. Bound state energy for the circular defect and for the first order perturbative result of the deformed circle defect versus R, where $\epsilon = 0.1$, $\lambda = 10$.

λ for all $\nu > 0$ which means that the bound state energies also decrease with increasing interaction strength λ, as expected.

3.3.2. Perturbative First Order Stationary Scattering Problem

Now we use analytical continuation of $\tilde{\Phi}$, i.e., taking ν to ik, to see the scattering behaviour of the deformed circle. When we evaluate $\tilde{\Phi}(E)$ in terms of the variable

$k > 0$, we get

$$\tilde{\Phi}(E) = \frac{1}{\lambda} - \frac{i}{4} J_0(kR) H_0^{(1)}(kR) + \frac{\epsilon}{2\pi^2}\left(-\frac{1}{2R} + \frac{i\pi k}{2} J_0(kR) H_1^{(1)}(kR)\right)\left(\int_0^{2\pi} h(\theta) d\theta\right) + O(\epsilon^2) \tag{3.3.40}$$

where $E = k^2$. We take θ' to be the angle between $\mathbf{k}'$ and $\mathbf{k}$, $\mathbf{k}$ being the momentum vector of the incoming particle which is chosen to be parallel to the x axis for simplicity. Then,

$$\langle \mathbf{k}' | \tilde{\Gamma} \rangle = J_0(kR) - \frac{\epsilon}{2\pi R} \int_0^{2\pi} e^{-ikR\cos(\theta - \theta')} h(\theta) d\theta - \frac{ik\epsilon}{2\pi} \int_0^{2\pi} e^{-ikR\cos(\theta-\theta')} \cos(\theta - \theta') h(\theta) d\theta + J_0(kR) \frac{\epsilon}{2\pi R} \int_0^{2\pi} h(\theta) d\theta + O(\epsilon^2) \, . \tag{3.3.41}$$

Hence, placing (3.3.40) and (3.3.41) in (3.1.28), the scattering amplitude of the deformed circle is given by

$$\begin{aligned}
\tilde{f}(\mathbf{k} \to \mathbf{k}') &= \frac{1}{4}\sqrt{\frac{2}{\pi k}} \langle \mathbf{k}' | \tilde{\Gamma} \rangle (\tilde{\Phi}(E))^{-1} \langle \tilde{\Gamma} | \mathbf{k} \rangle \\
&= \frac{1}{4}\sqrt{\frac{2}{\pi k}} \left(\frac{1}{\lambda} - \frac{i}{4} J_0(kR) H_0^1(kR)\right)^{-1} \\
&\times \Bigg[J_0^2(kR) + \epsilon \Bigg(\frac{1}{\pi R} \, J_0^2(kR) \int_0^{2\pi} h(\theta) d\theta \\
&- J_0(kR) \int_0^{2\pi} \left[e^{-ikR\cos(\theta-\theta')}(1 + ikR\cos(\theta - \theta')) \right. \\
&\left. + e^{ikR\cos(\theta)}(1 - ikR\cos(\theta)) \right] h(\theta) \frac{d\theta}{2\pi R} \\
&+ J_0^2(kR) \left(\frac{1}{\lambda} - \frac{i}{4} J_0(kR) H_0^{(1)}(kR)\right)^{-1} \\
&\times \left(\frac{1}{2\pi R} - \frac{ik}{2} J_0(kR) H_1^{(1)}(kR)\right) \frac{1}{2\pi} \int_0^{2\pi} h(\theta) d\theta \Bigg) \Bigg] + \mathcal{O}(\epsilon^2) \, .
\end{aligned} \tag{3.3.42}$$

Finally, using this result, we plot the differential cross sections as a function of k for the circular defect and deformed circular defect for the particular deformation $h(\theta) = \sin^2\theta$ in Figure 3.22.

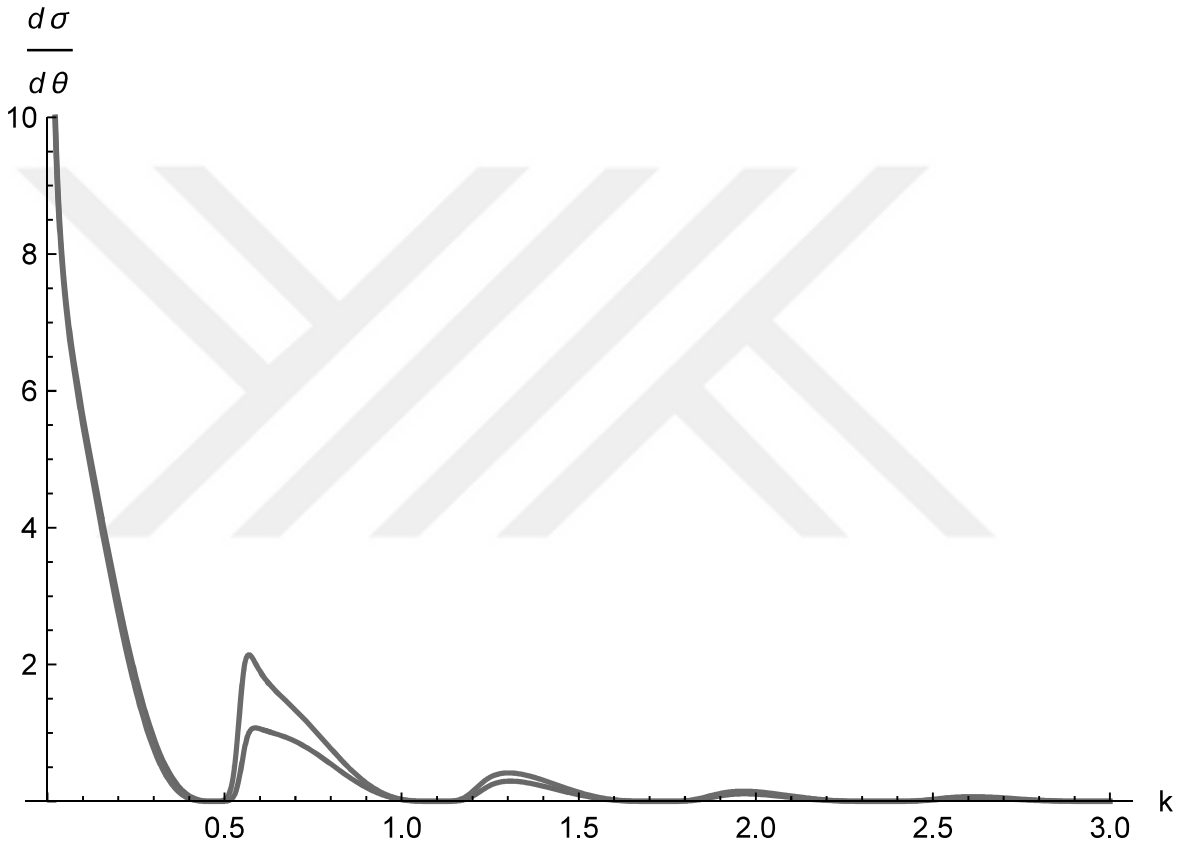

Figure 3.22. Differential cross sections as a function of k from a circular defect and deformed circular defect (red curve), where $h(\theta) = \sin^2\theta$, $R = 5$, $\lambda = 40$, $\epsilon = 0.1$.

3.4. Small Deformations of a Sphere

In this section, we consider deforming a sphere S^2 centered at the origin with radius R, as pictured in Figure 3.23. We perturb the original shell with $\tilde{\Sigma}$ which is the

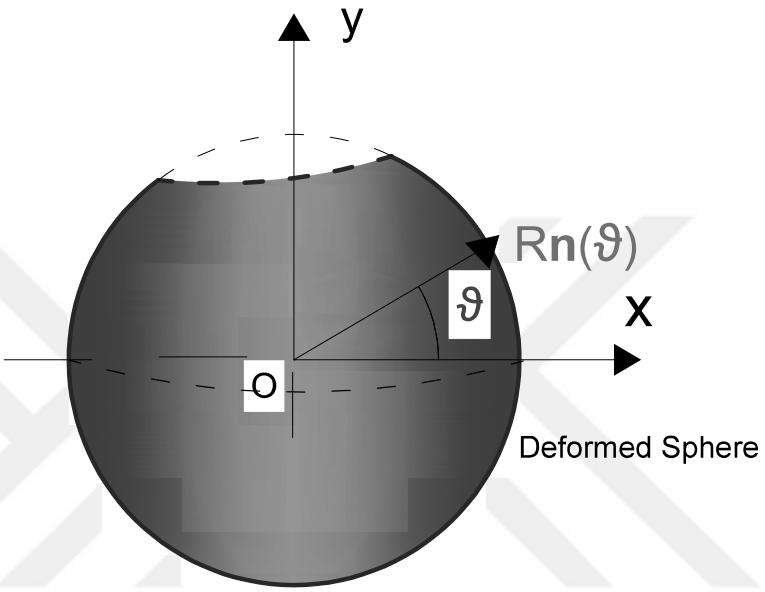

Figure 3.23. The deformed sphere setup where $R\mathbf{n}(\theta)$ is the position vector of the spherical defect.

small deformation along the sphere's normal direction. The location of the deformed shell is defined by

$$\tilde{\sigma}(\theta,\phi) := \sigma(\theta,\phi) + \epsilon h(\theta,\phi)\mathbf{N}(\theta,\phi)\ , \tag{3.4.1}$$

where ϵ is again a small deformation parameter, $\mathbf{N}$ is the normal vector of the sphere, and h is a smooth deformation function on the sphere. If $|\epsilon|$ is sufficiently small, it is well-known that the deformed sphere $\tilde{\Sigma}$ is a regular surface [70] and its surface area up to order ϵ is given by

$$A(\tilde{\Sigma}) = A(\Sigma) - 2\epsilon \int_0^{2\pi}\int_0^{\pi} H(\theta,\phi)h(\theta,\phi)R^2\sin\theta d\theta d\phi + O(\epsilon^2)\ , \tag{3.4.2}$$

where H is the mean curvature of the sphere. In our case H is a constant which is $1/R$, so it will be taken out of the integral in (3.4.2). We will write the solid angle

as $d\Omega$ instead of $\sin\theta d\theta d\phi$ for notational simplification and Ω as the argument of the functions on the sphere.

We express the resolvent operator for this case as below

$$R(E) = R_0(E) + R_0(E)|\tilde{\Sigma}\rangle\tilde{\Phi}^{-1}(E)\langle\tilde{\Sigma}|R_0(E)\ , \tag{3.4.3}$$

where the principal matrix has the form

$$\tilde{\Phi}(E) = \frac{1}{\lambda} - \langle\tilde{\Sigma}|R_0(E)|\tilde{\Sigma}\rangle\ . \tag{3.4.4}$$

3.4.1. Perturbative First Order Calculation of the Bound State Energy

For the bound state analysis, we use the expressions given in (3.3.7), (3.3.8), (3.3.9), and (3.3.10) analogously to construct $\tilde{\Phi}(E)$ as

$$\begin{aligned}
\tilde{\Phi}(E) &= \frac{1}{\lambda} - \langle\tilde{\Sigma}|R_0(E)|\tilde{\Sigma}\rangle \\
&= \frac{1}{\lambda} - \frac{1}{(4\pi)^2}\left(1 + \frac{\epsilon}{\pi R}\int_{S^2} h(\Omega)d\Omega\right)\Bigg[\int_{\mathbb{R}^3}\left(\int_{S^2\times S^2} e^{i\mathbf{p}\cdot(\sigma(\Omega)-\sigma(\Omega'))}d\Omega d\Omega'\right) \\
&\times \frac{1}{p^2+\nu^2}\frac{d^3p}{(2\pi)^3} + \epsilon\Bigg(2\int_{\mathbb{R}^3}\left(\int_{S^2\times S^2} e^{i\mathbf{p}\cdot(\sigma(\Omega)-\sigma(\Omega'))}(i\mathbf{p}\cdot\mathbf{N}(\Omega))\,h(\Omega)\,d\Omega d\Omega'\right) \\
&\times \frac{1}{p^2+\nu^2}\frac{d^3p}{(2\pi)^3} \\
&- \frac{4}{R}\int_{\mathbb{R}^3}\left(\int_{S^2\times S^2} e^{i\mathbf{p}\cdot(\sigma(\Omega)-\sigma(\Omega'))}h(\Omega)\,d\Omega d\Omega'\right)\frac{1}{p^2+\nu^2}\frac{d^3p}{(2\pi)^3}\Bigg)\Bigg] + O(\epsilon^2)
\end{aligned} \tag{3.4.5}$$

where $\sigma(\Omega)$ is the position vector of the spherical defect. These integrals can be calculated similarly to the deformed circle case. We have already computed the integral which gives the second diagonal term in equation (3.2.13) and found

$$\begin{aligned}
\langle\Sigma|R_0(-\nu^2)|\Sigma\rangle &= \frac{1}{(4\pi)^2}\int_{\mathbb{R}^3}\left(\int_{S^2\times S^2} e^{i\mathbf{p}\cdot(\sigma(\Omega)-\sigma(\Omega'))}d\Omega d\Omega'\right)\frac{1}{p^2+\nu^2}\frac{d^3p}{(2\pi)^3} \\
&= \frac{1}{4\pi R}K_{1/2}(\nu R)I_{1/2}(\nu R)\ .
\end{aligned} \tag{3.4.6}$$

We will use the derivative equation

$$(i\mathbf{p}\cdot\mathbf{N}(\Omega))\, e^{i\mathbf{p}\cdot\sigma(\Omega)} = \frac{\partial}{\partial R} e^{i\mathbf{p}\cdot\sigma(\Omega)} \tag{3.4.7}$$

for the second term. The exponential factors can be expressed in terms of the spherical Bessel functions of the first kind and spherical harmonics using the well-known expansion of plane waves in terms of the spherical harmonics [71]:

$$e^{i\mathbf{p}\cdot\sigma(\Omega)} = 4\pi \sum_{l=0}^{\infty} \sum_{m=-l}^{l} i^l j_l(pR) Y^*_{lm}(\Omega_p) Y_{lm}(\Omega)\ . \tag{3.4.8}$$

Here Ω_p and Ω are the polar angles of the vector $\mathbf{p}$ and σ, respectively. Using (3.4.7) and (3.4.8), we obtain

$$\begin{aligned}
&\int_{\mathbb{R}^3} \left(\int_{S^2\times S^2} e^{i\mathbf{p}\cdot(\sigma(\Omega)-\sigma(\Omega'))} (i\mathbf{p}\cdot\mathbf{N}(\Omega))\, h(\Omega)\, d\Omega d\Omega' \right) \frac{1}{p^2+\nu^2} \frac{d^3p}{(2\pi)^3} \\
&= (4\pi)^2 \int_0^{\infty} \int_{S^2} \left(\int_{S^2\times S^2} \sum_{l=0}^{\infty} \sum_{m=-l}^{l} i^l \frac{\partial j_l(pR)}{\partial R} Y^*_{lm}(\Omega_p) Y_{lm}(\Omega) h(\Omega) \right. \\
&\left. \times \sum_{l'=0}^{\infty} \sum_{m'=-l}^{l} (-i)^{l'} \frac{\partial j_{l'}(pR)}{\partial R} Y_{l'm'}(\Omega_p) Y^*_{l'm'}(\Omega') d\Omega d\Omega' \right) \frac{d\Omega_p p^2 dp}{(2\pi)^3}\ .
\end{aligned} \tag{3.4.9}$$

By the orthonormality relation of the spherical harmonics,

$$\int_{S^2} Y_{lm}(\Omega) Y_{l'm'}(\Omega) d\Omega = \delta_{ll'}\delta_{mm'}\ , \tag{3.4.10}$$

integrations over Ω_p and Ω' of the left-hand side of equation (3.4.9) lead to

$$\begin{aligned}
&\int_{\mathbb{R}^3} \left(\int_{S^2\times S^2} e^{i\mathbf{p}\cdot(\sigma(\Omega)-\sigma(\Omega'))} (i\mathbf{p}\cdot\mathbf{N}(\Omega))\, h(\Omega)\, d\Omega d\Omega' \right) \frac{1}{p^2+\nu^2} \frac{d^3p}{(2\pi)^3} \\
&= \frac{(4\pi)^2}{(2\pi)^3} \int_0^{\infty} j_0(pR)(-j_1(pR)) \frac{p^3}{p^2+\nu^2} dp \left(\int_{S^2} h(\Omega) d\Omega \right)\ ,
\end{aligned} \tag{3.4.11}$$

where we make use of $Y_{00}(\Omega) = 1/\sqrt{4\pi}$ and the identity

$$\frac{dj_0(x)}{dx} = -j_1(x)\ . \tag{3.4.12}$$

Replacing spherical Bessel's by the Bessel functions of the first kind according to

$$j_l(x) = \sqrt{\frac{\pi}{2x}} J_{l+1/2}(x)\ , \tag{3.4.13}$$

and decomposing

$$\frac{p^2}{p^2+\nu^2} = 1 - \frac{\nu^2}{p^2+\nu^2} \tag{3.4.14}$$

we obtain [61]

$$\int_0^\infty J_{1/2}(pR)J_{3/2}(pR)dp = \frac{1}{2R}\,, \tag{3.4.15}$$

$$\int_0^\infty J_{3/2}(pR)J_{1/2}(pR)\frac{dp}{p^2+\nu^2} = \frac{1}{\nu}I_{3/2}(\nu R)K_{1/2}(\nu R)\,. \tag{3.4.16}$$

Using the results given in (3.4.15) and (3.4.16), we get

$$\int_{\mathbb{R}^3}\left(\int_{S^2\times S^2} e^{i\mathbf{p}\cdot(\sigma(\Omega)-\sigma(\Omega'))}(i\mathbf{p}\cdot\mathbf{N}(\Omega))\,h(\Omega)\,d\Omega d\Omega'\right)\frac{1}{p^2+\nu^2}\frac{d^3p}{(2\pi)^3}$$
$$= -\frac{1}{R}\left(\int_{S^2} h(\Omega)d\Omega\right)\left(\frac{1}{2R} - \nu K_{1/2}(\nu R)I_{3/2}(\nu R)\right)\,. \tag{3.4.17}$$

Following similar arguments, we can find the result of the last integral of the equation (3.4.5) as

$$\int_{\mathbb{R}^3}\left(\int_{S^2\times S^2} e^{i\mathbf{k}\cdot(\sigma(\Omega)-\sigma(\Omega'))}h(\Omega)\,d\Omega d\Omega'\right)\frac{1}{k^2+\nu^2}\frac{d^3k}{(2\pi)^3}$$
$$= \frac{2}{R}K_{1/2}(\nu R)I_{1/2}(\nu R)\left(\int_{S^2} h(\Omega)d\Omega\right)\,. \tag{3.4.18}$$

Combining the results in equations (3.4.6), (3.4.17) and (3.4.18), we obtain

$$\tilde{\Phi}(-\nu^2) = \frac{1}{\lambda} - \frac{1}{4\pi R}I_{1/2}(\nu R)K_{1/2}(\nu R)$$
$$+\ \frac{\epsilon}{8\pi^2 R}\left(-\frac{1}{2R} + \nu I_{1/2}(\nu R)K_{3/2}(\nu R)\right)\left(\int_{S^2} h(\Omega)d\Omega\right)\,, \tag{3.4.19}$$

where we make use of the Wronskian relation $I_{1/2}(x)K_{3/2}(x) + I_{3/2}(x)K_{1/2}(x) = 1/x$ again.

We notice that the formula for the function $\tilde{\Phi}$ is very similar to the one obtained for the deformed circular defect case, however there is a difference. The eigenvalue flow can be obtained again by first considering the unperturbed case, $\epsilon = 0$ and $\tilde{\Phi} = 0$ and then writing $I_{1/2}(\nu R)K_{1/2}(\nu R)$ in its integral form:

$$\frac{1}{\lambda} = \frac{1}{4\pi R}I_{1/2}(\nu R)K_{1/2}(\nu R) = \frac{1}{4\pi R}\int_0^\infty \frac{x}{x^2+\nu^2R^2}J_{1/2}^2(x)dx\,. \tag{3.4.20}$$

As we take the derivative of the right hand side of the above equation with respect to ν, we see that it is a decreasing function of ν for given parameters λ and R. However, the product $I_{1/2}(\nu R)K_{1/2}(\nu R)$ is finite as $\nu \to 0^+$, so there may not always be a solution if λ is small enough. But if there is a solution then it is unique. To see how would the bound state energy change if we perturb the bound state solution by some small term, let us assume that there is a bound state solution ν as

$$\nu = \nu_* + \epsilon\nu_1 + O(\epsilon^2) \ . \tag{3.4.21}$$

Then the bound state energy up to order ϵ can be found by solving the zeroes of $\tilde{\Phi}$ by expanding terms around $\nu = \nu_*$. Therefore, we find

$$\begin{aligned} E_B = &- \nu_*^2 - \epsilon\,\nu_*^2 \\ &\times \left(\frac{\frac{1}{2\nu_* R} - I_{1/2}(\nu_* R)K_{3/2}(\nu_* R)}{I_{3/2}(\nu_* R)K_{1/2}(\nu_* R) - I_{1/2}(\nu_* R)K_{3/2}(\nu_* R) + \frac{1}{\nu_* R} I_{1/2}(\nu_* R)K_{1/2}(\nu_* R)} \right) \\ &\times \left(\frac{1}{\pi R} \int_{S^2} h(\Omega) d\Omega \right) + O(\epsilon^2) \ . \end{aligned} \tag{3.4.22}$$

Looking at this result, we see that this result has the same geometric interpretation as in the case of circle: We replace the original sphere with another sphere of slightly different radius $R - \epsilon R_1$, with

$$R_1 = \frac{1}{4\pi R^2} \int_{S^2} h(\Omega) R^2 d\Omega \tag{3.4.23}$$

and then look for the small change in the bound state energy because of this shrinking of the sphere. Therefore, we can summarize our observation once more for the spherical shell case: A small deformation in the normal direction of a given sphere, which supports an attractive delta function, leads to a perturbation of the original bound state energy, to first order the resulting change can be obtained as follows: increase the initial radius by an amount equal to the average of the deformation over the given sphere, then compute the first order perturbation of the bound state energy corresponding to this new sphere with the same coupling constant.

Again, for a special deformation function such as $h(\theta) = \sin\theta$, we numerically plot how the bound state energies change with respect to R for a given λ, as shown in

Figure 3.24.

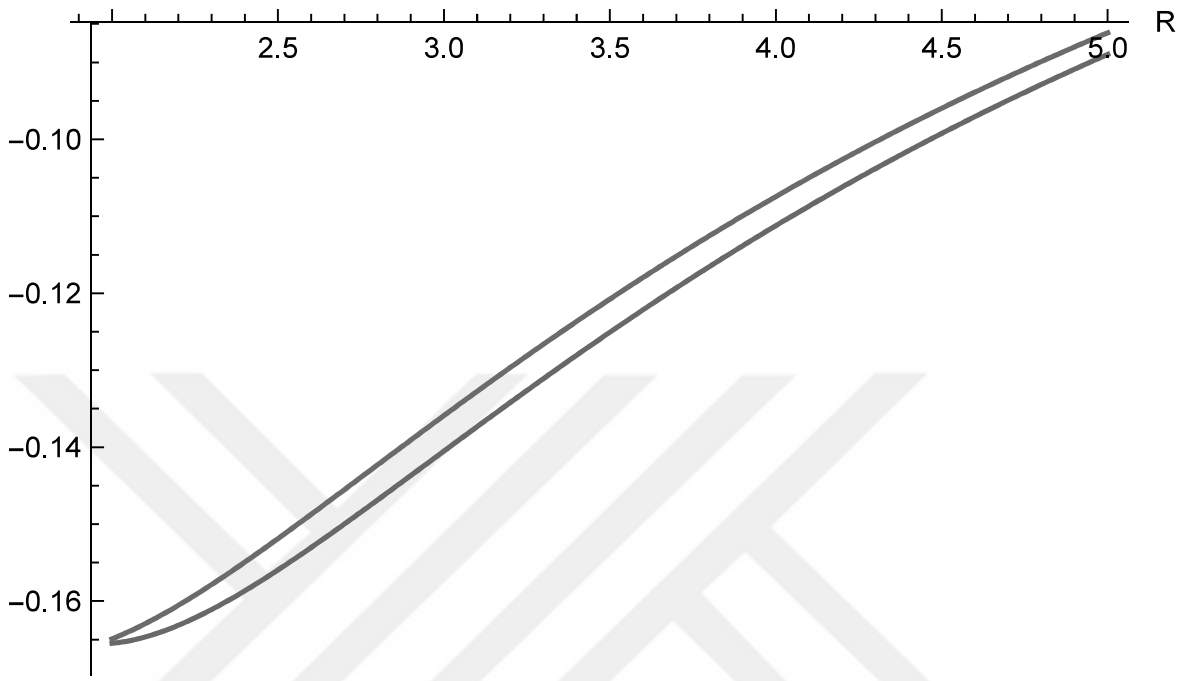

Figure 3.24. Bound state energy for the spherical defect and for the deformed spherical defect (red curve) versus R, where $\epsilon = 0.1$, $\lambda = 10$.

3.4.2. Perturbative First Order Stationary Scattering Problem

We use another analytical continuation of the function $\tilde{\Phi}$ and obtain

$$\tilde{\Phi}(E) = \frac{1}{\lambda} - \frac{i}{8R} J_{1/2}(kR) H^{(1)}_{1/2}(kR) + \frac{\epsilon}{8\pi^2 R}\left(-\frac{1}{2R} + \frac{i\pi k}{2} J_{1/2}(kR) H^{(1)}_{3/2}(kR)\right)\left(\int_{S^2} h(\Omega) d\Omega\right) + O(\epsilon^2) \quad (3.4.24)$$

for the scattering part of this case. We need to write the expression $\langle \tilde{\Sigma} | \mathbf{k} \rangle$ in terms of the deformation function $h(\Omega)$:

$$\langle \tilde{\Sigma} | \mathbf{k} \rangle = \frac{1}{A(\tilde{\Sigma})} \int_{S^2} e^{i\mathbf{k}\cdot\tilde{\sigma}(\Omega)} R^2 \left(1 - \frac{2\epsilon}{R} h(\Omega)\right) \, d\Omega \, . \quad (3.4.25)$$

We expand the exponential term as

$$e^{i\epsilon h(\Omega)\mathbf{k}\cdot\mathbf{N}(\Omega)} = 1 + i\epsilon h(\Omega)\mathbf{k}\cdot\mathbf{N}(\Omega) \tag{3.4.26}$$

and expanding $A(\tilde{\Sigma})$ in ϵ, we can easily show that

$$\begin{aligned}\langle\tilde{\Sigma}|\mathbf{k}\rangle = &\left(1 + \frac{\epsilon}{2\pi R}\int_{S^2} h(\Omega)d\Omega\right)\left(\frac{\sin(kR)}{kR} - \frac{\epsilon}{2\pi R}\int_{S^2} e^{i\mathbf{k}\cdot\sigma(\Omega)}h(\Omega)d\Omega\right.\\ &\left. + \frac{i\epsilon}{4\pi}\int_{S^2} e^{i\mathbf{k}\cdot\sigma(\Omega)}(\mathbf{k}\cdot\mathbf{N}(\Omega))h(\Omega)d\Omega\right) + O(\epsilon^2)\ .\end{aligned} \tag{3.4.27}$$

To simplify the integrals, we consider a particular class of deformations, where $h(\Omega) = h(\theta)$ only. Once more we take θ' to be the angle between $\mathbf{k}'$ and $\mathbf{k}$, and $\mathbf{k}$ is in the direction of z coordinate. Then, using (3.4.24) and (3.4.27) and keeping only the terms of the order of ϵ, we get the explicit expression for the scattering amplitude for a deformation $h(\theta)$, given by

$$\begin{aligned}\tilde{f}(\mathbf{k}\to\mathbf{k}') =& -\frac{1}{4\pi}\langle\mathbf{k}'|\tilde{\Sigma}\rangle(\tilde{\Phi}(E))^{-1}\langle\tilde{\Sigma}|\mathbf{k}\rangle\\ =&\frac{1}{4\pi}\left(\frac{1}{\lambda} - \frac{i}{8R}J_{1/2}(kR)H^{(1)}_{1/2}(kR)\right)^{-1}\\ &\times\left\{\frac{\sin^2 kR}{k^2R^2} + \epsilon\left[\frac{4\sin^2 kR}{k^2R^3}\frac{1}{4\pi}\int h(\Omega)d\Omega - \frac{\sin kR}{kR^2}\int_0^\pi\left[e^{-ikR\cos(\theta-\theta')}\right.\right.\right.\\ &\left.\times\left(1 + \frac{ikR}{2}\cos(\theta-\theta')\right) + e^{ikR\cos\theta}\left(1 - \frac{ikR}{2}\cos\theta\right)\right]\sin\theta\ h(\theta)\ d\theta\\ &+ \frac{\sin^2 kR}{k^2R^2}\left(\frac{1}{4\pi R^2} - \frac{ik}{4R}J_{1/2}(kR)H^{(1)}_{3/2}(kR)\right)\\ &\left.\left.\left.\times\left(\frac{1}{\lambda} - \frac{i}{8R}J_{1/2}(kR)H^{(1)}_{1/2}(kR)\right)^{-1}\frac{1}{4\pi}\int h(\Omega)d\Omega\right]\right\} + O(\epsilon^2)\right].\end{aligned} \tag{3.4.28}$$

Finally, the graphs of the differential cross sections as a function of k for the spherical defect and deformed spherical defect for a particular deformation $h(\theta) = \sin\theta$ are given in Figure 3.25.

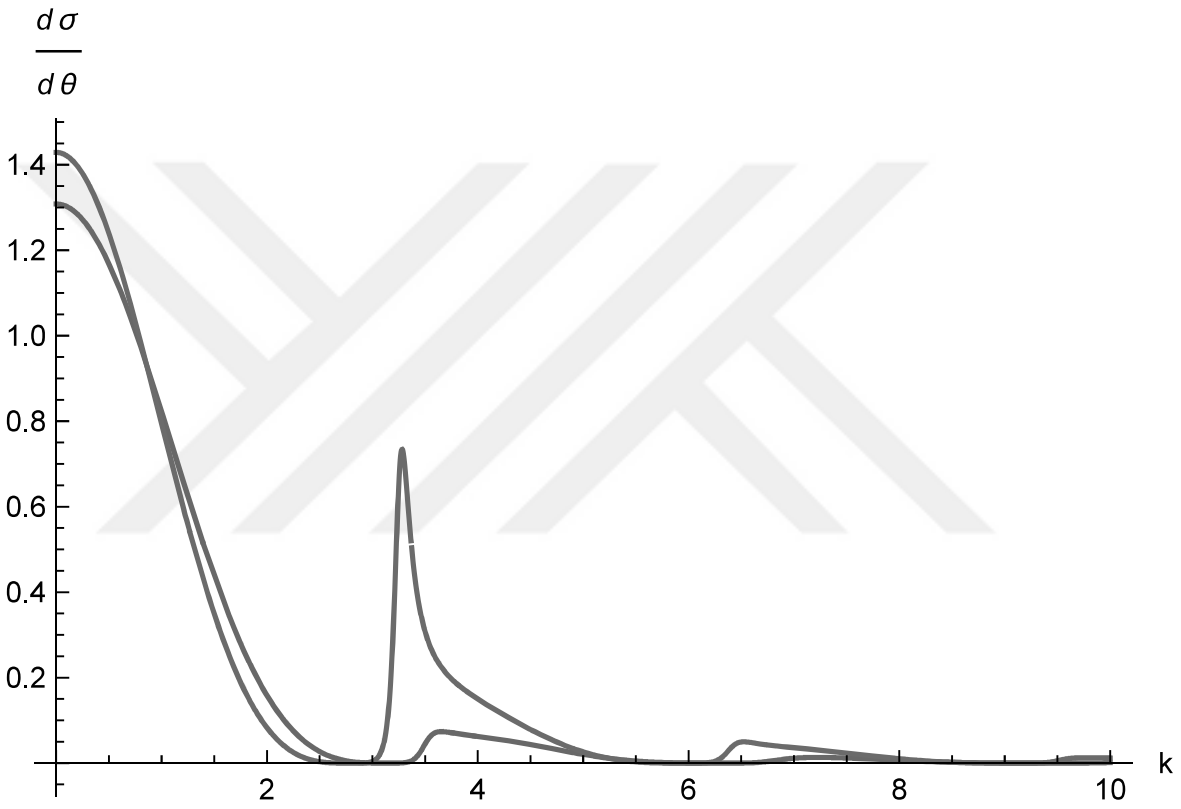

Figure 3.25. Differential cross sections as a function of k from a spherical defect and deformed spherical defect (red curve), where $h(\theta) = \sin\theta$, $R = 1$, $\lambda = 100$, and $\epsilon = 0.1$.

3.5. Deformed Circle and a Point Defect

Now we add a point delta potential to the case in (3.3). The setup is basically sketched in Figure 3.26. Let us remind ourselves the expressions of the circle defor-

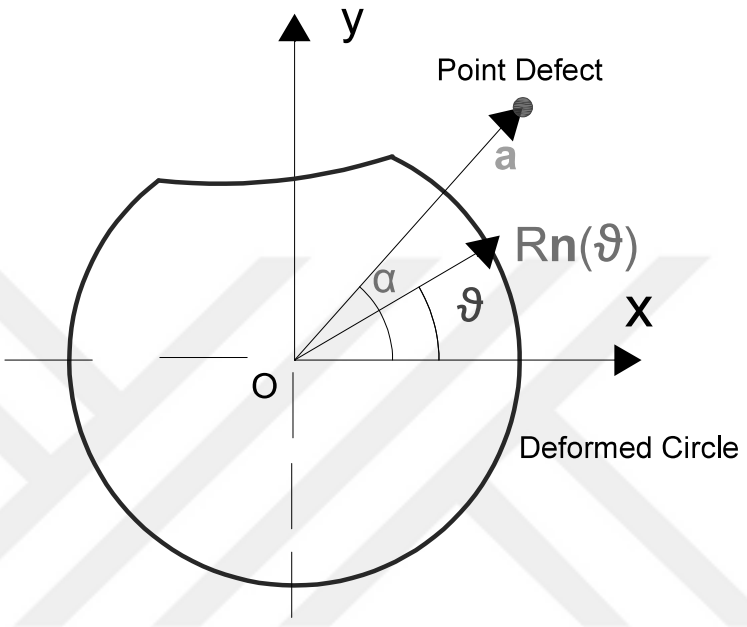

Figure 3.26. Deformed circle and point defects setup where $R\mathbf{n}(\theta)$ and $\mathbf{a}$ are the position vectors of the defects respectively.

mation. The position vector of the circle with radius R which is perturbed by $\epsilon h(s)$ is:

$$\tilde{\gamma}(s) = \gamma(s) + \epsilon h(s)\mathbf{n}(s) \ , \tag{3.5.1}$$

the magnitude of the derivative of this vector with respect to R is $|\tilde{\gamma}'(s)| = 1 - \frac{\epsilon}{R}h(s) + O(\epsilon^2)$, and we also have the total length of the deformed circle before in (3.3.4) as

$$L(\tilde{\Gamma}) = 2\pi R - \frac{\epsilon}{R}\int_0^L h(s)ds + O(\epsilon^2) \ , \text{ and } \ \langle \mathbf{p}|\tilde{\Gamma}\rangle = \frac{1}{L(\tilde{\Gamma})}\int_0^L e^{-i\mathbf{p}\cdot\tilde{\gamma}(s)}|\tilde{\gamma}'(s)|\,ds \ . \tag{3.5.2}$$

We also have the approximate equation

$$\frac{1}{L(\tilde{\Gamma})} = \frac{1}{2\pi R - \epsilon\int_0^{2\pi} h(\theta')d\theta'} = \frac{1}{2\pi R}\left(1 + \frac{\epsilon}{2\pi R}\int_0^{2\pi} h(\theta')d\theta'\right) \ . \tag{3.5.3}$$

In this scenario, we already have the 1×1 element of the principal matrix which is the point-point term from our earlier calculations. Therefore, what we need to find is

$$\begin{aligned}\Phi_{12}(-\nu^2) = \Phi_{21}(-\nu^2) &= -\left\langle \mathbf{a} \right| R_0(-\nu^2) \left| \tilde{\Gamma} \right\rangle = -\int \left\langle \mathbf{a} | \mathbf{p} \right\rangle \ \left\langle \mathbf{p} | R_0(-\nu^2) | \tilde{\Gamma} \right\rangle \ d^2p \\ &= -\int \frac{e^{i\ \mathbf{a}\cdot\mathbf{p}}}{(2\pi)^2} \ \frac{1}{p^2+\nu^2} \ \left\langle \mathbf{p} | \tilde{\Gamma} \right\rangle \ d^2p \end{aligned} \tag{3.5.4}$$

where, again $\mathbf{a}$ is the position of the point delta potential. We take the Taylor expansion of the exponential term, $e^{-i\epsilon h(\theta)\mathbf{p}\cdot\mathbf{n}(\theta)} \sim 1 - i\epsilon h(\theta)\mathbf{p}\cdot\mathbf{n}(\theta)$, then we get

$$\begin{aligned}\Phi_{12}(-\nu^2) = &-\int \frac{e^{i\ \mathbf{a}\cdot\mathbf{p}}}{(2\pi)^2} \ \frac{1}{p^2+\nu^2} \\ &\times \left(\frac{1}{L(\tilde{\Gamma})} \int_0^{2\pi} e^{-i\mathbf{p}\cdot\mathbf{R}} \left[1 - \frac{\epsilon}{R} h(\theta) - i\epsilon h(\theta)\mathbf{p}\cdot\mathbf{n}(\theta) \right] R d\theta \right) \ d^2p \\ = &-\int \frac{e^{i\ \mathbf{a}\cdot\mathbf{p}}}{(2\pi)^3} \ \frac{1}{p^2+\nu^2} \left(\int_0^{2\pi} \left(e^{-i\mathbf{p}\cdot\mathbf{R}} + e^{-i\mathbf{p}\cdot\mathbf{R}} \frac{\epsilon}{2\pi R} \left(\int_0^{2\pi} h(\theta') d\theta' \right) \right. \right. \\ &\left. \left. - e^{-i\mathbf{p}\cdot\mathbf{R}} \frac{\epsilon}{R} h(\theta) + \frac{\epsilon h(\theta)}{R} \frac{\partial}{\partial R} e^{-i\mathbf{p}\cdot\mathbf{R}} \right) d\theta \right) d^2p \end{aligned} \tag{3.5.5}$$

where we write $\gamma(\theta) = \mathbf{R}$. At this point, again we need to use the uniformly convergent plane wave expansion in two dimensions

$$e^{i\mathbf{p}\cdot\mathbf{a}} = \sum_{m=-\infty}^{\infty} i^m J_m(pa) \cos(m\varphi) \tag{3.5.6}$$

for each of the exponential terms in (3.5.5) since there are two different angles (the angle between the point defect and wave vector $\mathbf{p}$; the angle between the position vector of the circular defect and the wave vector $\mathbf{p}$) to be integrated. Let us take the angle between wave vector, $\mathbf{p}$, and the position vector of the circular defect, $\mathbf{R}(\theta)$, as ϕ. Rearranging these by getting rid of the terms of the order of ϵ^2,

$$\begin{aligned}\Phi_{12}(-\nu^2) = &-\int \frac{1}{(2\pi)^3} \sum_{m=-\infty}^{\infty} i^m J_m(pa) \cos(m\phi) \ \frac{1}{p^2+\nu^2} \left[\int_0^{2\pi} e^{-i\mathbf{p}\cdot\mathbf{R}} d\theta \right. \\ &+ \int_0^{2\pi} e^{-i\mathbf{p}\cdot\mathbf{R}} d\theta \frac{\epsilon}{2\pi R} \left(\int_0^{2\pi} h(\theta') d\theta' \right) - e^{-i\mathbf{p}\cdot\mathbf{R}} \frac{\epsilon}{R} \left(\int_0^{2\pi} h(\theta') d\theta' \right) \\ &\left. + \frac{\epsilon}{R} \left(\int_0^{2\pi} h(\theta') d\theta' \right) \frac{\partial}{\partial R} e^{-i\mathbf{p}\cdot\mathbf{R}} \right] d^2p \ . \end{aligned} \tag{3.5.7}$$

Here, it is important to mention that in the third term in the bracket, the angle between $\mathbf{p}$ and $\gamma(\theta) = \mathbf{R}$ is not the same as the angle variable in the deformation, $h(\theta')$. Then,

in terms of the Bessel functions, we have

$$\Phi_{12}(-\nu^2) = -\int \frac{1}{(2\pi)^3} \sum_{m=-\infty}^{\infty} i^m J_m(pa)\cos(m\phi)\ \frac{1}{p^2+\nu^2}\Bigg[2\pi J_0(pR) + \frac{\epsilon}{R}\Bigg(\int_0^{2\pi} h(\theta')d\theta'\Bigg)\Bigg[J_0(pR) - \sum_{k=-\infty}^{\infty} i^k J_k(pR)\cos(k\phi) + \frac{\partial}{\partial R}\sum_{k=-\infty}^{\infty} i^k J_k(pR)\cos(k\phi)\Bigg]\Bigg]\, d^2p\ . \tag{3.5.8}$$

For the last term of (3.5.8), we use the derivative relation of the Bessel functions:

$$\frac{d}{dx}J_k(x) = \frac{1}{2}(J_{k-1}(x) - J_{k+1}(x))\ , \tag{3.5.9}$$

and obtain

$$\Phi_{12}(-\nu^2) = -\int \frac{1}{(2\pi)^3} \sum_{m=-\infty}^{\infty} i^m J_m(pa)\cos(m\phi)\ \frac{1}{p^2+\nu^2}\Bigg[2\pi J_0(pR) + \frac{\epsilon}{R}\Bigg(\int_0^{2\pi} h(\theta')d\theta'\Bigg)\Bigg[J_0(pR) - \sum_{k=-\infty}^{\infty} i^k J_k(pR)\cos(k\phi) + \sum_{k=-\infty}^{\infty} i^k \frac{p}{2}[J_{k-1}(pR) - J_{k+1}(pR)]\cos(k\phi)\Bigg]\Bigg]\, pdpd\phi \tag{3.5.10}$$

Using the identity

$$\int_0^{2\pi} \cos(k\phi)\cos(m\phi)d\phi = \pi\delta_{mk} \tag{3.5.11}$$

we get

$$\Phi_{12}(-\nu^2) = -\frac{1}{8\pi^2}\int_0^{\infty} \frac{1}{p^2+\nu^2}\Bigg[2\pi J_0(pa)J_0(pR) + \frac{\epsilon}{R}\Bigg(\int_0^{2\pi} h(\theta')d\theta'\Bigg) \times \Bigg[J_0(pa)J_0(pR) + \sum_{m=-\infty}^{\infty} J_m(pa)J_m(pR) - \frac{p}{2}\sum_{m=-\infty}^{\infty} J_m(pa)J_{m-1}(pR) + \frac{p}{2}\sum_{m=-\infty}^{\infty} J_m(pa)J_{m+1}(pR)\Bigg]\Bigg]\, pdp\ . \tag{3.5.12}$$

At this point, we use the following summation formulae for the product of Bessel functions that is given in [62]

$$\sum_{m=1}^{\infty} J_m(\lambda r_1)J_m(\lambda r_2)\cos m\theta = J_0\Bigg(\lambda\sqrt{r_1^2 + r_2^2 - 2r_1 r_2\cos\theta}\Bigg)\ , \tag{3.5.13}$$

$$\sum_{-\infty}^{\infty} J_{\nu+m}(\lambda r_2)J_m(\lambda r_1)\begin{cases}\cos m\theta \\ \sin m\theta\end{cases} = J_\nu(\lambda d)\begin{cases}\cos\alpha \\ \sin\alpha\end{cases} \tag{3.5.14}$$

where $\vec{d} = \vec{r}_1 - \vec{2}_2$, θ indicates the angle between $\vec{r}_1$ and $\vec{r}_2$, α indicates the angle between $\vec{d}$ and $\vec{r}_2$ and $d = |\vec{d}| = \sqrt{r_1^2 + r_2^2 - 2r_1r_2cos\theta}$. We can always take the angle between the point defect position vector, $\mathbf{a}$, and the position vector of the circular defect, $\mathbf{R}$, as zero because of the cylindrical symmetry of the circular defect. Therefore, we take $\theta = \alpha = 0$ and rewrite the expression in (3.5.12) as

$$\begin{aligned}\Phi_{12}(-\nu^2) = -\frac{1}{8\pi^2}\Bigg[&\int_0^\infty 2\pi J_0(pa)J_0(pR)\frac{pdp}{p^2+\nu^2} + \frac{\epsilon}{R}\left(\int_0^{2\pi} h(\theta')d\theta'\right) \\ &\times\left[\int_0^\infty J_0(pa)J_0(pR)\frac{pdp}{p^2+\nu^2} + \int_0^\infty J_0(p\sqrt{a^2+R^2-2aR})\frac{pdp}{p^2+\nu^2}\right. \\ &+\int_0^\infty \frac{1}{2}J_1(p\sqrt{a^2+R^2-2aR})\frac{p^2dp}{p^2+\nu^2} \\ &\left.+\int_0^\infty \frac{1}{2}J_1(p\sqrt{a^2+R^2-2aR})\frac{p^2dp}{p^2+\nu^2}\right].\end{aligned} \tag{3.5.15}$$

Finally, we are left with the p-integral only where we used the Bessel identity $J_{-n}(z) = (-1)^n J_n(z)$. Using the relations given in [61] to calculate these integrals, we get

$$\begin{aligned}\Phi_{12}(-\nu^2) = -\frac{1}{8\pi^2}\Bigg[&2\pi K_0(\nu a)I_0(\nu R) + \frac{\epsilon}{R}\left(\int_0^{2\pi} h(\theta')d\theta'\right) \\ &\times\Big(K_0(\nu a)I_0(\nu R) + K_0(\nu(a-R)) + \nu K_1(\nu(a-R))\Big)\Bigg],\end{aligned} \tag{3.5.16}$$

using the assumption of $R < a$. We remark that $a < R$ case can be worked out analogously. We already have the 2×2 term of the principal matrix in equation (3.3.28):

$$\begin{aligned}\Phi_{22}(-\nu^2) =&\frac{1}{\lambda_2} - \frac{1}{2\pi}I_0(\nu R)K_0(\nu R) \\ &+\frac{\epsilon}{2\pi^2}\left(-\frac{1}{2R} + \nu I_0(\nu R)K_1(\nu R)\right)\left(\int_0^{2\pi} h(\theta)d\theta\right).\end{aligned} \tag{3.5.17}$$

Eventually, we have all of the elements of the principal matrix in terms of the deformation integral which is $\int_0^{2\pi} h(\theta)d\theta$. So we can look for the bound state energies and the scattering amplitude expression for this case.

3.5.1. Perturbative First Order Calculation of the Bound State Energy

Analogously, we rewrite the principal matrix by perturbing the assumed bound state energy ν_* by $\epsilon\nu_1$, i.e., $\nu = \nu_* + \epsilon\nu_1$ and $E_B = -\nu_*^2 - 2\epsilon\nu_*\nu_1$. Again, we Taylor expand its terms around ν_*. The first term is

$$\Phi_{11}(\nu_* + \epsilon\nu_1) = \frac{1}{\lambda_R} + \frac{1}{2\pi}\left[\ln\left(\frac{\nu_*}{\mu}\right) + \frac{\epsilon\nu_1}{\mu\nu_*}\right] + \mathcal{O}(\epsilon^2) \tag{3.5.18}$$

where μ is the renormalization constant. There is no contribution coming from the terms with $K_0'(\nu_*(a-R))$ and $K_1'(\nu_*(a-R))$ since they are of the order of $\mathcal{O}(\epsilon^2)$ and more, so we have:

$$\begin{aligned}\Phi_{12} =& -\frac{1}{4\pi}\Bigg[K_0(\nu_* a)I_0(\nu_* R) + \epsilon\nu_1 R K_0(\nu_* a)I_1(\nu_* R) - \epsilon\nu_1 a K_1(\nu_* a)I_0(\nu_* R) \\ &+ \frac{\epsilon}{2\pi R}\left(\int_0^{2\pi} h(\theta')d\theta'\right)\Big(K_0(\nu_* a)I_0(\nu_* R) + K_0(\nu_*(a-R)) \\ &+ \nu_* K_1(\nu_*(a-R))\Big)\Bigg] = \Phi_{21}(\nu_* + \epsilon\nu_1)\ ,\end{aligned} \tag{3.5.19}$$

for the off-diagonal elements. We already have Φ_{22} term in (3.4.19) and expanding it around ν_* we get

$$\begin{aligned}\Phi_{22} =& \frac{1}{\lambda_2} - \frac{1}{2\pi}I_0(\nu_* R)K_0(\nu_* R) + \frac{\epsilon\nu_1 R}{2\pi}\ I_0(\nu_* R)K_1(\nu_* R) - \frac{\epsilon\nu_1 R}{2\pi}I_1(\nu_* R)K_0(\nu_* R) \\ &- \frac{\epsilon}{2\pi^2}\left(\frac{1}{2R} - \nu_* I_0(\nu_* R)K_1(\nu_* R)\right)\left(\int_0^{2\pi} h(\theta)d\theta\right)\ .\end{aligned} \tag{3.5.20}$$

Through the standard perturbation theory, we can make the definition

$$\Phi \Rightarrow \Phi + \delta\Phi \tag{3.5.21}$$

and using this, we need to find an expression for ν_1 through the equation

$$\omega_1(\nu_* + \epsilon\nu_1) + \delta\omega_1 = \underbrace{\omega_1(\nu_*)}_{0} + \epsilon\nu_1 \frac{\partial\omega_1}{\partial\nu}\bigg|_{\nu_*} + \delta\omega_1 = 0 \tag{3.5.22}$$

where

$$\delta\omega_1 = A^{*T}\ \delta\Phi\ A\ . \tag{3.5.23}$$

So we write the Feynman-Hellman equation once more:

$$\left.\frac{\partial\omega_1}{\partial\nu}\right|_{\nu_*} = A^{*T}\left.\frac{\partial\Phi}{\partial\nu}\right|_{\nu_*} A \tag{3.5.24}$$

and then find

$$A_1^{*T}\left.\frac{\partial\Phi_{11}}{\partial\nu}\right|_{\nu_*} A_1 = A_1^{*T}\left[\frac{1}{2\pi}\frac{1}{\nu_*\mu}\right]A_1 \ , \tag{3.5.25}$$

$$A_1^{*T}\left.\frac{\partial\Phi_{12}}{\partial\nu}\right|_{\nu_*} A_2 = -\frac{1}{4\pi}A_1^{*T}\Big[-aK_1(\nu_* a)I_0(\nu_* R) + RK_0(\nu_* a)I_1(\nu_* R)\Big]A_2 \ , \tag{3.5.26}$$

$$A_2^{*T}\left.\frac{\partial\Phi_{22}}{\partial\nu}\right|_{\nu_*} A_2 = A_2^{*T}\Big[-\frac{1}{2\pi\nu_*} + \frac{R}{\pi}I_0(\nu_* R)K_1(\nu_* R)\Big]A_2 \ . \tag{3.5.27}$$

We find a normalized representative zero eigenvalue equation given below:

$$\begin{bmatrix}\Phi_{11} & \Phi_{12}\\ \Phi_{12} & \Phi_{22}\end{bmatrix}\begin{bmatrix}A_1\\ A_2\end{bmatrix} = \begin{bmatrix}0\\ 0\end{bmatrix} \quad \Rightarrow \quad \begin{bmatrix}A_1\\ A_2\end{bmatrix} = \frac{1}{\sqrt{\Phi_{11}^2+\Phi_{12}^2}}\begin{bmatrix}-\Phi_{12}\\ \Phi_{11}\end{bmatrix} \ . \tag{3.5.28}$$

Replacing A_1 and A_2, and multiplying with $\epsilon\nu_1$, we obtain

$$\begin{aligned}\epsilon\nu_1\frac{\partial\omega_1}{\partial\nu_*} =& \left[\left(\frac{1}{4\pi}K_0(\nu_* a)I_0(\nu_* R)\right)^2 + \left(\frac{1}{\lambda_R}+\frac{1}{2\pi}\ln\left(\frac{\nu_*}{\mu}\right)\right)^2\right]^{-1}\\ &\times\Bigg\{\frac{\epsilon\nu_1}{2\pi}\frac{1}{\nu_*\mu}\left(\frac{1}{4\pi}K_0(\nu_* a)I_0(\nu_* R)\right)^2 + \frac{\epsilon\nu_1}{2\pi}\left(\frac{1}{4\pi}K_0(\nu_* a)I_0(\nu_* R)\right)\\ &\times\Big[aK_1(\nu_* a)I_0(\nu_* R) - RK_0(\nu_* a)I_1(\nu_* R)\Big]\left(\frac{1}{\lambda_R}+\frac{1}{2\pi}\ln\left(\frac{\nu_*}{\mu}\right)\right)\\ &-\frac{\epsilon\nu_1}{2\pi}\Big[\frac{1}{\nu_*} - 2RI_0(\nu_* R)K_1(\nu_* R)\Big]\left(\frac{1}{\lambda_R}+\frac{1}{2\pi}\ln\left(\frac{\nu_*}{\mu}\right)\right)^2\Bigg\} \ .\end{aligned} \tag{3.5.29}$$

Now we obtain $\delta\omega_1$ via the equation (3.5.23):

$$\begin{aligned}\delta\omega_1 =& \left[\left(\frac{1}{4\pi}K_0(\nu_* a)I_0(\nu_* R)\right)^2 + \left(\frac{1}{\lambda_R} + \frac{1}{2\pi}\ln\left(\frac{\nu_*}{\mu}\right)\right)^2\right]^{-1} \\ & \times \frac{\epsilon\nu_1}{2\pi}\left(\int_0^{2\pi} h(\theta')d\theta'\right)\Bigg\{ -\frac{1}{4\pi}K_0(\nu_* a)I_0(\nu_* R)\ \frac{1}{\nu_1 R}\Big[K_0(\nu_* a)I_0(\nu_* R) \\ & + K_0(\nu_*(a-R)) + \nu_* K_1(\nu_*(a-R))\Big]\left(\frac{1}{\lambda_R} + \frac{1}{2\pi}\ln\left(\frac{\nu_*}{\mu}\right)\right) \\ & - \frac{1}{\nu_1\pi}\left(\frac{1}{2R} - \nu_* I_0(\nu_* R)K_1(\nu_* R)\right)\left(\frac{1}{\lambda_R} + \frac{1}{2\pi}\ln\left(\frac{\nu_*}{\mu}\right)\right)^2\Bigg\}. \end{aligned} \tag{3.5.30}$$

Placing the expressions given in (3.5.29) and (3.5.30) into (3.5.22), we get an expression for ν_1 as

$$\begin{aligned}\nu_1 =& \Bigg[\frac{1}{\nu_*\mu}\left(\frac{1}{4\pi}K_0(\nu_* a)I_0(\nu_* R)\right)^2 + \frac{1}{4\pi}K_0(\nu_* a)I_0(\nu_* R) \\ & \times\Big[aK_1(\nu_* a)I_0(\nu_* R) - RK_0(\nu_* a)I_1(\nu_* R)\Big]\left(\frac{1}{\lambda_R} + \frac{1}{2\pi}\ln\left(\frac{\nu_*}{\mu}\right)\right) \\ & - \left[\frac{1}{\nu_*} - 2RI_0(\nu_* R)K_1(\nu_* R)\right]\left(\frac{1}{\lambda_R} + \frac{1}{2\pi}\ln\left(\frac{\nu_*}{\mu}\right)\right)^2\Bigg] \\ & \times\Bigg[\int_0^{2\pi} h(\theta')d\theta'\Bigg\{\frac{1}{4\pi}K_0(\nu_* a)I_0(\nu_* R)\ \frac{1}{R}\Big[K_0(\nu_* a)I_0(\nu_* R) \\ & + K_0(\nu_*(a-R)) + \nu_* K_1(\nu_*(a-R))\Big]\left(\frac{1}{\lambda_R} + \frac{1}{2\pi}\ln\left(\frac{\nu_*}{\mu}\right)\right) \\ & + \frac{1}{\pi}\left(\frac{1}{2R} - \nu_* I_0(\nu_* R)K_1(\nu_* R)\right)\left(\frac{1}{\lambda_R} + \frac{1}{2\pi}\ln\left(\frac{\nu_*}{\mu}\right)\right)^2\Bigg\}\Bigg]^{-1} \end{aligned} \tag{3.5.31}$$

and for the bound state energy in terms of ν_1 as

$$
\begin{aligned}
E_B = & -\nu_*^2 - \epsilon\nu_* \\
& \times \left[\frac{1}{\nu_*\mu} \left(\frac{1}{4\pi} K_0(\nu_* a) I_0(\nu_* R) \right)^2 + \frac{1}{4\pi} K_0(\nu_* a) I_0(\nu_* R) \right. \\
& \times \left[a K_1(\nu_* a) I_0(\nu_* R) - R K_0(\nu_* a) I_1(\nu_* R) \right] \left(\frac{1}{\lambda_R} + \frac{1}{2\pi} \ln\left(\frac{\nu_*}{\mu} \right) \right) \\
& \left. - \left[\frac{1}{\nu_*} - 2R I_0(\nu_* R) K_1(\nu_* R) \right] \left(\frac{1}{\lambda_R} + \frac{1}{2\pi} \ln\left(\frac{\nu_*}{\mu} \right) \right)^2 \right] \\
& \times \left[\int_0^{2\pi} h(\theta') d\theta' \left\{ \frac{1}{4\pi} K_0(\nu_* a) I_0(\nu_* R) \, \frac{1}{R} \Big[K_0(\nu_* a) I_0(\nu_* R) \right. \right. \\
& \left. + K_0(\nu_*(a-R)) + \nu_* K_1(\nu_*(a-R)) \Big] \left(\frac{1}{\lambda_R} + \frac{1}{2\pi} \ln\left(\frac{\nu_*}{\mu} \right) \right) \\
& \left. \left. + \frac{1}{\pi} \left(\frac{1}{2R} - \nu_* I_0(\nu_* R) K_1(\nu_* R) \right) \left(\frac{1}{\lambda_R} + \frac{1}{2\pi} \ln\left(\frac{\nu_*}{\mu} \right) \right)^2 \right\} \right]^{-1} . \qquad (3.5.32)
\end{aligned}
$$

3.6. Deformed Sphere and a Point Defect

In this section, we combine a point defect with a deformed spherical defect with radius R. Let us remind ourselves that $\tilde{\sigma}$ is the position vector of the deformed sphere:

$$\tilde{\sigma}(\theta, \phi) := \sigma(\theta, \phi) + \epsilon h(\theta, \phi) \mathbf{N}(\theta, \phi) \, , \qquad (3.6.1)$$

where ϵ is a small deformation parameter, $\mathbf{N}$ is the normal vector. As before, h is going to be taken as a smooth function on the sphere. The area of the deformed sphere is given by

$$A(\tilde{\Sigma}) = 4\pi R^2 - 2\epsilon \int_0^{2\pi} H \int_0^{\pi} h(\theta, \phi) R^2 \sin\theta d\theta d\phi + O(\epsilon^2) \, , \qquad (3.6.2)$$

where $H = 1/R$ is the mean curvature of the sphere and we will use the notation $d\Omega$ instead of $\sin\theta d\theta d\phi$ to make our expressions more simple. Again, we have the diagonal elements of the principal matrix in (3.4.19) and (3.4.19). The only expression we need

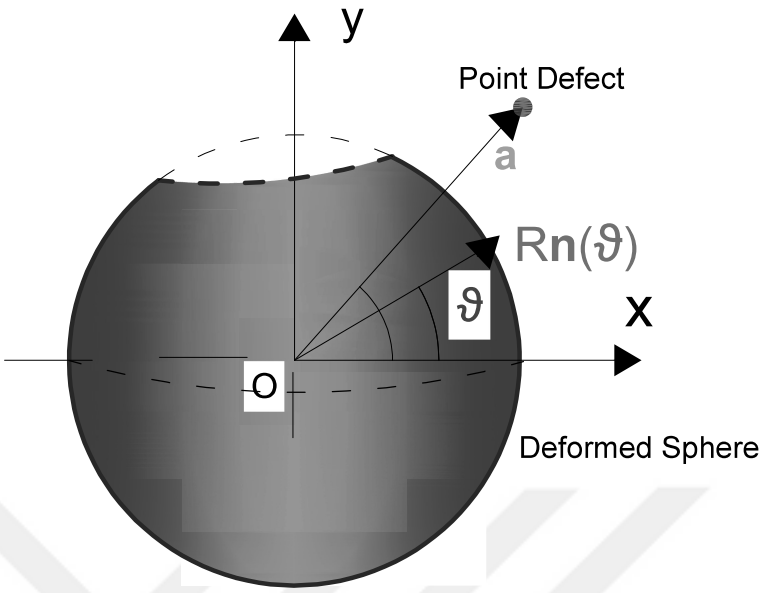

Figure 3.27. Deformed sphere and point defects setup where $R\mathbf{n}(\theta)$ and $\mathbf{a}$ are the position vectors of the defects respectively.

to find is $\Phi_{12} = \Phi_{21}$ element:

$$\Phi_{12}(-\nu^2) = \Phi_{21}(-\nu^2) = -\langle \mathbf{a}|\, R_0(-\nu^2)\, |\tilde{\Sigma}\rangle = -\int \langle \mathbf{a}|\mathbf{p}\rangle \;\langle \mathbf{p}|R_0(-\nu^2)|\tilde{\Sigma}\rangle \; d^3p$$
$$= -\int \frac{e^{i\ \mathbf{a}\cdot\mathbf{p}}}{(2\pi)^3}\; \frac{1}{p^2+\nu^2}\; \langle \mathbf{p}|\tilde{\Sigma}\rangle \; d^3p\ . \tag{3.6.3}$$

We have a momentum state projected on a deformed sphere as

$$\langle \mathbf{p}|\tilde{\Sigma}\rangle = \frac{1}{A(\tilde{\Sigma})}\int e^{-i\mathbf{p}\cdot\tilde{\sigma}(\Omega)}\ |\tilde{\sigma}'(\Omega)|\, R^2 d\Omega \tag{3.6.4}$$

where

$$|\tilde{\sigma}'(\Omega)| = \left|\frac{\partial}{\partial s}\tilde{\sigma}(\Omega)\right| = 1 - \epsilon h(\Omega)\kappa = 1 - \frac{2\epsilon}{R}h(\Omega)\ . \tag{3.6.5}$$

We use the approximation

$$\frac{1}{A(\tilde{\Sigma})} = \frac{1}{4\pi R^2}\left(1 + \frac{2\epsilon}{4\pi R}\int_0^{2\pi}\int_0^{\pi} h(\Omega)d\Omega\right)\ , \tag{3.6.6}$$

and the Taylor expansion of the exponential term

$$e^{-i\epsilon h(\Omega)\mathbf{p}\cdot\mathbf{N}(\Omega)} = 1 - i\epsilon h(\Omega)\mathbf{p}\cdot\mathbf{N}(\Omega)\ . \tag{3.6.7}$$

Substituting (3.6.4), (3.6.5), (3.6.6) and (3.6.7) in equation (3.6.3), we have

$$\begin{aligned}
\Phi_{12}(-\nu^2) =& -\frac{1}{4\pi}\int \frac{e^{i\ \mathbf{a}\cdot\mathbf{p}}}{(2\pi)^3}\ \frac{1}{p^2+\nu^2}\Bigg[\int_0^{2\pi}\int_0^{\pi} e^{-i\mathbf{p}\cdot\sigma(\Omega)}d\Omega \\
&+\frac{2\epsilon}{4\pi R}\Big(\int_0^{2\pi}\int_0^{\pi} h(\Omega')d\Omega'\Big)\int_0^{2\pi}\int_0^{\pi} e^{-i\mathbf{p}\cdot\sigma(\Omega)}d\Omega \\
&+\epsilon\int_0^{2\pi}\int_0^{\pi}\frac{\partial}{\partial R}e^{-i\mathbf{p}\cdot\sigma(\Omega)}h(\Omega)d\Omega-\frac{2\epsilon}{R}\int_0^{2\pi}\int_0^{\pi} e^{-i\mathbf{p}\cdot\sigma(\Omega)}h(\Omega)d\Omega\Bigg]d^3p \\
=& -\frac{1}{(2\pi)^3}\Bigg\{\int\frac{e^{i\ \mathbf{a}\cdot\mathbf{p}}}{p^2+\nu^2}\ \frac{\sin(pR)}{pR}d^3p+\Big(\int_0^{2\pi}\int_0^{\pi} h(\Omega')d\Omega'\Big) \\
&\times\Bigg[\frac{2\epsilon}{4\pi R}\int\frac{e^{i\ \mathbf{a}\cdot\mathbf{p}}}{p^2+\nu^2}\ \frac{\sin(pR)}{pR}d^3p+\frac{\epsilon}{4\pi}\frac{\partial}{\partial R}\int\frac{e^{i\ \mathbf{a}\cdot\mathbf{p}}}{p^2+\nu^2}e^{-i\mathbf{p}\cdot\sigma(\Omega)}d^3p \\
&-\frac{2\epsilon}{4\pi R}\int\frac{e^{i\ \mathbf{a}\cdot\mathbf{p}}}{p^2+\nu^2}e^{-i\mathbf{p}\cdot\sigma(\Omega)}\ d^3p\Bigg]\Bigg\}\ ,
\end{aligned} \tag{3.6.8}$$

again, getting rid of the higher order terms and using the fact that the angle between $\sigma(\Omega)$ and $\mathbf{p}$ is not Ω, so we can separate all the deformation function integrals. We can take the angle between $(\mathbf{a}-\sigma(\Omega))$ and $\mathbf{p}$ as φ, the angle variable of $d^3p = p^2dp\sin(\varphi)d\varphi d\alpha$. Using (2.2.14), the final form of $\Phi_{12}\equiv\Phi_{12}(\nu_*+\epsilon\nu_1)$ is then,

$$\begin{aligned}
\Phi_{12} =& -\frac{1}{(2\pi)^3}\Bigg\{\frac{2\pi^2}{\nu aR}e^{-\nu a}\sinh(\nu R)+\Big(\int_0^{2\pi}\int_0^{\pi} h(\Omega')d\Omega'\Big)\Bigg[\frac{\epsilon\pi}{\nu aR^2}e^{-\nu a}\sinh(\nu R) \\
&+\frac{\epsilon}{4\pi}\frac{\partial}{\partial R}\int_0^{2\pi}\int_0^{\pi}\int_0^{\infty}\frac{p^2\ dp}{p^2+\nu^2}e^{-ip(a-R)\cos\varphi}\sin\varphi d\varphi d\alpha \\
&-\frac{2\epsilon}{4\pi R}\int_0^{2\pi}\int_0^{\pi}\int_0^{\infty}\frac{p^2\ dp}{p^2+\nu^2}e^{-ip(a-R)\cos\varphi}\sin\varphi d\varphi d\alpha\Bigg]\Bigg\} \\
=& -\frac{1}{4\pi\nu aR}e^{-\nu a}\sinh(\nu R)-\Big(\int_0^{2\pi}\int_0^{\pi} h(\Omega')d\Omega'\Big) \\
&\times\Bigg[\frac{\epsilon}{8\pi^2\nu aR^2}e^{-\nu a}\sinh(\nu R)+\frac{\epsilon}{16\pi^2}[\nu(a-R)+1]\frac{e^{-\nu(a-R)}}{(a-R)^2}-\frac{\pi\epsilon}{R}\frac{e^{-\nu(a-R)}}{a-R}\Bigg] \\
=& -\frac{1}{4\pi\sqrt{aR}}K_{1/2}(\nu a)I_{1/2}(\nu R)-\Big(\int_0^{2\pi}\int_0^{\pi} h(\Omega')d\Omega'\Big) \\
&\times\epsilon\Bigg[\frac{1}{8\pi^2R\sqrt{aR}}K_{1/2}(\nu a)I_{1/2}(\nu R) \\
&+\Big(\frac{\nu+1/(a-R)}{16\pi^2}-\frac{\pi}{R}\Big)\sqrt{\frac{2\nu}{\pi}}\frac{K_{1/2}(\nu(a-R))}{\sqrt{a-R}}\Bigg]
\end{aligned} \tag{3.6.9}$$

where we used the integral result

$$\int_0^\infty \frac{p}{p^2+\nu^2}\sin(px)\,dp = e^{-\nu x}\frac{\pi}{2} \quad \text{for} \quad x>0. \tag{3.6.10}$$

3.6.1. Perturbative First Order Calculation of the Bound State Energy

We write the bound state energy perturbed as $E_B = -\nu_*^2 - 2\epsilon\nu_*\nu_1$ by taking $\nu = \nu_* + \epsilon\nu_1$, and perform the similar Taylor expansion around ν_*. Since we already have the expanded forms of $\Phi_{11}(\nu_* + \epsilon\nu_1)$ and $\Phi_{22}(\nu_* + \epsilon\nu_1)$, we write $\Phi_{12}(\nu_* + \epsilon\nu_1)$ as:

$$\begin{aligned}
\Phi_{12} =& -\frac{1}{4\pi\sqrt{aR}}K_{1/2}((\nu_*+\epsilon\nu_1)a)I_{1/2}((\nu_*+\epsilon\nu_1)R) - \left(\int_0^{2\pi}\int_0^{\pi} h(\Omega')d\Omega'\right) \\
&\times \epsilon\left[\frac{1}{8\pi^2 R\sqrt{aR}}K_{1/2}((\nu_*+\epsilon\nu_1)a)I_{1/2}((\nu_*+\epsilon\nu_1)R)\right. \\
&\left.+\left(\frac{(\nu_*+\epsilon\nu_1)+1/(a-R)}{16\pi^2}-\frac{\pi}{R}\right)\sqrt{\frac{2(\nu_*+\epsilon\nu_1)}{\pi}}\frac{K_{1/2}((\nu_*+\epsilon\nu_1)(a-R))}{\sqrt{a-R}}\right] \\
=& -\frac{1}{4\pi\sqrt{aR}}\Big[K_{1/2}(\nu_* a)I_{1/2}(\nu_* R) + \epsilon\nu_1 R K_{1/2}(\nu_* a)I_{3/2}(\nu_* R) \\
&- \epsilon\nu_1 a K_{3/2}(\nu_* a)I_{1/2}(\nu_* R)\Big] - \left(\int_0^{2\pi}\int_0^{\pi} h(\Omega')d\Omega'\right)\frac{\epsilon}{8\pi^2 R\sqrt{aR}} \\
&\times\left[K_{1/2}(\nu_* a)I_{1/2}(\nu_* R) + \left(\frac{\nu_*+1/(a-R)}{16\pi^2}-\frac{\pi}{R}\right)\sqrt{\frac{2\nu_*}{\pi}}\frac{K_{1/2}(\nu_*(a-R))}{\sqrt{a-R}}\right].
\end{aligned} \tag{3.6.11}$$

Again, using the standard perturbation theory, we will find an expression for ν_1 from the equation

$\epsilon\nu_1\left.\frac{\partial\omega_1}{\partial\nu}\right|_{\nu_*} = -\delta\omega_1$, where $A^{*T}\left.\frac{\partial\Phi}{\partial\nu}\right|_{\nu_*} A = \left.\frac{\partial\omega_1}{\partial\nu}\right|_{\nu_*}$. The only term we need is

$$A_1^{*T}\frac{\partial\Phi_{12}}{\partial\nu}\bigg|_{\nu_*}A_2=\Bigg[\left(\frac{1}{4\pi\sqrt{aR}}K_{1/2}(\nu_*a)I_{1/2}(\nu_*R)\right)^2+\left(\frac{1}{\lambda_R}+\frac{1}{2\pi}\ln\left(\frac{\nu_*}{\mu}\right)\right)^2\Bigg]^{-1}$$
$$\times\frac{1}{4\pi\sqrt{aR}}K_{1/2}(\nu_*a)I_{1/2}(\nu_*R)\Bigg\{\frac{1}{4\pi\sqrt{aR}}\Bigg[-aK_{3/2}(\nu_*a)I_{1/2}(\nu_*R)$$
$$+RK_{1/2}(\nu_*a)I_{3/2}(\nu_*R)\Bigg]-\left(\int_0^{2\pi}\int_0^{\pi}h(\Omega')d\Omega'\right)\frac{\epsilon}{8\pi^2R\sqrt{aR}}$$
$$\times\Bigg[-aK_{3/2}(\nu_*a)I_{1/2}(\nu_*R)+RK_{1/2}(\nu_*a)I_{3/2}(\nu_*R)$$
$$+\frac{1}{16\pi^2}\sqrt{\frac{2\nu_*}{\pi}}\frac{K_{1/2}(\nu_*(a-R))}{\sqrt{a-R}}+\left(\frac{\nu_*+1/(a-R)}{16\pi^2}-\frac{\pi}{R}\right)\sqrt{\frac{1}{2\nu_*\pi}}$$
$$\times\frac{K_{1/2}(\nu_*(a-R))}{\sqrt{a-R}}-\left(\frac{\nu_*+1/(a-R)}{16\pi^2}-\frac{\pi}{R}\right)\sqrt{\frac{2\nu_*}{\pi}}\sqrt{a-R}$$
$$\times K_{3/2}(\nu_*(a-R))\Bigg]\Bigg\}\left(\frac{1}{\lambda_R}+\frac{1}{2\pi}\ln\left(\frac{\nu_*}{\mu}\right)\right)\ . \tag{3.6.12}$$

Now we write

$$\delta\omega_1=A_1^{*T}\delta\Phi_{11}A_1+2A_1^{*T}\Phi_{12}A_2+A_2^{*T}\Phi_{22}A_2$$
$$=\Bigg[\left(\frac{1}{4\pi\sqrt{aR}}K_{1/2}(\nu_*a)I_{1/2}(\nu_*R)\right)^2+\left(\frac{1}{\lambda_R}+\frac{1}{2\pi}\ln\left(\frac{\nu_*}{\mu}\right)\right)^2\Bigg]^{-1}\frac{\epsilon\nu_1}{2\pi}$$
$$\times\Bigg\{-\left(\int_0^{2\pi}\int_0^{\pi}h(\Omega')d\Omega'\right)\frac{1}{4\pi\nu_1R\sqrt{aR}}\Bigg[K_{1/2}(\nu_*a)I_{1/2}(\nu_*R)$$
$$+\left(\frac{\nu_*+1/(a-R)}{16\pi^2}-\frac{\pi}{R}\right)\sqrt{\frac{2\nu_*}{\pi}}\frac{K_{1/2}(\nu_*(a-R))}{\sqrt{a-R}}\Bigg]\left(\frac{1}{\lambda_R}+\frac{1}{2\pi}\ln\left(\frac{\nu_*}{\mu}\right)\right)$$
$$-\frac{1}{\nu_1\pi}\left(\frac{1}{2R}-\nu_*I_0(\nu_*R)K_1(\nu_*R)\right)\left(\int_0^{2\pi}h(\theta)d\theta\right)\left(\frac{1}{\lambda_R}+\frac{1}{2\pi}\ln\left(\frac{\nu_*}{\mu}\right)\right)^2\Bigg\} \tag{3.6.13}$$

and find the expression for ν_1 as

$$\begin{aligned}
\nu_1 =&\Bigg\{ \Bigg(\int_0^{2\pi} \int_0^{\pi} h(\Omega')d\Omega' \Bigg) \frac{1}{4\pi R\sqrt{aR}} \Bigg[K_{1/2}(\nu_* a) I_{1/2}(\nu_* R) \\
&+ \left(\frac{\nu_* + 1/(a-R)}{16\pi^2} - \frac{\pi}{R} \right) \sqrt{\frac{2\nu_*}{\pi}} \frac{K_{1/2}(\nu_*(a-R))}{\sqrt{a-R}} \Bigg] \left(\frac{1}{\lambda_R} + \frac{1}{2\pi} \ln\left(\frac{\nu_*}{\mu} \right) \right) \\
&+ \frac{1}{\pi} \left(\frac{1}{2R} - \nu_* I_0(\nu_* R) K_1(\nu_* R) \right) \left(\int_0^{2\pi} h(\theta) d\theta \right) \left(\frac{1}{\lambda_R} + \frac{1}{2\pi} \ln\left(\frac{\nu_*}{\mu} \right) \right)^2 \Bigg\} \\
&\Bigg\{ \frac{1}{2\sqrt{aR}} K_{1/2}(\nu_* a) I_{1/2}(\nu_* R) \Bigg\{ \frac{1}{4\pi\sqrt{aR}} \Bigg[- aK_{3/2}(\nu_* a) I_{1/2}(\nu_* R) \\
&+ RK_{1/2}(\nu_* a) I_{3/2}(\nu_* R) \Bigg] - \Bigg(\int_0^{2\pi} \int_0^{\pi} h(\Omega')d\Omega' \Bigg) \frac{\epsilon}{8\pi^2 R\sqrt{aR}} \\
&\times \Bigg[- aK_{3/2}(\nu_* a) I_{1/2}(\nu_* R) + RK_{1/2}(\nu_* a) I_{3/2}(\nu_* R) \\
&+ \frac{1}{16\pi^2} \sqrt{\frac{2\nu_*}{\pi}} \frac{K_{1/2}(\nu_*(a-R))}{\sqrt{a-R}} + \left(\frac{\nu_* + 1/(a-R)}{16\pi^2} - \frac{\pi}{R} \right) \sqrt{\frac{1}{2\nu_*\pi}} \\
&\times \frac{K_{1/2}(\nu_*(a-R))}{\sqrt{a-R}} - \left(\frac{\nu_* + 1/(a-R)}{16\pi^2} - \frac{\pi}{R} \right) \sqrt{\frac{2\nu_*}{\pi}} \sqrt{a-R} \\
&\times K_{3/2}(\nu_*(a-R)) \Bigg] \Bigg\} \left(\frac{1}{\lambda_R} + \frac{1}{2\pi} \ln\left(\frac{\nu_*}{\mu} \right) \right) \\
&- 2 \Bigg[\frac{1}{\nu_*} - 2RI_0(\nu_* R) K_1(\nu_* R) \Bigg] \left(\frac{1}{\lambda_R} + \frac{1}{2\pi} \ln\left(\frac{\nu_*}{\mu} \right) \right)^2 \Bigg\} \Bigg\}^{-1} . \qquad (3.6.14)
\end{aligned}$$

Finally, using (3.5.22) and (3.5.23), we express the bound state energy in terms of ν_1 obtained above and get

$$
\begin{aligned}
E_B = & -\nu_*^2 - 2\epsilon\nu_* \\
& \times \Bigg\{ \Bigg(\int_0^{2\pi} \int_0^{\pi} h(\Omega') d\Omega' \Bigg) \frac{1}{4\pi R\sqrt{aR}} \Bigg[K_{1/2}(\nu_* a) I_{1/2}(\nu_* R) \\
& + \left(\frac{\nu_* + 1/(a-R)}{16\pi^2} - \frac{\pi}{R} \right) \sqrt{\frac{2\nu_*}{\pi}} \frac{K_{1/2}(\nu_*(a-R))}{\sqrt{a-R}} \Bigg] \left(\frac{1}{\lambda_R} + \frac{1}{2\pi} \ln\left(\frac{\nu_*}{\mu} \right) \right) \\
& + \frac{1}{\pi} \left(\frac{1}{2R} - \nu_* I_0(\nu_* R) K_1(\nu_* R) \right) \left(\int_0^{2\pi} h(\theta) d\theta \right) \left(\frac{1}{\lambda_R} + \frac{1}{2\pi} \ln\left(\frac{\nu_*}{\mu} \right) \right)^2 \Bigg\} \\
& \Bigg\{ \frac{1}{2\sqrt{aR}} K_{1/2}(\nu_* a) I_{1/2}(\nu_* R) \Bigg\{ \frac{1}{4\pi\sqrt{aR}} \Bigg[- aK_{3/2}(\nu_* a) I_{1/2}(\nu_* R) \\
& + RK_{1/2}(\nu_* a) I_{3/2}(\nu_* R) \Bigg] - \Bigg(\int_0^{2\pi} \int_0^{\pi} h(\Omega') d\Omega' \Bigg) \frac{\epsilon}{8\pi^2 R\sqrt{aR}} \\
& \times \Bigg[- aK_{3/2}(\nu_* a) I_{1/2}(\nu_* R) + RK_{1/2}(\nu_* a) I_{3/2}(\nu_* R) \\
& + \frac{1}{16\pi^2} \sqrt{\frac{2\nu_*}{\pi}} \frac{K_{1/2}(\nu_*(a-R))}{\sqrt{a-R}} + \left(\frac{\nu_* + 1/(a-R)}{16\pi^2} - \frac{\pi}{R} \right) \sqrt{\frac{1}{2\nu_*\pi}} \\
& \times \frac{K_{1/2}(\nu_*(a-R))}{\sqrt{a-R}} - \left(\frac{\nu_* + 1/(a-R)}{16\pi^2} - \frac{\pi}{R} \right) \sqrt{\frac{2\nu_*}{\pi}} \sqrt{a-R} \\
& \times K_{3/2}(\nu_*(a-R)) \Bigg] \Bigg\} \left(\frac{1}{\lambda_R} + \frac{1}{2\pi} \ln\left(\frac{\nu_*}{\mu} \right) \right) \\
& - 2 \Bigg[\frac{1}{\nu_*} - 2RI_0(\nu_* R) K_1(\nu_* R) \Bigg] \left(\frac{1}{\lambda_R} + \frac{1}{2\pi} \ln\left(\frac{\nu_*}{\mu} \right) \right)^2 \Bigg\} \Bigg\}^{-1} . \qquad (3.6.15)
\end{aligned}
$$

4. GEOMETRIC SCATTERING IN THE PRESENCE OF LINE DEFECTS

In this chapter, we will concentrate on solely the scattering state of a scalar particle which scatters from an asymptotically flat curved surface in the presence of line defects. We will mention the concept of geometric scattering and as the singular potentials, the scattering by infinitely long linear delta potentials. We will give the calculations and graphs obtained in our work [49].

The research on the quantum mechanical problems on a curved surface is a very interesting topic [19, 21–25]. Consequently, studies on quantum scattering on a curved surface are also very influential since they provide very important tools to quantum gravitational theories. A relatively fundamental approach on this manner is analyzed in [26]. In this paper, the scattering of a scalar particle freely moving on an asymptotically flat surface S is examined. Following this work, we see that we can express the non-trivial geometry to the Hamiltonian as a perturbation to the kinetic energy and a correction to the potential because of the curvature effects. To realize such a system, we can think of a dilute electron gas formed on bumpy surface. Therefore, adding some singular potentials to the geometric problem is crucial since there could be some defects in this gas. In their work [28], authors also do the calculations of the geometric scattering of a scalar particle, an electron in particular, in the presence of many point-like delta potentials and observe an amplification of the geometric scattering effects by the point defects. For the study of the linear delta potentials, we will follow the formulation obtained in [28]. We note that in this chapter we use the normalization $\langle x|k\rangle = \frac{e^{ikx}}{\sqrt{2\pi}}$ instead of the earlier chapter (which takes $\frac{e^{ikx}}{2\pi}$) in one dimension.

4.1. Scattering by parallel line defects in a plane

First, we start with the case where the space is flat. We work in two dimensions and the non-relativistic scalar particle scatters by N linear delta potentials which are

pictured in Figure 4.1 and can be described as

$$V_0(x,y) = \sum_{n=1}^{N} \xi_n \delta(x - a_n) \tag{4.1.1}$$

where ξ_n is the interaction strength which can be either complex or real and a_n's are the locations of the linear defects.

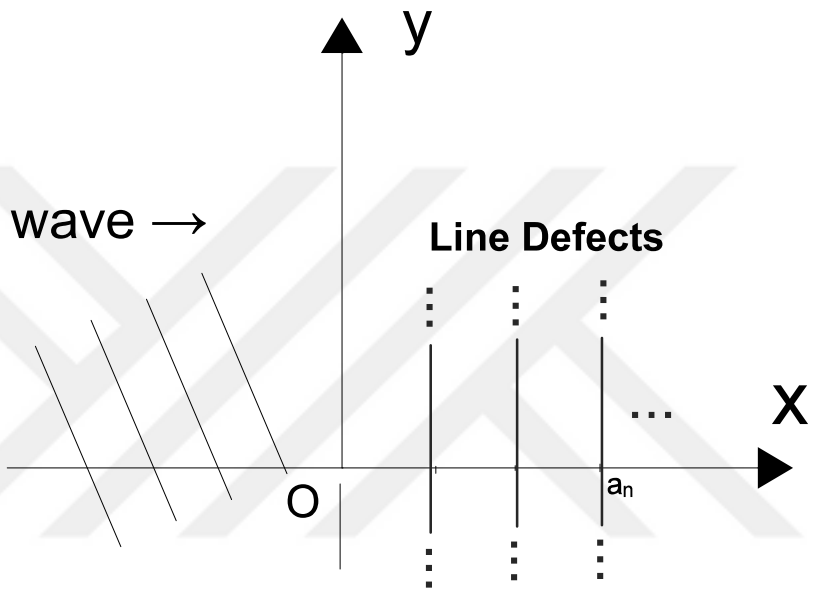

Figure 4.1. Line Defects where a_n is the location of the defect.

The Hamiltonian of such a system can be written as below

$$H = H_0 + V_0 = -\nabla^2 + \sum_{n=1}^{N} \xi_n \delta(x - a_n) \ . \tag{4.1.2}$$

Because of the definition of the potential does not have a polar symmetry, we will work on the cartesian coordinates for this part of the problem. In position space, the time-independent Schrödinger equation is

$$\Big[-\partial_x^2 - \partial_y^2 + \sum_{n}^{N} \xi_n \delta(x - a_n) \Big] \psi_0(x,y) = k^2 \psi_0(x,y) \, , \tag{4.1.3}$$

where $k^2 = E$. Now, to solve this equation, we can use the separation of variables method since the potential is in terms of the x-coordinate only and we already know that the momentum dependent scattering solution, $\langle x, y | \psi_0(\mathbf{k}) \rangle$, should satisfy the

Lippmann-Schwinger equation,

$$\langle x, y|\psi_0(\mathbf{k})\rangle = \langle x, y|\mathbf{k}\rangle + \langle x, y|R_0^+(E)V_0|\psi_0(\mathbf{k})\rangle \ , \tag{4.1.4}$$

where $\mathbf{k}$ is the incoming wavevector. We can express $\mathbf{k}$ as

$$\mathbf{k} = k_x\mathbf{e}_x + k_y\mathbf{e}_y = k(\cos\theta_0\mathbf{e}_x + \sin\theta_0\mathbf{e}_y) \tag{4.1.5}$$

where $\mathbf{e}_x$ and $\mathbf{e}_y$ are respectively the unit vectors along the x- and y-axes, $|\mathbf{k}| = k$ and θ_0 is the incidence angle. So we can write the solution to (4.1.3) as

$$\psi_0(\mathbf{x}) = \psi_0(x, y) = \chi(x)\phi(y) \tag{4.1.6}$$

where

$$\phi(y) = e^{ik_y y}/2\pi \tag{4.1.7}$$

since the potential is not y-dependent. For the x-component of the Schrödinger equation we have

$$\frac{\partial^2}{\partial x^2}\chi(x) + k_x^2\ \chi(x) = \sum_{n=1}^{N}\xi_n\delta(x - a_n)\chi(a_n)\ . \tag{4.1.8}$$

At this point, we need to make connection between momentum and position spaces and obtain the full wave solution $\psi_0(\mathbf{k}, \mathbf{x})$. To do that, we identify the Hilbert space $L^2(\mathbb{R}^2)$ of square-integrable functions of $\mathbf{x} = (x, y)$ with $\mathcal{H}_1 \otimes \mathcal{H}_2$, where $\mathcal{H}_1$ and $\mathcal{H}_2$ are respectively the Hilbert space of the square-integrable functions of x and y. This allows us to express the momentum dependent wave solution $|\psi_0(\mathbf{k})\rangle$ as an inner product of position functions:

$$\begin{aligned} |\psi_0(\mathbf{k})\rangle = |\chi, \phi\rangle = |\chi\rangle \otimes |\phi\rangle\,, \\ \Rightarrow \quad \psi_0(\mathbf{k}, \mathbf{x}) = \chi(x)\phi(y)\ . \end{aligned} \tag{4.1.9}$$

Similarly, we are now able to write V_0 in the form,

$$V_0 = \sum_{n=1}^{N}\xi_n|a_n\rangle\langle a_n| \otimes I_2 \tag{4.1.10}$$

where I_2 is the identity operator for $\mathcal{H}_2$. Now it is admissible to write the second term

in the Lippmann-Schwinger equation directly as

$$\begin{aligned}\langle x,y|R_0^+(E)V_0|\psi_0(\mathbf{k})\rangle =& \sum_{n=1}^{N}\xi_n \langle x,y|\, R_0^+(E)\,|a_n\rangle\,\langle a_n|\chi\rangle\,|\phi\rangle \\ =& \sum_{n=1}^{N}\xi_n \int_{-\infty}^{\infty}\langle x,y|\, R_0^+(E)\,|k_x,k_y\rangle\,\langle k_x|a_n\rangle\,\langle a_n|\chi\rangle\,\langle k_y|\phi\rangle\, dk_x dk_y \\ =& \sum_{n=1}^{N}\xi_n \int_{-\infty}^{\infty}\langle x,y|\, R_0^+(E)\,|k_x,k_y\rangle\,\frac{e^{-ik_x a_n}}{\sqrt{2\pi}}\chi(a_n)\,\langle k_y|\phi\rangle\, dk_x dk_y\ .\end{aligned} \tag{4.1.11}$$

Now we place the resolvent operator, $R_0(E) = (E-\hat{\mathbf{p}}_x^2)^{-1}$ in the equation above where $\hat{\mathbf{p}}_x\,|k_x\rangle = k_x\,|k_x\rangle$ and get

$$\begin{aligned}\langle x,y|R_0^+(E)V_0|\psi_0(\mathbf{k})\rangle =& \sum_{n=1}^{N}\xi_n \int_{-\infty}^{\infty}\frac{\langle x|k_x'\rangle\,\langle y|k_y\rangle\,\langle k_x'|k_x\rangle}{E-k_x'^2+i\epsilon}\frac{e^{-ik_x a_n}}{\sqrt{2\pi}} \\ & \times\chi(a_n)\,\langle k_y|\phi\rangle\, dk_x dk_y dk_x' \\ =& \sum_{n=1}^{N}\xi_n \int_{-\infty}^{\infty}\frac{e^{ik_x x}}{\sqrt{2\pi}}\frac{1}{E-k_x^2+i\epsilon}\frac{e^{-ik_x a_n}}{\sqrt{2\pi}}\chi(a_n)\,\langle y|\phi\rangle\, dk_x \\ =& \phi(y)\sum_{n=1}^{N}\xi_n\chi(a_n)\mathcal{G}(x-a_n),\end{aligned} \tag{4.1.12}$$

where $\mathcal{G}$ is the Green's function for the x-component of the differential equation,

$$\mathcal{G}(x-x') := \langle x|\left(-E+k_x^2+i\epsilon\right)^{-1}|x'\rangle = -\frac{ie^{ik_x|x-x'|}}{2k_x}, \tag{4.1.13}$$

where it is important to note that, in this chapter, we take the signature of the Green's function opposite to the last chapter to stick to the notation in our relevant paper. Substituting these results in the Lippmann-Schwinger equation, we find the x-component of the solution as

$$\chi(x) = e^{ik_x x} - \frac{i}{2k_x}\sum_{n}^{N}\xi_n e^{ik_x|x-a_n|}\chi(a_n)\ . \tag{4.1.14}$$

At this point, we do the similar calculation to the principal matrix calculation earlier: We take $x = a_m$, with $m = 1,\ldots,N$, and arrive at the following system of linear

equations for $\chi(a_n)$.

$$\sum_{n=1}^{N} T_{nm}\chi(a_n) = e^{ik_x a_m}, \tag{4.1.15}$$

where

$$T_{nm} = \delta_{nm} + \frac{i\xi_n}{2k_x} e^{ik_x|a_m - a_n|} = \begin{cases} 1 + \frac{i\xi_n}{2k_x} & \text{for} \quad n = m, \\ \frac{i\xi_n}{2k_x}\, e^{ik_x|a_m - a_n|} & \text{for} \quad n \neq m, \end{cases} \tag{4.1.16}$$

plays the role of the principal matrix in this case. Hence, combining the equations (4.1.7) and (4.1.14) and inserting the expression in (4.1.15), we can express the scattering solution (4.1.6) of the Schrödinger equation (4.1.3) in the form,

$$\langle \mathbf{x}|\psi_0(\mathbf{k})\rangle = \frac{1}{2\pi}\left[e^{i\mathbf{k}\cdot\mathbf{x}} - i\sum_{m,n=1}^{N} e^{ik_x a_m} A^{-1}_{mn}\, e^{i(k_x|x-a_n|+k_y y)}\right], \tag{4.1.17}$$

where we make another simplification in the notation as we introduce A-matrix in terms of T as

$$A_{mn} = \frac{2k_x T_{mn}}{\xi_m} = \frac{2k_x\,\delta_{mn}}{\xi_m} + ie^{ik_x|a_m - a_n|} = \begin{cases} \frac{2k_x}{\xi_m} + i & \text{for} \quad n = m, \\ ie^{ik_x|a_m - a_n|} & \text{for} \quad n \neq m. \end{cases} \tag{4.1.18}$$

We need to compare the solution in (4.1.17) with the well-known form of the scattering solution in two dimensions which is

$$\psi(\mathbf{k},\mathbf{x}) = \frac{1}{2\pi}\Big[e^{i\mathbf{k}\cdot\mathbf{x}} + f(\mathbf{k}',\mathbf{k})\frac{e^{ikr}}{\sqrt{r}}\Big] \qquad \text{for} \quad r \to \infty \tag{4.1.19}$$

to obtain the scattering amplitude expression, $f(\mathbf{k}',\mathbf{k})$. Therefore, we should look at the long distance behaviour of the solution in (4.1.17). To do that, we need to obtain the asymptotic expression for the second term of the right-hand side of (4.1.17).

Let us start with writing the scattering part of the wave function as

$$\psi_{\text{scatt}}(\mathbf{x}) = \frac{-i}{2\pi}\sum_{m,n=1}^{N} e^{ik_x a_m} A^{-1}_{mn}\, e^{i(k_x|x-a_n|+k_y y)}. \tag{4.1.20}$$

We already know that the scattering part of the wave solution should look like

$$\psi_{\text{scatt}}(\mathbf{x}) \to \frac{e^{ikr}}{2\pi\sqrt{r}}\, f(\mathbf{k}', \mathbf{k}) \quad \text{for} \quad r \to \infty \tag{4.1.21}$$

in two dimensions according to the expression in (4.1.19). So we need to compare the right-hand side of (4.1.20) with (4.1.21). We can rewrite the scattering part by expressing the magnitude term in the exponential as below

$$\psi_{\text{scatt}}(\mathbf{x}) = \frac{e^{ik_y y}}{2\pi} \sum_{n=1}^{N} \Big[\mathfrak{t}_n^{+}\ \Theta(x - a_n) e^{ik_x x} + \mathfrak{t}_n^{-}\ \Theta(a_n - x) e^{-ik_x x} \Big], \tag{4.1.22}$$

where

$$\mathfrak{t}_n^{\pm} := -i \sum_{m=1}^{N} A_{mn}^{-1}\ e^{ik_x(a_m \mp a_n)} \tag{4.1.23}$$

and $\Theta(x)$ is the step function. Because $k_x > 0$ and the incidence angle θ_0 takes values in the interval $(-\frac{\pi}{2}, \frac{\pi}{2})$. Therefore, the scattering angle θ ranges over the interval $[-\frac{\pi}{2}, \frac{3\pi}{2})$ and we can define θ^+ and θ^- angles as:

$$\begin{aligned} \theta^+ &:= \theta \qquad\quad \text{for} \quad \theta \in (-\tfrac{\pi}{2}, \tfrac{\pi}{2}), \\ \theta^- &:= \pi - \theta \quad \text{for} \quad \theta \in (\tfrac{\pi}{2}, \tfrac{3\pi}{2})\ . \end{aligned}$$

We introduce these angles to be able to use the asymptotic expansion expression given in Appendix A of the reference [85] which is

$$e^{ik_y y} e^{\pm ik_x x} \to \sqrt{\frac{2\pi}{kr}}\ \Big[e^{i(kr - \frac{\pi}{4})} \delta(\theta_0 - \theta^{\pm}) + e^{-i(kr - \frac{\pi}{4})} \delta(\theta_0 - \theta^{\pm} + \pi) \Big] \tag{4.1.24}$$

as $r \to \infty$. We need this expansion to write the exponential terms of (4.1.22) more clearly. Putting (4.1.24) in (4.1.20), we obtain

$$\begin{aligned} \psi_{\text{scatt}}(\mathbf{x}) = &- e^{ikr} \sqrt{\frac{i}{2\pi r k}} \\ &\times \sum_{n,m=1}^{N} A_{mn}^{-1} \Big[e^{ik_x(a_m - a_n)} \delta(\theta - \theta_0) + e^{ik_x(a_m + a_n)} \delta(\theta + \theta_0 - \pi) \Big], \end{aligned} \tag{4.1.25}$$

which gives the scattering amplitude as

$$f_0(\mathbf{k}',\mathbf{k}) = -\sqrt{\frac{2\pi i}{k}}\sum_{n,m=1}^{N} A^{-1}_{mn}\Big[e^{ik_x(a_m-a_n)}\delta(\theta-\theta_0)+e^{ik_x(a_m+a_n)}\delta(\theta+\theta_0-\pi)\Big]$$
$$=\sqrt{\frac{2\pi}{k}}\,e^{-i\pi/4}\Big[\mathfrak{t}^+(\mathbf{k})\delta(\theta-\theta_0)+\mathfrak{t}^-(\mathbf{k})\delta(\theta+\theta_0-\pi)\Big], \tag{4.1.26}$$

where we have introduced

$$\mathfrak{t}^+(\mathbf{k}) := -i\sum_{n,m=1}^{N} A^{-1}_{mn}e^{ik_x(a_m-a_n)} = -i\sum_{n,m=1}^{N} A^{-1}_{mn}\cos[k_x(a_m-a_n)], \tag{4.1.27}$$

$$\mathfrak{t}^-(\mathbf{k}) := -i\sum_{n,m=1}^{N} A^{-1}_{mn}e^{ik_x(a_m+a_n)}, \tag{4.1.28}$$

and used the fact that A^{-1} is a symmetric matrix, i.e., $A^{-1}_{nm} = A^{-1}_{mn}$. As we look at the expression in (4.1.26), we see that the scattering is determined at only two angles; at $\theta = \theta_0$ and $\theta = \pi - \theta_0$. This is an expected result since the potential is only x-dependent and there is nothing to change the y-component of the momentum vector and this is why our setup acts like the basic scattering problem in one dimension: there are only reflected and transmitted parts of the incoming wave.

4.2. Geometric scattering as a perturbation to line defects

To see how the presence of the line defects affect the geometric scattering, we will add the locally curved geometry of the space to the Hamiltonian as a perturbation. We need to be careful when defining this space dependent perturbation. We need to embed the locally curved surface in the flat space, $\mathbb{R}^3$, and force the scattering particle to stay on this surface to obtain a problem in two dimensions. In this work, we follow the calculations which model the effect of the confining forces in terms of the thin-layer quantization scheme of Ref. [77]. The Hamiltonian operator written on a curved space is

$$H_{\text{curved}} = -g^{1/2}\partial_i(g^{ij}g^{1/2})\partial_j + \left(\lambda_1 K + \lambda_2 M^2\right), \tag{4.2.1}$$

where g is the metric tensor, K and M are the Gaussian and the mean curvatures of the surface respectively and their couplings are λ_1 and λ_2. According to da Costa [77],

$\lambda_1 = \lambda_2 = -1/2$ and we give the plots for different values of the couplings such as 0, $1/2$ and $-1/2$. In our case, the Hamiltonian can be written as

$$H = -g^{1/2}\partial_i(g^{ij}g^{1/2})\partial_j + (\lambda_1 K + \lambda_2 M^2) + V_0 \tag{4.2.2}$$

where V_0 is the potential defining the linear defects. Our claim that we can write this Hamiltonian as

$$H = H_0 + V_0 + \zeta V_1 = H_0 + V \tag{4.2.3}$$

where H_0 is the free Hamiltonian and ζ is the perturbation parameter that we will use to keep track of the strength of the geometric contributions. We can use the standard perturbation theory to write the scattering solution [28]

$$|\psi(\mathbf{k})\rangle = \sum_{n=0}^{\infty} \zeta^n |\psi_n(\mathbf{k})\rangle, \tag{4.2.4}$$

and using the Lippmann-Schwinger equation we have

$$|\psi_n(\mathbf{k})\rangle = \begin{cases} \left[1 - R_0^+(E)V_0\right]^{-1} |\mathbf{k}\rangle & \text{for} \quad n = 0, \\ \left[1 - R_0^+(E)V_0\right]^{-1} R_0^+(E)V_1|\psi_{n-1}(\mathbf{k})\rangle & \text{for} \quad n \geq 1, \end{cases} \tag{4.2.5}$$

where $|\mathbf{k}\rangle$ is the plane wave solution. We can also write the total scattering amplitude as a series as

$$f(\mathbf{k}', \mathbf{k}) = \sum_{n=0}^{\infty} \zeta^n f_n(\mathbf{k}', \mathbf{k}) \ . \tag{4.2.6}$$

Combining (4.1.19) and (4.1.4), we know that we can write the scattering amplitude for the potential V as

$$f(\mathbf{k}', \mathbf{k}) \ := \ -\pi\sqrt{\frac{2\pi i}{k}}\, \langle \mathbf{k}'|V|\psi(\mathbf{k})\rangle \tag{4.2.7}$$

where we use a slightly different convention then the earlier chapter (as we keep $\sqrt{i}$ term). So for the nth term of the scattering amplitude we can write

$$f_n(\mathbf{k}', \mathbf{k}) = \ -\pi\sqrt{\frac{2\pi i}{k}} \times \begin{cases} \langle \mathbf{k}'|V_0|\psi_0(\mathbf{k})\rangle & \text{for} \quad n = 0, \\ \langle \mathbf{k}'|V_0|\psi_n(\mathbf{k})\rangle + \langle \mathbf{k}'|V_1|\psi_{n-1}(\mathbf{k})\rangle & \text{for} \quad n \geq 1. \end{cases} \tag{4.2.8}$$

We take the first Born approximation in our calculations and it implies ignoring all the terms except of the order of ζ. Hence, we are interested in the $n = 0$ and $n = 1$ terms only which are

$$f_0(\mathbf{k}', \mathbf{k}) = -\pi\sqrt{\frac{2\pi i}{k}}\langle \mathbf{k}'|V_0|\psi_0(\mathbf{k})\rangle, \tag{4.2.9}$$

and

$$f_1(\mathbf{k}', \mathbf{k}) = -\pi\sqrt{\frac{2\pi i}{k}}\left[\langle \mathbf{k}'|V_0|\psi_1(\mathbf{k})\rangle + \langle \mathbf{k}'|V_1|\psi_0(\mathbf{k})\rangle\right] \ . \tag{4.2.10}$$

We note that the zeroth order wave solution and the scattering amplitude, $|\psi_0(\mathbf{k})\rangle$ and $f_0(\mathbf{k}', \mathbf{k})$, are already calculated in section 4.1. Setting $n = 1$ in (4.2.5) and replacing $|\psi_1(\mathbf{k})\rangle$ with the obtained expression, we get

$$\begin{aligned}
\langle \mathbf{k}'|V_0|\psi_1(\mathbf{k})\rangle + \langle \mathbf{k}'|V_1|\psi_0(\mathbf{k})\rangle =& \langle \mathbf{k}'|V_0[1 - R_0^+(E)V_0]^{-1}R_0^+(E)V_1|\psi_0(\mathbf{k})\rangle \\
&+ \langle \mathbf{k}'|V_1|\psi_0(\mathbf{k})\rangle \\
=& \langle \mathbf{k}'|(V_0[1 - R_0^+(E)V_0]^{-1}R_0^+(E) + 1)V_1|\psi_0(\mathbf{k})\rangle \\
=& \langle \tilde{\psi}_0(\mathbf{k}')|V_1|\psi_0(\mathbf{k})\rangle,
\end{aligned} \tag{4.2.11}$$

where we define

$$\langle \tilde{\psi}_0(\mathbf{k})| = \langle \mathbf{k}|\, V_0[1 - R_0^+(E)V_0]^{-1}R_0^+(E) + \langle \mathbf{k}| \tag{4.2.12}$$

Now using the series expansion

$$(1 - R_0^+(E)V_0)^{-1} = 1 + R_0^+(E)V_0 + ... \tag{4.2.13}$$

we obtain

$$\begin{aligned}
\langle \tilde{\psi}_0(\mathbf{k})| &= \langle \mathbf{k}|\left[V_0(1 + R_0^+(E)V_0 + ...)R_0^+(E) + 1\right] \\
&= \langle \mathbf{k}|\left[(1 + V_0R_0^+(E) + ...)V_0R_0^+(E) + 1\right] \\
&= \langle \mathbf{k}|\left[(1 - V_0R_0^+(E))^{-1}V_0R_0^+(E) + (1 - V_0R_0^+(E))^{-1}(1 - V_0R_0^+(E))\right] \\
&= \langle \mathbf{k}|\,(1 - V_0R_0^+(E))^{-1} \ .
\end{aligned} \tag{4.2.14}$$

With this expression in (4.2.14), we can write f_1 as

$$\begin{aligned} f_1(\mathbf{k}', \mathbf{k}) &= -\pi\sqrt{\frac{2\pi i}{k}}\langle\tilde{\psi}_0(\mathbf{k}')|V_1|\psi_0(\mathbf{k})\rangle \\ &= -\pi\sqrt{\frac{2\pi i}{k}}\int\int \langle\tilde{\psi}_0(\mathbf{k}')|\mathbf{x}'\rangle\,\langle\mathbf{x}'|V_1|\mathbf{x}\rangle\,\langle\mathbf{x}|\psi_0(\mathbf{k})\rangle\, d\mathbf{x}'d\mathbf{x}\ . \end{aligned} \tag{4.2.15}$$

Subtracting the free part, H_0, and V_0 from the Hamiltonian given in (4.2.2), we can write the ζV_1 part of the potential as

$$\zeta\langle\mathbf{x}'|V_1|\mathbf{x}\rangle = \mathcal{L}_{\mathbf{x}'}\,\delta(\mathbf{x}'-\mathbf{x}), \tag{4.2.16}$$

where $\mathcal{L}_{\mathbf{x}}$ is the differential operator,

$$\mathcal{L}_{\mathbf{x}} := \left[g_0^{ij}(x) - g^{ij}(x)\right]\partial_i\partial_j - \frac{\partial_i[\sqrt{g(x)}g^{ij}(x)]}{\sqrt{g(x)}}\partial_j + 2\lambda_1 K(x) + 2\lambda_2 M(x)^2, \tag{4.2.17}$$

and g_0^{ij} are the components of the inverse of the Euclidean metric tensor $\mathfrak{g}_0$. According to our observation in section 4.1 which says that $f_0(\mathbf{k}', \mathbf{k})$ vanishes for angles θ other than θ_0 and $\pi - \theta_0$, we can claim that

$$f(\mathbf{k}', \mathbf{k}) \approx \zeta\, f_1(\mathbf{k}', \mathbf{k}) \quad \text{for} \quad \theta \notin \{\theta_0, \pi - \theta_0\}.$$

Delta potential in (4.2.16) drops $d\mathbf{x}$ integral and we are left with the scattering amplitude expression that we need to handle as below

$$\zeta\, f_1(\mathbf{k}', \mathbf{k}) = -\pi\sqrt{\frac{2\pi i}{k}}\int_{\mathbb{R}^2} d^2\mathbf{x}'\,\langle\tilde{\psi}_0(\mathbf{k}')|\mathbf{x}'\rangle\,\mathcal{L}_{\mathbf{x}'}\langle\mathbf{x}'|\psi_0(\mathbf{k})\rangle. \tag{4.2.18}$$

So we need to compute $\langle\tilde{\psi}_0(\mathbf{k})|\mathbf{x}\rangle$. Projecting the equation (4.2.14) onto position space

$$\langle\tilde{\psi}_0(\mathbf{k})|\mathbf{x}\rangle = \langle\mathbf{k}|\,(1 - V_0 R_0^+(E))^{-1}\,|\mathbf{x}\rangle \tag{4.2.19}$$

which can be written as

$$\langle\tilde{\psi}_0(\mathbf{k})|\mathbf{x}\rangle = \langle\mathbf{k}|\mathbf{x}\rangle + \langle\mathbf{k}|\,V_0 R_0^+(E)\,|\mathbf{x}\rangle\ , \tag{4.2.20}$$

then we have

$$\tilde{\psi}_0(\mathbf{k}, \mathbf{x}) = \frac{1}{2\pi}\left[e^{i\mathbf{k}\cdot\mathbf{x}} + i\sum_{m,n=1}^{N} e^{ik_x a_m} A^{-1*}_{mn}\, e^{i(-k_x|x-a_n|+k_y y)}\right]. \tag{4.2.21}$$

Finally, we substitute (4.1.17) and (4.2.21) in (4.2.18) to obtain

$$\zeta f_1(\mathbf{k}',\mathbf{k}) = -\frac{1}{2}\sqrt{\frac{i}{2\pi k}}\Bigg[I_0 - i\sum_{m,n=1}^{N}\left(A'^{-1}_{mn}I_{mn} + A^{-1}_{mn}J_{mn}\right) - \sum_{m,n,m',n'=1}^{N} A'^{-1}_{mm'}A^{-1}_{nn'}I_{mm'nn'}\Bigg], \tag{4.2.22}$$

where A'^{-1}_{mn} stands for A^{-1}_{mn} with k_x replaced with k'_x, and I_0, I_{mn}, J_{mn}, and $I_{mm'nn'}$ are complex coefficients given by

$$I_0 := \int_{\mathbb{R}^2} d^2\mathbf{x}'\, e^{-i\mathbf{k}'\cdot\mathbf{x}'}\mathcal{L}_{\mathbf{x}'}\, e^{i\mathbf{k}\cdot\mathbf{x}'}, \tag{4.2.23}$$

$$I_{mn} := \int_{\mathbb{R}^2} d^2\mathbf{x}'\left(e^{-ik'_{x'}a_m}\; e^{-ik'_{y'}y'}\, e^{-ik'_{x'}|x'-a_n|}\right)\mathcal{L}_{\mathbf{x}'}\, e^{i\mathbf{k}\cdot\mathbf{x}'}, \tag{4.2.24}$$

$$J_{mn} := \int_{\mathbb{R}^2} d^2\mathbf{x}' e^{-i\mathbf{k}'\cdot\mathbf{x}'}\mathcal{L}_{\mathbf{x}'}\left(e^{ik_{x'}a_m}\; e^{ik_{y'}y'}e^{ik_{x'}|x'-a_n|}\right), \tag{4.2.25}$$

$$I_{mm'nn'} := \int_{\mathbb{R}^2} d^2\mathbf{x}'\left(e^{-ik'_{x'}a_{m'}}\; e^{-ik'_{y'}y'}e^{-ik'_{x'}|x'-a_m|}\right) \times \mathcal{L}_{\mathbf{x}'}\left(e^{ik_{x'}a_{n'}}\; e^{ik_{y'}y'}e^{ik_{x'}|x'-a_n|}\right). \tag{4.2.26}$$

4.3. Scattering by a Gaussian Bump with Line Defects

Let us take the asymptotically flat surface S considered here as it has a cylindrical symmetry. The setup of such a system is pictured in Figure 4.2. In other words, we have a surface defined by

$$z = f(r), \tag{4.3.1}$$

where (r,θ,z) are the cylindrical coordinates in $\mathbb{R}^3$ and f is a smooth function satisfying

$$\lim_{r\to\infty}\dot{f}(r) = \lim_{r\to 0}\dot{f}(r) = 0 \tag{4.3.2}$$

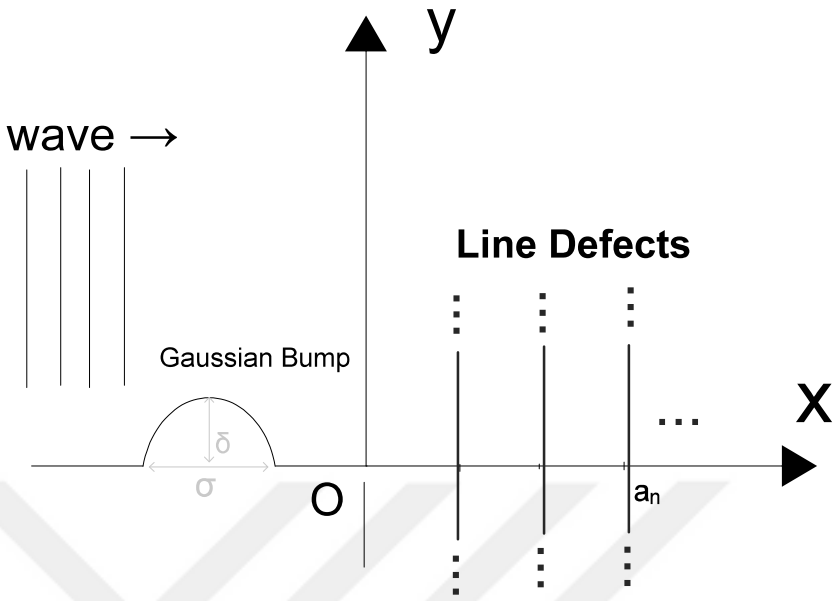

Figure 4.2. Line Defects and a Gaussian Bump.

being $\dot{f}(r) = \frac{\partial}{\partial r} f(r)$ [27]. We need to write operator $\mathcal{L}$ accordingly. The components of the metric tensor take the form [26]:

$$g_{11} = 1 + \dot{f}^2, \qquad g_{12} = g_{21} = 0, \qquad g_{22} = r^2, \tag{4.3.3}$$

and also we can express the Gaussian and mean curvatures of the surface S as

$$K = \frac{G\dot{G}}{r}, \qquad M = \frac{1}{2}\left(\frac{G}{r} + \dot{G}\right), \tag{4.3.4}$$

respectively, where we define G as

$$G = \frac{\dot{f}}{\sqrt{1 + \dot{f}^2}}. \tag{4.3.5}$$

We insert the expressions given in (4.3.3) and (4.3.4) into $\mathcal{L}$ and obtain

$$\mathcal{L}_{\mathbf{x}} = G^2 \left[\partial_r^2 + \tfrac{1}{r}\left(1 + \tfrac{r\dot{G}}{G}\right)\partial_r + \tfrac{2\lambda_1 \dot{G}}{rG} + \tfrac{\lambda_2}{2r^2}\left(1 + \tfrac{r\dot{G}}{G}\right)^2\right]. \tag{4.3.6}$$

To describe a local Gaussian bump, we take

$$f(r) = \delta \quad e^{-r^2/2\sigma^2}, \tag{4.3.7}$$

where δ and σ are real and indicate the height and width of Gaussian bump respectively. We assume that $(\delta/\sigma)^2 = \eta \ll 1$, i.e., the bump is very low. We will ignore the terms higher orders of η in our calculations. We choose $\Delta k = k - k^{'}$ lies along the x'-axis for simplicity.

If we use Θ (respectively θ) to denote the angle between k and $k^{'}$ (respectively $\mathbf{k}'$ and the x'-axis), we can show that $\theta = (\pi + \Theta)/2$ and $|\mathbf{k}' - \mathbf{k}| = 2ks$, where we define

$$s = \sin(\Theta/2).$$

We use all these and calculate the integral in (4.2.23), we find [27, 28]:

$$I_0 = \frac{\pi\,\eta\, e^{-s^2\mathfrak{K}^2}}{2}\Big[(4\lambda_1 s^2 - 1)\mathfrak{K}^2 + \lambda_2(s^4\mathfrak{K}^4 + 2)\Big] + \mathcal{O}(\eta^2). \tag{4.3.8}$$

where $\mathfrak{K} := k\sigma$. The rest of the coefficient integrals in (4.2.24), (4.2.25) and (4.2.26) are a bit more difficult to calculate since they involve functions of Cartesian coordinates (x', y'). We therefore perform a coordinate transformation to express the right-hand side of (4.3.6) in Cartesian coordinates. Using the Cartesian $\mathcal{L}$ various properties of Bessel functions and the identities,

$$\frac{d|x|}{dx} = \mathrm{sgn}(x), \qquad\qquad \frac{d^2|x|}{dx^2} = 2\delta(x),$$

we can compute I_{mn}, J_{mn}, and $I_{mnm'n'}$ in terms of the error and complementary error functions with the help of Mathematica. The results of these integrals are given in Appendix A since they are very long and complicated. So in principle, we have an explicit expression for the scattering amplitude of the Gaussian bump (4.3.7) in the presence of N parallel line defects located at $x = a_n$ with $n = 1, .., N$. We will look at the behaviour of the scattering amplitude with the help of plots since it is very complicated to examine analytically. So we need to set some numbers.

We take the delta function potential $\xi_n \delta(x - a_n)$ as a barrier potential,

$$V_n(x, y) := \begin{cases} V_0 & \text{for} \quad |x - a_n| \leq \rho/2, \\ 0 & \text{for} \quad |x - a_n| > \rho/2, \end{cases} \tag{4.3.9}$$

where $V_0 := \xi_n/\rho$ and ρ are respectively the height and width of the barrier. We compare V_0 with the energy of the incoming electron $E = k^2$. V_0 must be much larger than k^2 to be able to behave as a delta potential. Also ρ must be much smaller than the length scales of the problem which are the de Broglie wavelength $\lambda_{\text{dB}} = 2\pi/k$ and the width of the Gaussian bump σ , i.e.,

$$V_0 \gg E, \qquad \rho \ll \lambda_{\text{dB}}, \qquad \rho \ll \sigma. \tag{4.3.10}$$

Since we want our system to be sensitive to the non-trivial local geometry, we consider the scattering of the particles with wavelengths λ_{dB} which are of the same order of magnitude as σ. This means that $\mathfrak{K} = k\sigma$ should be of the order of 1. For these waves, we only need to satisfy the first two of the conditions listed in (4.3.10). We can express the first of these condition as $\xi_n \gg k^2\rho$. Therefore it will be fulfilled, if $\sigma\xi_n \gg k\rho$. Note also that the second condition in (4.3.10) is equivalent to $k\rho \ll 1$.

In our numerical settings, we take

$$V_0 \approx 1 \text{ eV}, \qquad \rho \approx 1 \text{ nm}, \qquad \mathfrak{z}_n = \sigma^{-1}, \tag{4.3.11}$$

and suppose that the effective mass of the electron is given by $m \approx 10^{-2} m_{\text{e}}$ since it is a part of a dilute electron gas. Then it is easy to show that $E \ll V_0$ will imply $k\rho \ll 1$. For example, for $E \approx 10^{-3}$ eV we find $k\rho \approx 0.02$.

We have the differential cross section, $|f(\mathbf{k}', \mathbf{k})|^2$, plots for a Gaussian bump when there are none, one or two line defects as a function of $\mathfrak{K} = k\sigma$.

In Figure 4.3, we plot the differential cross section versus $\mathfrak{K}$ when there is only one line defect accompanies the Gaussian bump with fixing the other parameters. As we can see, the scattering effect is more sensible when the line defect is not located on

the center of the Gaussian bump, but before or after the bump. We see that locating the line defect before or after the bump, i.e., taking $x = 3\sigma$ or $x = -3\sigma$, does not make any difference on the cross section plot. Also when we look at our numerical results, we see that the values for the cross section are not identical but very close which are not visible in our plots. In Figure 4.4, there are two line defects. We see that when we locate the bump between the line defects, the amplification in the differential cross section seems drastic. There is still an amplification, which does not seem identical this time, when we locate one of the line defects on the center of the bump, and the other before or after the bump (first and second plots in Figure 4.4). However, as we look at the numerical values, we see that the boost is much larger in the geometric scattering demonstrated in the third plot of Figure 4.4 and we can make the interpretation that when line defects located symmetrically to the bump, they function as a resonator. We also see that, the amplification seems higher at the relatively small angles, $\theta = 5^\circ$ and $\theta = 30^\circ$.

In Figures 4.5 and 4.6, we plot $|f(\mathbf{k}', \mathbf{k})|^2$ versus θ for a Gaussian bump with one or two line defects, respectively. In this case, we fix $\mathfrak{K} = k\sigma = 1$ and take different values of the curvature coefficients λ_1 and λ_2. These graphs are compatible with the observations in Figures 4.3 and 4.4. For the one line defect, the plots seem identical and the values are a bit higher then the case when the line is located on the center of the bump. Also, there is a sharp amplification in the third plot of Figure 4.6, which is the case when the bump is located between the lines and this points to the resonance effect.

We also have the graph when there is no line defects, but the Gaussian bump only which is given in Figure 4.7. Comparing the numerical values, we see that the presence of line defects indeed magnify the geometric scattering effects. Despite to the case when there are point defects which have effects on the cross section at every scattering angle θ [28], line defects only produce reflected and transmitted waves at angles $\theta = \theta_0$ and $\pi - \theta_0$ as we calculated earlier. Therefore, we see the effects of the line defects on the scattering from the bump at angles other than θ_0 and $\pi - \theta_0$.

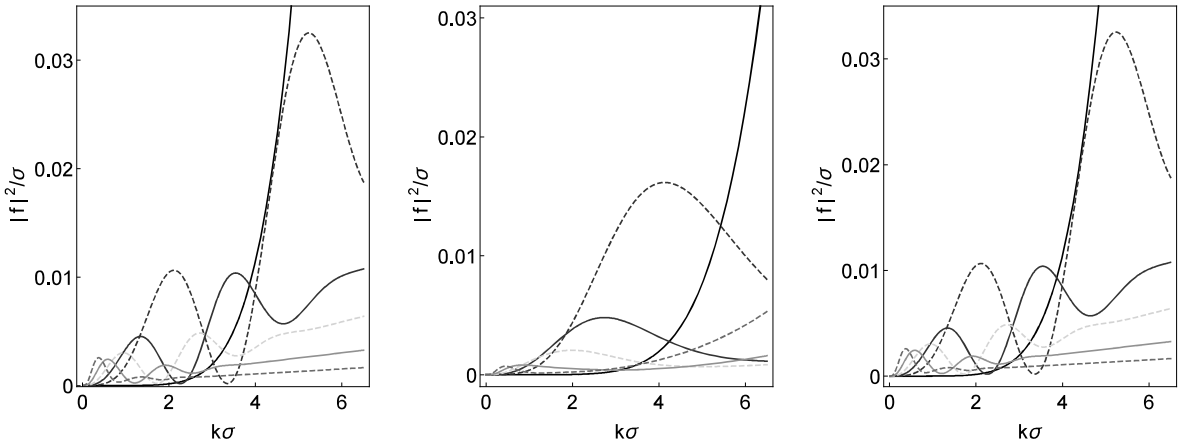

Figure 4.3. Plots of $|f(k',k)|^2/\sigma$ as functions of $k\sigma$ for the Gaussian bump (4.3.7) with a line defect at $x=-3\sigma$ (on the left), $x=0$ (in the middle), and $x=3\sigma$ (on the right) for $\theta_0=0^\circ$, $\eta=0.1$, $\sigma\mathfrak{z}_1=1$, $\lambda_1=-\lambda_2=1/2$, and different values of θ, namely $\theta=5^\circ$ (black), $\theta=30^\circ$ (dashed purple), 45° (blue), 60° (dashed green), 90° (orange), and 175° (dashed red).

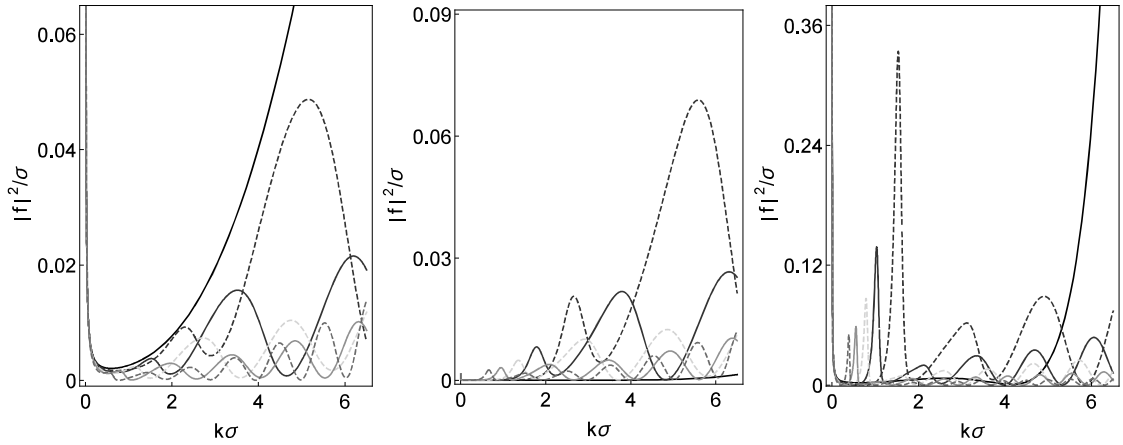

Figure 4.4. Plots of $|f(k',k)|^2/\sigma$ as functions of $k\sigma$ for the Gaussian bump (4.3.7) with two line defects at $x=-3\sigma$ and $x=0$ (on the left), $x=0$ and $x=3\sigma$ (in the middle), and $x=\pm 3\sigma$ (on the right) for $\theta_0=0^\circ$, $\eta=0.1$, $\sigma\mathfrak{z}_1=1$, $\lambda_1=-\lambda_2=1/2$, and different values of θ, namely $\theta=5^\circ$ (black), $\theta=30^\circ$ (dashed purple), 45° (blue), 60° (dashed green), 90° (orange), and 175° (dashed red).

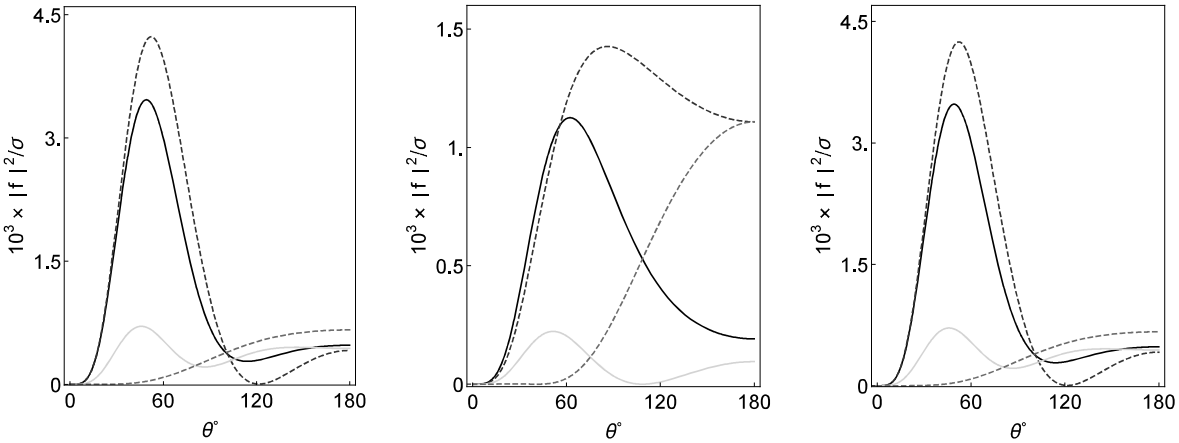

Figure 4.5. Plots of $|f(k', k)|^2/\sigma$ as functions of θ for the Gaussian bump (4.3.7) with a line defect at $x = -3\sigma$ (on the left), $x = 0$ (in the middle), and $x = 3\sigma$ (on the right) for $\theta_0 = 0^\circ$, $\eta = 0.1$, $\sigma\mathfrak{z}_1 = k\sigma = 1$, and different values of λ_1 and λ_2, namely $\lambda_1 = -\lambda_2 = 1/2$ (black), $\lambda_1 = 0$ and $\lambda_2 = -1/2$ (dashed blue), $\lambda_1 = 1/2$ and $\lambda_2 = 0$ (green), and $\lambda_1 = \lambda_2 = 1/2$ (dashed red).

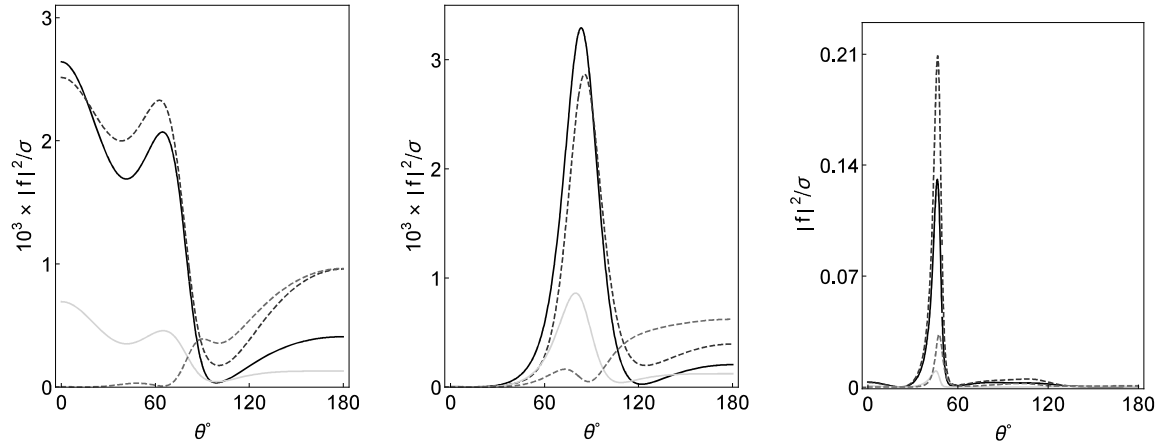

Figure 4.6. Plots of $|f(k', k)|^2/\sigma$ as functions of θ for the Gaussian bump (4.3.7) with two line defects at $x = -3\sigma$ and $x = 0$ (on the left), $x = 0$ and $x = 3\sigma$ (in the middle), and $x = \pm 3\sigma$ (on the right) for $\theta_0 = 0^\circ$, $\eta = 0.1$, $\sigma\mathfrak{z}_1 = k\sigma = 1$, and different values of λ_1 and λ_2, namely $\lambda_1 = -\lambda_2 = 1/2$ (black), $\lambda_1 = 0$ and $\lambda_2 = -1/2$ (dashed blue), $\lambda_1 = 1/2$ and $\lambda_2 = 0$ (green), and $\lambda_1 = \lambda_2 = 1/2$ (dashed red).

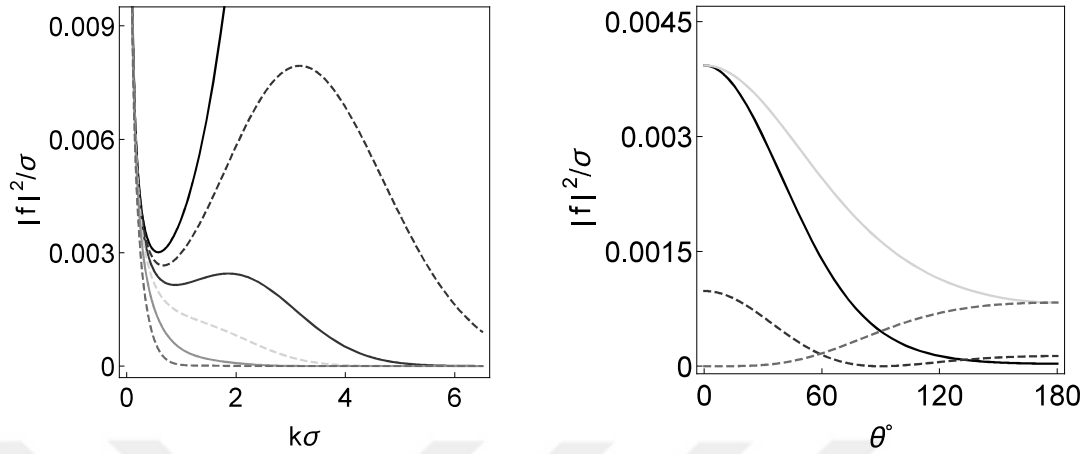

Figure 4.7. Plots of $|f(k^{'}, k)|^2/\sigma$ as functions of $\mathfrak{K} = k\sigma$ (on the left) and θ (on the right) for the Gaussian bump (4.3.7) in the absence of the line defects with the same values of the physical parameters as in Figures 4.3 and 4.4. The graphs in the left panel correspond to the scattering angles: $\theta = 5^\circ$ (black), $\theta = 30^\circ$ (dashed purple), 45° (blue), 60° (dashed green), 90° (orange), and 175° (dashed red). Those in the right panel correspond to the curvature coefficients: $\lambda_1 = -\lambda_2 = 1/2$ (black), $\lambda_1 = 0$ and $\lambda_2 = -1/2$ (dashed blue), $\lambda_1 = 1/2$ and $\lambda_2 = 0$ (green), and $\lambda_1 = \lambda_2 = 1/2$ (dashed red).

4.4. Scattering From a Line Segment and a Point Defect

Following these calculations, we want to combine the cases when there are line defects and point defects. However, we could not succeed to obtain an analytical solution of this problem since Mathematica can not calculate the integrals containing the product of two Hankel functions. So instead, we will make an approximation. In [55], authors also give another approximate solution to this problem. We will use a line "segment" with length L approximation on the line defect (kL is small compared to the wavelength) to search for the scattering on a flat space, as pictured in Figure 4.8. The principal matrix, Φ, for a general curve defect and a point defect is

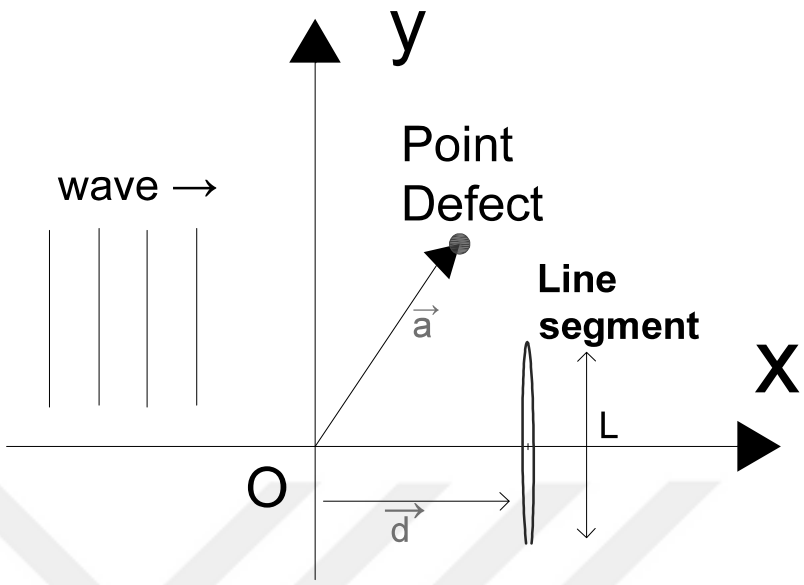

Figure 4.8. Line segment and a point defect.

$$\Phi = \begin{bmatrix} \frac{1}{\xi_1} - \langle f_1 | \, R_0^+(E) \, | f_1 \rangle & \langle f_1 | \, R_0^+(E) \, | f_2 \rangle \\ \langle f_2 | \, R_0^+(E) \, | f_1 \rangle & \frac{1}{\xi_2} - \langle f_2 | \, R_0^+(E) \, | f_2 \rangle \end{bmatrix}. \tag{4.4.1}$$

Here $|f_1\rangle = |\mathbf{a}\rangle$ represents the point defect and $|f_2\rangle = |\Gamma\rangle$ is the curve defect. We already have Φ_{11} renormalized

$$\Phi_{11}(E) = \frac{1}{\xi_R} - \frac{1}{2\pi} \ln\left(\frac{k}{\mu}\right) - \frac{i}{4} \tag{4.4.2}$$

and we introduce the renormalized coupling as

$$\frac{1}{\xi_1} - \frac{1}{2\pi} \ln\left(\frac{\Lambda}{\mu}\right) = \frac{1}{\xi_R} \tag{4.4.3}$$

where Λ is the cut-off regularization parameter, μ is the renormalization constant and ξ_R is the renormalized interaction strength. The off-diagonal terms of the Φ matrix are not divergent. To get the elements of the Φ-matrix we consider the definition of the resolvent operator as $R_0^+ = (E - k^2)^{-1}$. The general resolvent of this case in terms of the T-matrix is:

$$R(E) = R_0^+(E) + R_0^+(E) \; T(E) \; R_0^+(E) \tag{4.4.4}$$

where, R_0^+ has the integral kernel which is the free Green's function in two dimensions which is

$$R_0^+(\mathbf{x},\mathbf{x}') = \frac{i}{4}H_0^{(1)}(k|\mathbf{x}-\mathbf{x}'|)\ . \tag{4.4.5}$$

We can write $T-$matrix as

$$T = |f_i\rangle\, \Phi_{ij}^{-1}\, \langle f_j| \tag{4.4.6}$$

where the inverse of the Φ-matrix is given by

$$\begin{aligned}\Phi^{-1} = &\left[(\frac{1}{\xi_R} - \frac{1}{2\pi}\ln\left(\frac{k}{\mu}\right) - \frac{i}{4})(\frac{1}{\xi_2} - \frac{i}{4}\int\int_0^L H_0^{(1)}(k|\gamma(s)-\gamma(s')|)\ \frac{dsds'}{L^2})\right.\\ &\left. + \frac{1}{16}\left(\int_0^L H_0^{(1)}(k|\gamma(s)-\mathbf{a}|)\frac{ds}{L}\right)^2\right]^{-1}\\ &\times\begin{bmatrix}\left(\frac{1}{\xi_2} - \frac{i}{4}\int\int_0^L H_0^{(1)}(k|\gamma(s)-\gamma(s')|)\frac{dsds'}{L^2}\right) & \left(\frac{i}{4}\int_0^L H_0^{(1)}(k|\gamma(s)-\mathbf{a}|)\frac{ds}{L}\right)\\ \left(\frac{i}{4}\int_0^L H_0^{(1)}(k|\gamma(s)-\mathbf{a}|)\frac{ds}{L}\right) & (\frac{1}{\xi_R} - \frac{1}{2\pi}\ln\left(\frac{k}{\mu}\right) - \frac{i}{4})\end{bmatrix}.\end{aligned} \tag{4.4.7}$$

Here L is the length of the curve, $\gamma(s)$ represents the position vector of the curve Γ, $s \in [0, L]$, $\mathbf{a}$ is the position vector of the point defect. We already have the form of the solution to Lippmann-Schwinger equation in terms of the T-matrix as

$$\psi(x) = \frac{e^{i\mathbf{k}\cdot\mathbf{x}}}{2\pi} - \frac{i}{4}\int H_0^{(1)}(k|\mathbf{x}-\mathbf{x}'|)\,\langle\mathbf{x}|\,T\,|\mathbf{k}\rangle\, d^2\mathbf{x}' \tag{4.4.8}$$

when $\mathbf{k}$ is a two dimensional vector. Hankel function has the following asymptotic expansion:

$$H^0(k|\mathbf{x}-\mathbf{x}'|) \simeq \sqrt{\frac{2}{\pi kr}}e^{-i\mathbf{k}'\cdot\mathbf{x}'-\frac{i\pi}{4}}e^{ikr} \quad \text{as } r\to\infty. \tag{4.4.9}$$

Here $r = |\mathbf{x}|$ and $|\mathbf{x}| >> |\mathbf{x}'|$. Now for $r \to \infty$

$$\int H_0^1(k|\mathbf{x}-\mathbf{x}'|)\,\langle\mathbf{x}'|\,T(E)\,|\mathbf{k}\rangle\, d^2\mathbf{x}' = \frac{e^{ikr}}{\sqrt{r}}\int\sqrt{\frac{2}{\pi k}}e^{-i\mathbf{k}'\cdot\mathbf{x}'-\frac{i\pi}{4}}\,\langle\mathbf{x}'|\,T(E)\,|\mathbf{k}\rangle\, d^2\mathbf{x}'$$

where $\mathbf{k}' = k\mathbf{x}'/r$. One can compare this expression with the general form of the scattering expression, $\frac{e^{ikr}}{\sqrt{r}} f(k,k')$, and get the scattering amplitude as

$$f(k,k') = -2\pi \frac{1}{4}\sqrt{\frac{2}{\pi k}} \int e^{-i\mathbf{k}'\cdot\mathbf{x}'} \langle \mathbf{x}' | T(E) | \mathbf{x}'' \rangle \frac{e^{i\mathbf{k}\cdot\mathbf{x}''}}{2\pi} d^2\mathbf{x}' d^2\mathbf{x}'' \tag{4.4.10}$$

where we exclude $\sqrt{i}$, since the plane wave expansion in two dimensions brings the phase factor $e^{i\pi/4}$, [54]. Now we take the Γ function as a line segment. Corresponding potential contains a delta function in two dimensions. The line defect is located at $x = 0$ and along $y = [-L/2, L/2]$. We will take the small distance approximation of the Hankel functions to calculate the elements of the $T-$matrix. Even though we will do the scattering amplitude calculations for only one point and one line defects, here we will write the Hankel integral for the case where there is N point and M line defects. There are two terms we need to handle in (4.4.7):

$$H_0^{(1)}(k|\vec{a_\alpha} - \vec{\gamma}_j|)\frac{ds}{L} \quad \text{and} \quad H_0^{(1)}(k|\vec{\gamma}_j - \vec{\gamma}_j'|)\frac{dsds'}{L^2} \ . \tag{4.4.11}$$

Here, we write the location of the α'th point defect as $\vec{a_\alpha}$ and position of the j'th line defect as $\vec{\gamma}_j$ where $\alpha = 1, 2, \cdots, N$ and $j = 1, 2, \cdots, M$. First, we start with the calculation of the term $H_0(k|\vec{a_\alpha} - \vec{\gamma}_j|)\frac{ds}{L}$. As mentioned above, the mid points of the lines are along the x-axis for simplicity. We write the argument of the Hankel function as

$$\begin{aligned} |\vec{a_\alpha} - (\vec{\xi}_j + y_j\hat{j})|^2 &= [\vec{a_\alpha} - (\vec{\xi}_j + y_j\hat{j})] \cdot [\vec{a_\alpha} - (\vec{\xi}_j + y_j\hat{j})] \\ &= [\underbrace{\vec{a_\alpha} - \vec{\xi}_j}_{\vec{d_{\alpha j}}} - y_j\hat{j}][\vec{a_\alpha} - \vec{\xi}_j - y_j\hat{j}] \end{aligned} \tag{4.4.12}$$

where, $\vec{\xi}_j$ represents the vector which is the projection of the position vector of the j'th line defect onto x-axis and $\vec{d_{\alpha j}}$ is the vector giving the distance between the point defect and the mid point of the line defect. First, we ignore the $\mathcal{O}(y_j^2)$ term since the length of the line segment is small compared to the distance d:

$$\begin{aligned} |\vec{a_\alpha} - (\vec{\xi}_j + y_j\hat{j})|^2 &\simeq \vec{d_{\alpha j}}^{\,2} - 2\vec{d_{\alpha j}} \cdot y_j \simeq \vec{d_{\alpha j}}(1 - \frac{2\vec{d_{\alpha j}} \cdot y_j}{d_{\alpha j}})^{1/2} \simeq \vec{d_{\alpha j}}(1 - \frac{\vec{d_{\alpha j}} \cdot y_j}{d_{\alpha j}}) \\ &= \vec{d_{\alpha j}} - \vec{d_{\alpha j}} \cdot y_j = \vec{d_{\alpha j}} - [\vec{a_\alpha} - \vec{\xi}_j] \cdot y_j \end{aligned} \tag{4.4.13}$$

Therefore we get

$$H_0^{(1)}(kd_{\alpha j} - ky_j(a_\alpha - \xi_j)) = H_0^{(1)}(kd_{\alpha j}) - H_1^{(1)}(kd_{\alpha j})(ky_j(a_\alpha - \xi_j)). \tag{4.4.14}$$

Now if we take the integral of the second term in (4.4.14) which is in the order of y:

$$\frac{1}{L}\Big[\int_{-L/2}^{L/2} ky_j \; dy_j\Big] H_1^{(1)}(kd_{\alpha j})(a_\alpha - \xi_j) = 0. \tag{4.4.15}$$

Therefore, the contribution coming from the first order of y correction to the distance between the defects turns out to be zero. We need to look at the higher order. We will keep the y^2 correction to the leading term:

$$|\vec{d_{\alpha j}} + y_j\hat{j}|^2 = d_{\alpha j}^2 - 2\vec{d_{\alpha j}}\cdot\hat{j}y_j + y_j^2 = d_{\alpha j}^2\left(1 - \frac{2\vec{d_{\alpha j}}\cdot\hat{j}y_j}{d_{\alpha j}^2} + \frac{y_j^2}{d_{\alpha j}^2}\right) \tag{4.4.16}$$

$$\Rightarrow |\vec{d_{\alpha j}} + y_j\hat{j}| = d_{\alpha j}\left(1 - \frac{2\vec{d_{\alpha j}}\cdot\hat{j}y_j}{d_{\alpha j}^2} + \frac{y_j^2}{d_{\alpha j}^2}\right)^{1/2}. \tag{4.4.17}$$

To consider the case where there is only one point and one finite line defects, we take $\vec{d_{\alpha j}} = \vec{d}$ and $y_j = y$ and we get:

$$\begin{aligned}\left(1 - \frac{2\vec{d}\cdot\hat{j}y}{d^2} + \frac{y^2}{d^2}\right)^{1/2} &\simeq 1 + \frac{1}{2}\Big[-\frac{2\vec{d}\cdot\hat{j}y}{d^2} + \frac{y^2}{d^2}\Big] + \frac{1}{2}\frac{1}{2}(\frac{1}{2} - 1)\Big(-\frac{2\vec{d}\cdot\hat{j}y}{d^2} + \frac{y^2}{d^2}\Big)^2 \\ &= 1 - \frac{\vec{d}\cdot\hat{j}y}{d^2} + \frac{1}{2}\frac{y^2}{d^2} - \frac{1}{4}\frac{(\vec{d}\cdot\hat{j})^2y^2}{d^4}.\end{aligned} \tag{4.4.18}$$

Here, we ignore the higher orders of y^2 and we have:

$$\Rightarrow\; d\Big[1 - \frac{\vec{d}\cdot y\hat{j}}{d^2} + \frac{1}{2}\frac{y^2}{d^2} - \frac{1}{4}\frac{(\vec{d}\cdot\hat{j})^2y^2}{d^4}\Big] = d - \frac{\vec{d}\cdot y\hat{j}}{d} + \frac{1}{2}\frac{y^2}{d} - \frac{1}{4}\frac{(\vec{d}\cdot\hat{j})^2y^2}{d^3}. \tag{4.4.19}$$

We put this expression back in the Hankel function and use the expansion below:

$$\begin{aligned}&H_0^{(1)}\left(kd - \underbrace{\hat{d}\cdot\hat{j}\;ky + \frac{1}{2}\frac{ky^2}{d} - \frac{1}{4}(\hat{d}\cdot\hat{j})^2\frac{ky^2}{d}}_{\text{small}}\right) \\ &\simeq H_0^{(1)}(kd) - H_1^{(1)}(kd)\left(\hat{d}\cdot\hat{j}\;ky + \frac{1}{2}\frac{ky^2}{d} - \frac{1}{4}(\hat{d}\cdot\hat{j})^2\frac{ky^2}{d}\right) \\ &\quad + \frac{1}{2}\underbrace{H_1^{(1)}(kd)}_{(H_0^{(1)} - H_2^{(1)})(kd)}\left(\frac{(\hat{d}\cdot\hat{j})^2}{d}ky^2\right)\end{aligned} \tag{4.4.20}$$

where $\hat{d}$ is the unit vector along $\vec{d}$. We take the integral of the correction:

$$\begin{aligned}\int_{-L/2}^{L/2}\frac{dy}{L}\Bigg[&-H_1^{(1)}(kd)\left(\hat{d}\cdot\hat{j}\;ky+\frac{1}{2}\frac{ky^2}{d}-\frac{1}{4}(\hat{d}\cdot\hat{j})^2\frac{ky^2}{d}\right)\\&+\frac{1}{2}\underbrace{H_1^{(1)}(kd)}_{(H_0^{(1)}-H_2^{(1)})(kd)}\left(\frac{(\hat{d}\cdot\hat{j})^2}{d}ky^2\right)\Bigg]\\&=\frac{k}{L}\frac{L^3}{24d}\Bigg[-H_1^{(1)}(kd)\left(1-\frac{1}{2}(\hat{d}\cdot\hat{j})^2\right)+H_0^{(1)}(kd)(\hat{d}\cdot\hat{j})^2-H_2^{(1)}(kd)(\hat{d}\cdot\hat{j})^2\Bigg]\end{aligned}\tag{4.4.21}$$

and we get the expression below for the first term of (4.4.11):

$$\begin{aligned}H_0(k|\vec{a}-\gamma(s)|)\frac{ds}{L}=&H_0^{(1)}(kd)+\frac{k}{L}\frac{L^3}{24d}\Bigg[-H_1^{(1)}(kd)\left(1-\frac{1}{2}(\hat{d}\cdot\hat{j})^2\right)\\&+H_0^{(1)}(kd)(\hat{d}\cdot\hat{j})^2-H_2^{(1)}(kd)(\hat{d}\cdot\hat{j})^2\Bigg].\end{aligned}\tag{4.4.22}$$

The integral in the second diagonal term of Φ, $H_0^{(1)}(k|\vec{\gamma}-\vec{\gamma}'|)\frac{dsds'}{L^2}$, is a bit tricky:

$$\begin{aligned}\frac{i}{2}H_0^{(1)}(k|\underbrace{\gamma(s)-\gamma(s')}_{small}|)dsds'&=\frac{i}{2}\int H_0^{(1)}(k|y_1-y_2|)\frac{dy_1dy_2}{L^2}\\&\simeq\frac{i}{2}\int_{-L/2}^{L/2}\left[i\frac{2}{\pi}\left(\ln(\frac{k}{2}|y_1-y_2|)+\gamma\right)+1\right]\frac{dy_1dy_2}{L^2}\\&=-\frac{1}{\pi}\int_{-L/2}^{L/2}\left[\ln(\frac{k}{2}|y_1-y_2|)+\gamma-\frac{i\pi}{2}\right]\frac{dy_1dy_2}{L^2}\\&=-\frac{1}{\pi}\int_{-L/2}^{L/2}\ln(\frac{k}{2}|y_1-y_2|)\frac{dy_1dy_2}{L^2}\underbrace{-\frac{1}{\pi}(\gamma-\frac{i\pi}{2})\frac{L^2}{L^2}}_{\text{constant term}}\end{aligned}\tag{4.4.23}$$

Here we used the fact that $H_0^{(1)}(z)\sim i\;2/\pi\;[\ln(z/2)+\gamma]+1\quad z\to 0^+$ where γ is the Euler's constant. Now we change the variables $u=y_1-y_2$, $v=y_1+y_2$, therefore we have $dy_1dy_2=\frac{1}{2}\;dudv$. So let us calculate the integral in the right-hand side of the

equation (4.4.23) in the new frame:

$$\begin{aligned}\frac{1}{\pi}\int_{-L/2}^{L/2}\ln(\frac{k}{2}|y_1-y_2|)\frac{dy_1dy_2}{L^2} &= \int_{-L}^{0}\frac{1}{2}\int_{L-u}^{-L+u}dv\ln(\frac{k}{2}|u|)du\\ &\quad+\int_{0}^{L}\frac{1}{2}\int_{-L+u}^{L-u}dv\ln(\frac{k}{2}|u|)du\\ &=\int_{-L}^{0}(u-L)\ln(\frac{k}{2}|u|)du+\int_{0}^{L}(L-u)\ln(\frac{k}{2}|u|)du\\ &=\int_{-L}^{0}\frac{1}{2}(u-L)\ln(\frac{k^2}{4}u^2)du\\ &\quad+\int_{0}^{L}\frac{1}{2}(L-u)\ln(\frac{k^2}{4}u^2)du\ .\end{aligned}\tag{4.4.24}$$

If we let $u\to -u$ for the first integral in the last line of (4.4.24), then the whole sum in (4.4.24) becomes:

$$-\int_{0}^{L}u\ln(\frac{k^2}{4}u^2)\ du\ .\tag{4.4.25}$$

Then we have

$$\begin{aligned}&-\frac{1}{\pi}\int_{-L/2}^{L/2}[\ln(\frac{k}{2}|y_1-y_2|)\frac{dy_1dy_2}{L^2}=\frac{1}{L^2\pi}\int_{0}^{L}u\ln(\frac{k^2}{4}u^2)\ du\\ &=\frac{1}{\pi}\frac{4}{k^2L^2}\frac{1}{2}\left[(\frac{k}{2}u)^2\ln(\frac{k^2}{4}u^2)-(\frac{k}{2}u)^2\right]_0^L=\frac{4}{2\pi k^2L^2}[(\frac{k}{2}L)^2\ln(\frac{k^2}{4}L^2)-\frac{k^2}{4}L^2]\end{aligned}\tag{4.4.26}$$

and we combine this result with the constant term:

$$\frac{1}{2\pi}\ln\frac{k^2L^2}{4e}-\frac{1}{2\pi}-\frac{1}{\pi}(\gamma-\frac{i\pi}{2})=\frac{1}{2\pi}\ln[\frac{k^2L^2e^{i\pi}}{4e^{1+2\gamma}}]\tag{4.4.27}$$

we obtain

$$\frac{1}{\xi_2}-\frac{1}{4\pi}\ln[\frac{k^2L^2e^{i\pi}}{4e^{1+2\gamma}}]\ .\tag{4.4.28}$$

We assume for this case $1/\xi_2$ is also large enough (ξ_2 is small enough) to compensate for this. For the scattering amplitude, $f(k,k')$, we get the expression below:

$$\begin{aligned}
f(k,k') = &-2\pi\frac{1}{4}\sqrt{\frac{2}{\pi k}}\Bigg[(\frac{1}{\xi_R}-\frac{1}{2\pi}\ln\left(\frac{k}{\mu}\right)-\frac{i}{4})(\frac{1}{\xi_2}-\frac{1}{4\pi}\ln[\frac{k^2L^2e^{i\pi}}{4e^{1+2\gamma}}]\ ) \\
&+\frac{1}{16}\Bigg(H_0^{(1)}(kd)+\frac{kL^2}{24d}\Bigg[-H_1^{(1)}(kd)\left(1-\frac{1}{2}(\hat{d}\cdot\hat{j})^2\right)+H_0^{(1)}(kd)(\hat{d}\cdot\hat{j})^2 \\
&-H_2^{(1)}(kd)(\hat{d}\cdot\hat{j})^2\Bigg]\Bigg)^2\Bigg]^{-1}\times\Bigg[e^{-i\mathbf{k'}\cdot\mathbf{a}}-\left(\frac{1}{\xi_2}-\frac{1}{4\pi}\ln[\frac{k^2L^2e^{i\pi}}{4e^{1+2\gamma}}]\right)\frac{e^{i\mathbf{k}\cdot\mathbf{a}}}{2\pi} \\
&+e^{-i\mathbf{k'}\cdot\mathbf{a}}\Bigg(\frac{i}{4}\Bigg(H_0^{(1)}(kd)+\frac{k}{L}\frac{L^3}{24d}\Bigg[-H_1^{(1)}(kd)\left(1-\frac{1}{2}(\hat{d}\cdot\hat{j})^2\right) \\
&+H_0^{(1)}(kd)(\hat{d}\cdot\hat{j})^2-H_2^{(1)}(kd)(\hat{d}\cdot\hat{j})^2\Bigg]\Bigg)\Bigg)\frac{\sin(kL/2)}{\pi kL} \\
&+2\frac{\sin(k'L/2)}{k'L}\Bigg(\frac{i}{4}\Bigg(H_0^{(1)}(kd)+\frac{k}{L}\frac{L^3}{24d}\Bigg[-H_1^{(1)}(kd)\left(1-\frac{1}{2}(\hat{d}\cdot\hat{j})^2\right) \\
&+H_0^{(1)}(kd)(\hat{d}\cdot\hat{j})^2-H_2^{(1)}(kd)(\hat{d}\cdot\hat{j})^2\Bigg]\Bigg)\Bigg)\frac{e^{i\mathbf{k}\cdot\mathbf{a}}}{2\pi} \\
&+2\frac{\sin(k'L/2)}{k'L}(\frac{1}{\xi_R}-\frac{1}{2\pi}\ln\left(\frac{k}{\mu}\right)-\frac{i}{4})\frac{\sin(kL/2)}{\pi kL}\Bigg]. \qquad (4.4.29)
\end{aligned}$$

As a simpler example, to look at the case when the line segment is perpendicular to the $y-$axis, we take $\hat{d}\cdot\hat{j}=0$ in this expression, we get:

$$\begin{aligned}
f(k,k') = &-2\pi\frac{1}{4}\sqrt{\frac{2}{\pi k}}\Bigg[(\frac{1}{\xi_R}-\frac{1}{2\pi}\ln\left(\frac{k}{\mu}\right)-\frac{i}{4})(\frac{1}{\xi_2}-\frac{1}{4\pi}\ln[\frac{k^2L^2e^{i\pi}}{4e^{1+2\gamma}}]\ ) \\
&+\frac{1}{16}\left[H_0^{(1)}(kd)-\frac{kL^2}{24d}H_1^{(1)}(kd)\right]^2\Bigg]^{-1}\Bigg[e^{-i\mathbf{k'}\cdot\mathbf{a}}\left(\frac{1}{\xi_2}-\frac{1}{4\pi}\ln[\frac{k^2L^2e^{i\pi}}{4e^{1+2\gamma}}]\right)\frac{e^{i\mathbf{k}\cdot\mathbf{a}}}{2\pi} \\
&+e^{-i\mathbf{k'}\cdot\mathbf{a}}\frac{i}{4}\left(H_0^{(1)}(kd)-\frac{k}{L}\frac{L^3}{24d}H_1^{(1)}(kd)\right)\frac{\sin(kL/2)}{\pi kL} \\
&+2\frac{\sin(k'L/2)}{k'L}\frac{i}{4}\left(H_0^{(1)}(kd)-\frac{k}{L}\frac{L^3}{24d}H_1^{(1)}(kd)\right)\frac{e^{i\mathbf{k}\cdot\mathbf{a}}}{2\pi} \\
&+2\frac{\sin(k'L/2)}{k'L}(\frac{1}{\xi_R}-\frac{1}{2\pi}\ln\left(\frac{k}{\mu}\right)-\frac{i}{4})\frac{\sin(kL/2)}{\pi kL}\Bigg]. \qquad (4.4.30)
\end{aligned}$$

If we look at the ξ_2 and $kL\to 0$ limit where the wavelength is large to compare this expression with the known two point defects result, we get the exact same result. For this limit to make sense k is also taken small.

5. A DIRECT METHOD FOR THE LOW ENERGY SCATTERING OF DELTA SHELL POTENTIALS

In this chapter, we will give the idea provided in [50] briefly. The approach discussed here is solving the bound state and scattering problems of some singular potentials with a direct method rather to the conventional partial wave analysis. We will work in momentum space and study the distributional solutions. We will extend the ideas for point-like Dirac delta potentials given in [46]. In this approach, the boundary conditions explicitly take place instead of the $i\epsilon$ prescription of the partial wave analysis.

First, we start with reminding ourselves that we can express the Hamiltonian with a spherical delta shell potential as

$$H = H_0 - \lambda |\delta_{S^2}\rangle\langle\delta_{S^2}| \,, \tag{5.0.1}$$

where H_0 is the free Hamiltonian, and λ is the interaction strength. The Dirac delta function δ_S supported on the sphere S^2 with the radius R is defined by the relation [56]

$$\langle\delta_{S^2}|\psi\rangle \;=\; \frac{1}{\sqrt{A(S^2)}} \int_{S^2} \psi \; d^2S \,, \tag{5.0.2}$$

where $d^2S = R^2 d\Omega = R^2 \sin\theta d\theta d\phi$ and the area of the shell is $A(S^2) = 4\pi R^2$. We note that this definition of the Hamiltonian corresponds directly to the $l = 0$ sector of the usual differential equation approach in spherical coordinates.

5.1. Bound State Results

We consider one of the most basic cases of the singular interactions at first: the Dirac delta potential supported by a point. The bound state and scattering state of the point defect can be solved in momentum space as well, as discussed in [46].

In one dimension, we can write the time-independent Schödinger equation with

the attractive point-like Dirac delta potential $V(x) = -\lambda\delta(x)$ in momentum space as

$$(p^2 + \nu^2)\widehat{\psi}(p) = \lambda\psi(0) \ . \tag{5.1.1}$$

where $E = -\nu^2$ and $\hat{\psi}(p)$ is the Fourier transform of the solution of $\psi(x)$ which is

$$\psi(x) = \int_{-\infty}^{\infty} \hat{\psi}(p) \ e^{ipx} \ \frac{dp}{2\pi} \ . \tag{5.1.2}$$

We can divide both sides of equation (5.1.1) by $p^2 + \nu^2$, and we get

$$\widehat{\psi}(p) = \frac{\lambda\psi(0)}{p^2 + \nu^2} \ , \tag{5.1.3}$$

where we can consider $\psi(0)$ just as a number. To find ν, let us impose the following consistency condition which means that the inverse Fourier transform of the above wave function (5.1.3) evaluated at $x = 0$ should be equal to $\psi(0)$:

$$\psi(0) = \int_{-\infty}^{\infty} \widehat{\psi}(p)\frac{dp}{2\pi} = \int_{-\infty}^{\infty} \frac{\lambda\psi(0)}{p^2 + \nu^2}\frac{dp}{2\pi} \ . \tag{5.1.4}$$

We find the bound state energy by evaluating the above elementary integral and solving for ν. The result is $\nu = \frac{1}{2}$. Hence

$$E = -\frac{\lambda^2}{4} \ . \tag{5.1.5}$$

It follows from the consistency condition (5.1.4) that the bound state energy exists as long as $\lambda > 0$ since if $\lambda < 0$, it is not an attractive potential anymore. We can check if this result is true by easily taking the inverse Fourier transformation of $\widehat{\psi}(p)$ given in Equation (5.1.3). The inverse Fourier transformation of $\hat{\psi}(p)$ integral can be computed by the residue theorem [100] and we get

$$\psi(x) = \sqrt{\frac{\lambda}{2}} \ e^{-\frac{\lambda}{2}|x|} \tag{5.1.6}$$

which is the well-known bound state wave function [31] indeed.

Secondly, the wave function in momentum space for a spherical interaction is

$$\begin{aligned}(p^2+\nu^2)\,\widehat{\psi}(\mathbf{p}) &= \lambda\langle\mathbf{p}|\delta_{S^2}\rangle\langle\delta_{S^2}|\psi\rangle \\ &= \frac{\lambda}{4\pi R^2}\left(\int_{S^2} e^{-i\mathbf{p}\cdot\sigma}R^2d\Omega\right)\left(\int_{S^2}\psi(\sigma)R^2d\Omega\right)\ , \qquad (5.1.7)\end{aligned}$$

where again

$$\sigma(\theta,\phi) := (R\sin\theta\cos\phi, R\sin\theta\sin\phi, R\cos\theta)\ . \qquad (5.1.8)$$

We calculate the momentum space wave function as

$$\widehat{\psi}(\mathbf{p}) = \frac{\lambda}{p^2+\nu^2}\frac{\sin(pR)}{pR}\left(\int_{S^2}\psi(\sigma)R^2d\Omega\right)\ . \qquad (5.1.9)$$

Imposing the consistency condition given in (5.1.4) in three dimensions, we find,

$$\begin{aligned}\int_{S^2}\psi(\sigma)R^2d\Omega = &\left(\int_{S^2}\psi(\sigma)R^2d\Omega\right) \\ &\times\int_{S^2}\left(\int_{\mathbb{R}^3}\frac{\lambda}{p^2+\nu^2}\frac{\sin(pR)}{pR}e^{i\mathbf{p}\cdot\sigma(\theta',\phi')}\,\frac{d^3p}{(2\pi)^3}\right)R^2d\Omega'\ . \qquad (5.1.10)\end{aligned}$$

Integrating over the angular variables [100] and using the identities

$$\int_0^\infty\frac{\sin^2(pR)}{p^2+\nu^2}dp = e^{-R\nu}\frac{\pi\sinh(\nu R)}{2\nu} \qquad (5.1.11)$$

and

$$\sinh x = \frac{e^x-e^{-x}}{2}\ , \qquad (5.1.12)$$

we are left with the equation below

$$(1-e^{-2R\nu}) = \frac{2\nu}{\lambda} \qquad (5.1.13)$$

for the bound state energy. This equation says that there is always one solution as long as the slope of the left hand side is greater than the slope of the right hand side around $\nu=0$ which leads to the condition

$$\frac{1}{\lambda R} < 1 \qquad (5.1.14)$$

to have at least one bound state.

Isolating ν in the equation (5.1.13), we solve (5.1.13) as

$$\begin{aligned} e^{-R\lambda}e^{-2R\nu}(R\lambda+2R\nu) &= e^{-R\lambda}R\lambda \\ \Rightarrow R\lambda+2R\nu &= -W(-\lambda Re^{-R\lambda}) \\ \Rightarrow \nu &= -\frac{\lambda}{2}-\frac{1}{2R}W(-\lambda Re^{-R\lambda}) \end{aligned} \tag{5.1.15}$$

where W is the Lambert W function which is the solution of x of equation $xe^x = c$ as $W(c)$ [102]. We write the bound state energy in terms of the Lambert W function

$$E = -\nu^2 = -\left(\frac{\lambda}{2}+\frac{1}{2R}W\left(-\lambda Re^{-\lambda R}\right)\right)^2 . \tag{5.1.16}$$

The position space wave function of this bound state is obtained by the inverse Fourier transformation of $\psi(\mathbf{p})$.

And lastly, our concern is a circular Dirac delta potential in two dimensions when the circle is centered at the origin with radius R and it's parametrization is given by

$$\gamma(\theta) := (R\cos(\theta), R\sin(\theta)) . \tag{5.1.17}$$

So the Schrödinger equation in momentum space can be written as

$$(p^2+\nu^2)\widehat{\psi}(\mathbf{p}) = \frac{\lambda}{L(S^1)}\left(\int_0^{2\pi} e^{-i\mathbf{p}\cdot\gamma(\theta)}Rd\theta\right)\left(\int_0^{2\pi}\psi(\gamma(\theta))Rd\theta\right) \tag{5.1.18}$$

which has the following solution

$$\widehat{\psi}(\mathbf{p}) = \frac{\lambda J_0(pR)}{p^2+\nu^2}\left(\int_0^{2\pi}\psi(\gamma(\theta))Rd\theta\right) . \tag{5.1.19}$$

By following the similar approach as in the spherical shell case, we obtain

$$\frac{1}{\lambda R} = I_0(\nu R)K_0(\nu R) \tag{5.1.20}$$

for the bound state energy. we cannot solve this transcendental equation analytically. However, there is a unique solution ν for given λ and R. This can be seen by simply going back to the integral representations of the modified Bessel's and taking the derivative of it with respect to ν. The derivation gives a monotonically decreasing

function. Therefore, the solution always exists for all λ's and R's. Assuming ν_* is the bound state energy, using ν_* we can write the wave function in position space.

5.2. Scattering State Analysis

For the scattering case of the point interaction, we have $E = k^2$, $\nu = ik$, then the Schrödinger equation in momentum space is

$$(p^2 - k^2)\widehat{\psi}(p) = \lambda\psi(0) \ . \tag{5.2.1}$$

Now since dividing both sides by $p^2 - k^2$ leads to singularities as $\mathbf{p} = \pm\mathbf{k}$, we cannot solve this equation directly as it was in the bound state. As usual we add some $-i\epsilon$ term in the denominator to calculate the integral which corresponds to putting the outgoing boundary condition by hand [86]. So instead, we will use generalized functions [56] which are also called as distributions. Distributions, which are denoted as T's in this chapter, can be described as continuous linear functionals acting on functions. They take test functions and give real numbers as the output. The rigorous calculations on condition of continuity of distributions can be found in [56] and [101].

The point interaction can be defined as a Dirac delta distribution as [31, 86]

$$\langle \delta, \psi \rangle = \int_{-\infty}^{\infty} \delta(x)\psi(x)dx = \psi(0) \ . \tag{5.2.2}$$

Fourier transform of T acting on a test function can be defined as [56]

$$\langle \mathcal{F}(T), \psi \rangle = \langle T \ , \mathcal{F}(\psi) \rangle \ . \tag{5.2.3}$$

We will use the distributional solution for an equation like

$$(x^2 - a^2)T(x) = 0 \ , \tag{5.2.4}$$

which is

$$T(x) = A\delta(x - a) + B\delta(x + a) + \mathrm{pv}\left(\frac{1}{x^2 - a^2}\right) \ , \tag{5.2.5}$$

given in [56], where $a > 0$, A and B are arbitrary complex numbers. The principle value has the property

$$\mathrm{pv}\left(\frac{1}{x^2-a^2}\right) = \frac{1}{2a}\left(\mathrm{pv}\left(\frac{1}{x-a}\right) - \mathrm{pv}\left(\frac{1}{x+a}\right)\right) \tag{5.2.6}$$

which is also given in [56]. Therefore, using this property in (5.2.5), we can write the equation (5.2.1) as

$$\widehat{\psi}(p) = A\delta(p-k) + B\delta(p+k) + \lambda\psi(0)\mathrm{pv}\left(\frac{1}{p^2-k^2}\right) . \tag{5.2.7}$$

Substituting this back into inverse Fourier transformation, we find

$$\psi(x) = \frac{A}{2\pi}e^{ikx} + \frac{B}{2\pi}e^{-ikx} + \lambda\psi(0)\ \mathrm{pv}\int_{-\infty}^{\infty}\frac{e^{ipx}}{p^2-k^2}\,\frac{dp}{2\pi} . \tag{5.2.8}$$

Using residue theorem, the integral in the last term above can be calculated. Implying the continuity of the wave function at $x = 0$,

$$\psi(0) = \frac{A+B}{2\pi} \tag{5.2.9}$$

we find

$$\psi(x) = \begin{cases} \frac{A}{2\pi}e^{ikx} + \frac{B}{2\pi}e^{-ikx} - \frac{i\lambda(A+B)}{8\pi k}\left(e^{ikx} - e^{-ikx}\right) & \text{for } x \le 0 , \\ \\ \frac{A}{2\pi}e^{ikx} + \frac{B}{2\pi}e^{-ikx} + \frac{i\lambda(A+B)}{8\pi k}\left(e^{ikx} - e^{-ikx}\right) & \text{for } x \ge 0 . \end{cases} \tag{5.2.10}$$

for the wave function in position space and this result is compatible with the well-known results given in the literature [31].

For the scattering from spherical shell, we write the Schrödinger equation as

$$(p^2-k^2)\widehat{\psi}(\mathbf{p}) = \alpha(p) , \tag{5.2.11}$$

where

$$\alpha(p) := \frac{\lambda}{pR}\sin(pR)\left(\int_0^{2\pi}\int_0^{\pi}\psi(\sigma(\theta,\phi))R^2\sin\theta d\theta d\phi\right) . \tag{5.2.12}$$

Then the distributional expression for the wave function in momentum space is

$$\widehat{\psi}(\mathbf{p}) = A\delta(\mathbf{p}-\mathbf{k}) + B\delta(\mathbf{p}+\mathbf{k}) + C\delta(p-k) + \mathrm{pv}\left(\frac{\alpha(p)}{p^2-k^2}\right) . \tag{5.2.13}$$

The first two terms coming from $(p^2-k^2)\delta(\mathbf{p}\pm\mathbf{k}) = 0$ are similar to the one dimensional case. However, since we work in three dimensions now, we need to add the term coming from the magnitude of the wave vector, $(p^2-k^2)\delta(p-k) = 0$, where $k > 0$. Then, taking the inverse Fourier transformation of the above distributional solution

$$\psi(\mathbf{r}) = \frac{A}{(2\pi)^3}e^{i\mathbf{k}\cdot\mathbf{r}} + \frac{B}{(2\pi)^3}e^{-i\mathbf{k}\cdot\mathbf{r}} + \frac{2Ck}{(2\pi)^2}\,\frac{\sin(kr)}{r} + \mathrm{pv}\int_{\mathbb{R}^3}\frac{e^{i\mathbf{p}\cdot\mathbf{r}}\alpha(p)}{p^2-k^2}\,\frac{d^3p}{(2\pi)^3} \tag{5.2.14}$$

and imposing the consistency condition, we obtain the position space wave function.

And lastly, distributional wave solution for the circular interaction in momentum space can be expressed as

$$\widehat{\psi}(\mathbf{p}) = A\delta(\mathbf{p}-\mathbf{k}) + B\delta(\mathbf{p}+\mathbf{k}) + C\delta(p-k) + \left(\int_0^{2\pi}\psi(\gamma(\theta))Rd\theta\right)\mathrm{pv}\left(\frac{\lambda J_0(pR)}{p^2-k^2}\right) \tag{5.2.15}$$

similarly. We get the position space wave solution as

$$\begin{aligned}\psi(\mathbf{r}) =& \frac{A}{(2\pi)^2}e^{i\mathbf{k}\cdot\mathbf{r}} + \frac{B}{(2\pi)^2}e^{i\mathbf{k}\cdot\mathbf{r}} + \frac{Ck}{2\pi}J_0(kr) \\ &+ \left(\int_0^{2\pi}\psi(\gamma(\theta))Rd\theta\right)\mathrm{pv}\int_{\mathbb{R}^2}\left(\frac{\lambda J_0(pR)}{p^2-k^2}\right)e^{i\mathbf{p}\cdot\mathbf{r}}\frac{d^2p}{(2\pi)^2}\end{aligned} \tag{5.2.16}$$

by taking the Fourier transform of (5.2.15). Using the consistency condition, i.e., taking the line integral of both sides of (5.2.16), we find the term in the bracket in (5.2.16) and we have the explicit form of the scattering wave function under the out going boundary conditions [50].

6. CONCLUSION

In this thesis, we study the scattering properties and bound state energies of some hybrid systems of Dirac-delta potentials. We apply a proper regularization to the problem for each case and use renormalization for the necessary components of the Hamiltonians. The Dirac-delta potentials are supported by a circle/sphere together with potentials supported by a point outside of the circle/sphere in $\mathbb{R}^2$ and $\mathbb{R}^3$. We give the plots describing the behaviour of the bound state energies and scattering cross sections. We provide also analytical expressions for scattering amplitudes. We also look at the cases where the circular or spherical delta shells are deformed. We give the important result that the first order change in the bound state energies under small deformations of the shells is equal to the first order perturbative solution of the bound state energy when the volume of the support is increased by the average of the deformation over the shell. We also give the change in the bound state energy analytically when we add the point defects to the deformed shells.

The second main part of this thesis is about scattering from linear Dirac-delta potentials in two dimensions and geometric scattering problem on an asymptotically flat curved surface. We express the curved surface as a potential and take it as a perturbation. We search for the effect of the linear delta potentials on geometric scattering properties as these kinds of defects are seen in such dilute electron gas scattering setups. From the graphs we produced, we observe that placing the center of the curvature, which is a bump, between a pair of parallel line defects produce an effective resonator capable of achieving much larger amplification of the geometric scattering effects. We also obtain an analytic formulation when there are N line defects. Scalar particle scatters along two directions when the line defects are placed on a Euclidean surface. The scattering amplitude vanishes expect for the scattering angles θ_0 and $180^\circ - \theta_0$, where θ_0 is the angle of incidence. We also state an analytical expression for the case combining a point defect and a line defect in two dimensions using a short line segment approximation.

In the third part of the thesis, we use a direct formal operator approach to solve the bound state and stationary scattering problems of circular and spherical delta shell potentials for the $l = 0$ sector. Using the distributional solutions, we obtain the same results with the standard partial wave analysis for scattering problem. The interaction is expressed as a rank one operator and in two dimensions as a circle and in three dimensions as a sphere.

REFERENCES

1. Weinberg, S., *Lectures on Quantum Mechanics*, 2nd ed., Cambridge University Press, 2015.

2. Gasiorowicz, S., *Quantum Physics*, 2nd ed., John Wiley & Sons, 1996.

3. Taylor, J. R., *Scattering Theory: Quantum Theory on Non-relativistic Collisions*, John Wiley & Sons, 1972.

4. Gottfried, K., Yan, T. M., *Quantum Mechanics: Fundamentals*, 2nd ed., Springer-Verlag New York, 2003.

5. Mott, N. F., Massey, H. S. W., *The Theory of Atomic Collisions*, 3rd ed., Oxford University Press, 1965.

6. Goldberger, M. L., Watson, K. M., *Collision Theory*, John Wiley & Sons, 1964.

7. Rodberg, L. S., Thaler, R. M., *Introduction to the Quantum Theory of Scattering*, Academic Press, 1967.

8. Newton, R. G., *Scattering Theory of Waves and Particles*, 2nd ed., Springer-Verlag New York, 1982.

9. Farina, J. E. G., *Quantum Theory of Scattering Processes*, Pergamon Press Ltd., 1973.

10. Faddeev, L. D., Merkuriev, S. P., *Quantum Scattering Theory for Several Particle Systems*, Kluwer Academic Publishers, 1993.

11. Lax, P. D., Phillips, R. S., *Scattering Theory*, Academic Press, 1967.

12. Albeverio, S., Gesztesy, F., Hoegh-Krohn, R., Holden, H., *Solvable models in Quantum Mechanics*, 2nd ed., American Mathematical Society, 2004.

13. Albeverio, S., Kurasov, P., *Singular Perturbation of Differential Operators*, Cambridge University Press, 2000.

14. Silva, K. V. R. A., de Freitas, C. F., Filgueiras, C., "Geometry-Induced Quantum Dots on Surfaces with Gaussian Bumps", *The European Physical Journal B*, Vol. 86, No. 4, p. 147, 2013.

15. Encinosa, M., Etemadi, B., "Energy Shifts Resulting from Surface Curvature of Quantum Nanostructures", *Physical Review A*, Vol. 58, No. 1, pp. 77-81, 1998.

16. Taira, H., Shima, H., "Curvature Effects on Surface Electron States in Ballistic Nanostructures", *Surface Science*, Vol. 601, No. 22, pp. 5270-5275, 2007.

17. Atanasov, V., Dandoloff, R., Saxena, A., "Geometry-Induced Charge Separation on a Helicoidal Ribbon", *Physical Review B* Vol. 79, No. 3, p. 033404, 2009.

18. Brandt, F. T., Sánchez-Monroy, J. A., "Induced Magnetic Moment for a Spinless Charged Particle in the Thin-Layer Approach", *Europhysics Letters*, Vol. 111, No. 6, p. 67004, 2015.

19. DeWitt, B. S., "Dynamical Theory in Curved Spaces. I. A Review of the Classical and Quantum Action Principles", *Reviews of Modern Physics*, Vol. 29, No. 3, pp. 377-397, 1957.

20. Dewitt, B. S., "Point Transformations in Quantum Mechanics", *Physical Review*, Vol. 85, No. 4, pp. 653-661, 1952.

21. Penrose, R., "Zero Rest-Mass Fields Including Gravitation: Asymptotic Behaviour", *Proceedings of the Royal Society London A*, Vol. 284, No. 1397, pp. 159-203, 1965.

22. DeWitt-Morette, C., Elworthy, K. D., Nelson, B. L., Sammelman, G. S., "A Stochastic Scheme for Constructing Solutions of the Schrödinger Equation", *Annales de l'Institut Henri Poincaré*, Vol. 32, No. 4, pp. 327-341, 1980.

23. Marinov, M. S., "Path Integrals in Quantum Theory: An Outlook of Basic Concepts", *Physics Reports*, Vol. 60, No. 1, pp. 1-57, 1980.

24. Kleinert, H., "Path Integral on Spherical Surfaces in D Dimensions and on Group Spaces", *Physics Letters B*, Vol. 236, No. 3, pp. 315-320, 1990.

25. DeWitt, B. S., *Supermanifolds*, Cambridge University Press, 1992.

26. Mostafazadeh, A., "Scalar Curvature Factor in the Schrödinger Equation and Scattering on a Curved Surface", *Physical Review A*, Vol. 54, No. 2, pp. 1165-1170, 1996.

27. Oflaz, N., Mostafazadeh, A., Ahmady, M., "Scattering Due to Geometry: Case of a Spinless Particle Moving on an Asymptotically Flat Embedded Surface", *Physical Review A*, Vol. 98, No. 2, p. 022126, 2018.

28. Bui, H. V., Mostafazadeh, A., "Geometric Scattering of a Scalar Particle Moving on a Curved Surface in the Presence of Point Defects", *Annals of Physics*, Vol. 407, pp. 228-249, 2019.

29. Demkov, Yu. N., Ostrovskii, N. V., *Zero-Range Potentials and Their Applications in Atomic Physics*, Springer, 2013.

30. Gottfried, K., *Quantum Mechanics Vol I Fundamentals*, New York: Benjamin, 1966.

31. Griffiths, D. J., *Introduction to Quantum Mechanics*, Prentice Hall, 2016.

32. Antoinet, J. P., Gesztesy, F., Shabani, J., "Exactly Solvable Models of Sphere

Interactions in Quantum Mechanics", *Journal of Physics A: Mathematical and General*, 20, pp. 3687-3712, 1987.

33. Huang, K., *Quarks, Leptons and Gauge Fields*, World Scientific, 1982.

34. Jackiw, R., *Delta-Function Potentials in Two- and Three-Dimensional Quantum Mechanics, M. A. B. Bég Memorial Volume*, World Scientific, 1991.

35. Exner, P., Ichinose, T., "Geometrically Induced Spectrum in Curved Leaky Wires", *Journal of Physics A: Mathematical and General*, Vol. 34, No. 7, p. 1439, 2001.

36. Exner, P., Kondej, S., "Curvature-Induced Bound States for an Interaction Supported by a Curve" in , Annales Henri Poincaré, Vol. 3, No. 5, pp. 967-981, 2002.

37. Exner, P., Kondej, S., "Bound States Due to a Strong δ Interaction Supported by a Curved Surface", *Journal of Physics A: Mathematical and General*, Vol. 36, No. 2, p. 443, 2002.

38. Exner, P., Kovarik, H., *Quantum Waveguides*, Springer, 2015.

39. Kaynak, B. T. and Turgut O. T., "Singular Interactions Supported by Embedded Curves", *Journal of Physics A: Mathematical and Theoretical*, Vol. 45, No. 26, p. 265202, 2012.

40. Kaynak, B. T. and Turgut, O. T., "Compact Submanifolds Supporting Singular Interactions", *Annals of Physics*, Vol. 339, No. 3, pp. 266-292, 2013.

41. A. C. Maioli, and Alexandre G. M. Schmidt, "Exact Solution to Lippmann-Schwinger Equation for a Circular Billiard", *Journal of Mathematical Physics*, Vol. 59, No. 12, p. 122102, 2018.

42. Azado, P. C., Maioli, A. C., Schmidt, A. G. M., "Quantum Scattering by a Spherical Barrier with an Arbitrary Coupling Strength", *Physica Scripta*, Vol. 96, No.

8, p. 085205, 2021.

43. Demiralp, E., Beker, H., "Properties of Bound States of the Schrödinger Equation with Attractive Dirac Delta Potentials", *Journal of Physics A: Mathematical and General*, Vol. 36, No. 26, pp. 7449-7459, 2003.

44. Exner, P., Fraas, M., "On Geometric Perturbations of Critical Schrödinger Operators with a Surface Interaction", *Journal of Mathematical Physics*, Vol. 50, No. 11, p. 112101, 2009.

45. Cacciapuoti, C., Fermi, D., Posilicano, A., *Scattering Theory for Delta-Potentials Supported by Locally Deformed Planes, Mathematical Challenges of Zero-Range Physics Models, Methods, Rigorous Results, Open Problems, Editor: Assist. Prof. A. Michelangeli*, Springer International Publishing, 2021.

46. Lieber, M., "Quantum Mechanics in Momentum Space: An Illustration", *American Journal of Physics*, Vol. 43, No. 6, pp. 486-491, 1975.

47. Schmalz, J. A., Schmalz, G., Gureyev, T. E., Pavlov, K. M., "On the Derivation of the Green's Function for the Helmholtz Equation Using Generalized Functions", *American Journal of Physics*, Vol. 78, No. 2, pp. 181-186, 2010.

48. Erman, F., Seymen, S., Turgut, O. T., "Rank One Perturbations Supported by Hybrid Geometries and Their Deformations", arXiv:2202.10599v3 [math-ph], 2022.

49. Bui, H. V., Mostafazadeh, A., Seymen, S., "Geometric Scattering in the Presence of Line Defects", *European Physical Journal Plus*, Vol. 136, No. 109, pp. 1-17, 2021.

50. Erman, F., Seymen, S., "A Direct Method For the Low Energy Scattering Solution of Delta Shell Potentials", *European Physical Journal Plus*, Vol. 137, No. 3, p. 308, 2022.

51. Faddeev, L. D., Yakubovskii, O. A., *Lectures on Quantum Mechanics for Mathe-*

matics Students, American Mathematical Society, 2009.

52. Lapidus, I. R., "Quantum-mechanical scattering in Two Dimensions", *American Journal of Physics*, Vol. 50, No. 1, pp. 45-47, 1982.

53. Sakurai, J., J., *Modern Quantum Mechanics Revised Edition*, Addison-Wesley Publishing Company, 1994.

54. Adhikari, S. K., "Quantum Scattering in Two Dimensions", *American Journal of Physics*, Vol. 54, No. 4, pp. 362-367, 1986.

55. Bui, H. V., Loran, F., Mostafazadeh, A., "Scattering by a Collection of δ-Function Point and Parallel Line Defects in Two Dimensions", *Annals of Physics*, Vol. 434, No. 3, p. 168649, 2021.

56. Appel, W., *Mathematics for Physics and Physicists*, Princeton University Press, 2007.

57. Evans, L. C., *Partial Differential Equations, Graduate Series in Mathematics, Vol. 19, Second Edition*, American Mathematical Society, 2008.

58. Reed, M., Simon, B., *Methods of Modern Mathematical Physics II: Self Adjointness*, Academic Press, 1975.

59. Altunkaynak, B. İ., Erman, F., Turgut, O. T., "Finitely Many Dirac-Delta Interactions on Riemannian Manifolds", *Journal of Mathematical Physics*, Vol. 47, No. 8, pp. 1-23, 2006.

60. Erman, F., Turgut, O. T. , "Point Interactions in Two and Three Dimensional Riemannian Manifolds", *Journal of Physics A: Mathematical and Theoretical*, Vol. 43, No. 33, p. 335204, 2010.

61. Gradshteyn, I. S., Ryzhik, I. M., *Table of Integrals, Series, and Products*, Academic

Press, 2014.

62. Lebedev, N. N., *Special Functions and Their Applications*, Prentice-Hall, 1965.

63. Dogan, C., Erman, F., Turgut, O. T., "Existence of Hamiltonians for Some Singular Interactions on Manifolds", *Journal of Mathematical Physics*, Vol. 53, No. 4, p. 043511, 2012.

64. Dimock, J., Rajeev, S. G., "Multi-Particle Schrödinger Operators with Point Interactions in the Plane", *Journal of Physics A: Mathematical and General*, Vol. 37, No. 39, pp. 9157-9173, 2004.

65. Thirring, W., *Quantum Mathematical Physics: Atoms, Molecules and Large Systems*, Springer, 2013.

66. Reed, M., Simon, N., *Methods of Modern Mathematical Physics, Volume IV, Analysis of Operators*, Academic Press, 1978.

67. Blank, J., Exner, P., Havlicek, M., *Hilbert Space Operators in Quantum Physics*, Springer, 2008.

68. Do Carmo, M. P., *Differential Geometry of Curves and Surfaces: Revised and Updated Second Edition*, Courier Dover Publications, 2016.

69. Erman, F., Turgut, O. T., "A Perturbative Approach to the Tunneling Phenomena", *Frontiers in Physics*, Vol. 7, No. 2296, p. 69, 2019.

70. Bar, C., *Elementary Differential Geometry*, Cambridge University Press, 2010.

71. Stone, M., Goldbart, P., *Mathematics for Physics: A Guided Tour For Graduate Students*, Cambridge University Press, 2009.

72. Ferrari, G., Cuoghi, G., "Schrödinger Equation for a Particle on a Curved Surface

in an Electric and Magnetic Field", *Physical Review Letters*, Vol. 100, No. 23, p. 230403, 2008.

73. Szameit, A., Dreisow, F., Heinrich, M., Keil, R., Nolte, S., Tünnermann, A., Longhi, S., "Geometric Potential and Transport in Photonic Topological Crystals", *Physical Review Letters*, Vol. 104, No. 15, 2010.

74. Della Valle, G., Longhi, S., "Geometric Potential for Plasmon Polaritons on Curved Surfaces", *Journal of Physics B: Atomic, Molecular and Optical Physics*, Vol. 43, No. 5, p. 150403, 2010.

75. Jensen, B., Dandoloff, R., "Remarks on Quantum Mechanics on Surfaces", *Physics Letters A*, Vol. 375, No. 3, pp. 448-451, 2011.

76. Pahlavani, H., Botshekananfard, M., "Two-dimensional Electron Gas Under the Effect of Constrained Potential and Magnetic Field in Curved Space", *Physica B: Condensed Matter*, Vol. 459, No. 3, pp. 88-92, 2015.

77. da Costa, R. C. T., "Quantum Mechanics of a Constrained Particle", *Physical Review A*, Vol. 23, No. 4, pp. 1982-1987, 1981.

78. Atanasov, V., Saxena, A., "Electronic Properties of Corrugated Graphene: the Heisenberg Principle and Wormhole Geometry in the Solid State", *Journal of Physics: Condensed Matter*, Vol. 23, No. 17, p. 175301, 2011.

79. Wang, Y.-L., Du, L., Xu, C.-T., Liu, X.-J., Zong, H.-S., "Pauli Equation for a Charged Spin Particle on a Curved Surface in an Electric and Magnetic Field", *Physical Review A*, Vol. 90, No. 4, p. 042117, 2014.

80. Souza, P. H., Silva, Moises Rojas, E. O., Filgueiras, C., "A Curved Noninteracting 2D Electron Gas with Anisotropic Mass", *Annalen der Physik*, Vol. 530, No. 7, p. 1800112, 2018.

81. Serafim, F., Santos, F. A. N., Lima, J. R. F., Filgueiras, C., Moraes, F., "Position-Dependent Mass Effects in the Electronic Transport of Two-Dimensional Quantum Systems: Applications to Nanotubes", *Physica E: Low-dimensional Systems and Nanostructures*, Vol. 108, No. 1386, pp. 139-146, 2019.

82. Wang, Y.-L., Zong, H.-S., "Quantum Particle Confined to a Thin-Layer Volume: Non-uniform Convergence Toward the Curved Surface", *Annals of Physics*, Vol. 364, No. 3, pp. 68-78, 2016.

83. Kaplan, L., Maitra, N. T., Heller, J., "Quantizing Constrained Systems", *Physical Review A*, Vol. 56, No. 4, pp. 2592-2599, 1997.

84. Golovnev, A. V., "Canonical Quantization of Motion on Submanifolds", *Reports on Mathematical Physics*, Vol. 64, No. 1-2, pp. 59-77, 2009.

85. Loran, F., Mostafazadeh, A., "Transfer Matrix Formulation of Scattering Theory in Two and Three Dimensions", *Physical Review A*, Vol. 93, No. 4, p. 042707, 2016.

86. Shankar, R., *Principles of Quantum Mechanics*, Springer, 2013.

87. Bonneau, G., Faraut, J., Valent, G., "Self-adjoint Extensions of Operators and the Teaching of Quantum Mechanics", *American Journal of Physics*, Vol. 69, No. 3, pp. 322-331, 2001.

88. Araujo, V. S., Coutinho, F. A. B., Fernando Perez, J., "Operator Domains and Self-adjoint Operators", *American Journal of Physics*, Vol. 72, No. 2, pp. 203-213, 2004.

89. Böhm, A., *Quantum Mechanics: Foundations and Applications*, Springer Science & Business Media, 2013.

90. Erman, F., Gadella, M., Uncu, H., "On Scattering From the One-Dimensional Multiple Dirac Delta Potentials", *European Journal of Physics*, Vol. 39, No. 3, p.

035403, 2018.

91. Ashcroft, N. W., Mermin, N. D., *Solid State Physics*, Harcourt Collage Publishers, 1976.

92. Belloni, M., Robinett, R. W., "The Infinite Well and Dirac Delta Function Potentials as Pedagogical, Mathematical and Physical Models in Quantum Mechanics", *Physics Reports*, Vol. 540, No. 2, pp. 25-122, 2014.

93. Mead, L. R., Godines, J., "An Analytical Example of Renormalization in Two-Dimensional Quantum Mechanics", *American Journal of Physics*, Vol. 59, No. 10, pp. 935-937, 1991.

94. Jackiw, R., *Diverse Topics in Theoretical and Mathematical Physics: Lectures by Roman Jackiw*, World Scientific, 1995.

95. Mitra, I., DasGupta, A., Dutta-Roy, B., "Regularization and Renormalization in Scattering From Dirac-Delta Potentials", *American Journal of Physics*, Vol. 66, No. 12, pp. 1101-1109, 1998.

96. Gosdzinsky, P., Tarrach, R., "Learning Quantum Field Theory From Elementary Quantum Mechanics", *American Journal of Physics*, Vol. 59, No. 1, pp. 70-74, 1991.

97. Manuel, C., Tarrach, R., "Perturbative Renormalization in Quantum Mechanics", *Physics Letters B*, Vol. 328, No. 1-2, pp. 113-118, 1994.

98. Nyeo, S. L., "Regularization Methods for Delta-Function Potential in Two-Dimensional Quantum Mechanics", *American Journal of Physics*, Vol. 68, No. 571, pp. 571-575, 2000.

99. Fassari, S., Gadella, M., Nieto, L. M., Rinaldi, F., "The Schrödinger Particle on the Half-Line With an Attractive δ-Interaction: Bound States and Resonances",

European Physical Journal Plus, Vol. 136, No. 6, p. 673, 2021.

100. Brown, J. W., Churchill, R. V., *Complex Variables and Applications*, 8th ed., McGraw-Hill Book Company, 2009.

101. Kanwal, R. P., *Generalized Functions: Theory and Technique*, Springer Science & Business Media, 1998.

102. Verebič, D., "Lambert W Function For Applications in Physics", *Computer Physics Communications*, Vol. 183, No. 12, pp. 2622-2628, 2012.

103. Arfken G. B., Weber, H. J., *Mathematical Methods for Physicists*, 6th ed., Academic Press, 2005.

104. Abramovitz, M., Stegun, I. A., *Handbook of Mathematical Functions with Formulas, Graphs, and Mathematical Tables*, National Bureau of Standards, Applied Mathematics Series, 1988.

105. Reed, M., Simon, B., *Methods of Modern Mathematical Physics, Volume I*, Elsevier, 1972.

106. Landau, L. D., Lifshitz, E. M., *Quantum Mechanics: Non-Relativistic Theory*, 3rd ed., Vol. 3, Elsevier, 2013.

APPENDIX A: Formulas for I_{mn}, J_{mn}, and $I_{mnm'n'}$

The following are the formulas we have obtained for I_{mn}, J_{mn}, and $I_{mnm'n'}$ by performing the integrals in (4.2.24) - (4.2.26). Here $\alpha_n := a_n/\sigma$, and Erf$[x]$ and Erfc$[x]$ are respectively the error and complementary error functions.[1]

$$\begin{aligned}
I_{mn} =& \frac{1}{8}\eta e^{-s\mathfrak{K}(-i\alpha_m+i\alpha_n+s\mathfrak{K})}\Bigg\{\sqrt{\pi}s\mathfrak{K}e^{(s\mathfrak{K}+i\alpha_n)^2}\Big[-2i\alpha_n^2\lambda_2-2\alpha_n(\lambda_2-2)s\mathfrak{K} \\
&+i\left(8\lambda_1+\lambda_2-2\lambda_2 s^2\mathfrak{K}^2\right)\Big]+2\pi\mathrm{Erf}[\alpha_n-is\mathfrak{K}]\Big[2\lambda_2+\lambda_2 s^4\mathfrak{K}^4 \\
&+\mathfrak{K}^2(4\lambda_1 s^2-1)\Big]-2\pi\mathrm{Erfc}[\alpha_n](\mathfrak{K}^2-2\lambda_2)e^{s\mathfrak{K}(s\mathfrak{K}+2i\alpha_n)} \\
&+2\pi\Big[2\lambda_2+\lambda_2 s^4\mathfrak{K}^4+\mathfrak{K}^2(4\lambda_1 s^2-1)\Big]\Bigg\}+\mathcal{O}(\eta^2),
\end{aligned}$$

$$\begin{aligned}
J_{mn} =& \frac{1}{8}\eta e^{i\alpha_m s\mathfrak{K}}\sqrt{\pi}\Bigg\{2e^{-s\mathfrak{K}(i\alpha_n+s\mathfrak{K})}\sqrt{\pi}\left[\mathfrak{K}^2\left(-1+4s^2\lambda_1\right)+2\lambda_2+s^4\mathfrak{K}^4\lambda_2\right] \\
&\times\mathrm{Erfc}[\alpha_n-is\mathfrak{K}]-2e^{i\alpha_n s\mathfrak{K}}\sqrt{\pi}(\mathfrak{K}^2-2\lambda_2)\mathrm{Erf}[\alpha_n]+e^{-\alpha_n(\alpha_n-is\mathfrak{K})}\Big[(-2e^{\alpha_n{}^2} \\
&\times\sqrt{\pi}(\mathfrak{K}^2-2\lambda_2)-is\mathfrak{K}(-4+8\lambda_1-2i\alpha_n s\mathfrak{K}(-2+\lambda_2)+\lambda_2+2s^2\mathfrak{K}^2\lambda_2 \\
&-2\alpha_n{}^2(4+\lambda_2))\Big]\Bigg\}+\mathcal{O}(\eta^2),
\end{aligned}$$

$$I_{mm'nn'} = g_{mm'nn'}+\Theta(m-n)h_{mm'nn'}+\Theta(n-m)k_{mm'nn'}+l_{mm'nn'},$$

where

$$g_{mm'nn'} := \begin{cases} q_{mm'nn'} & \text{for} \quad m=n, \\ s_{mm'nn'} & \text{for} \quad m>n, \\ t_{mm'nn'} & \text{for} \quad m<n, \end{cases}$$

[1] By definition, Erfc$[x] := 1-\mathrm{Erf}[x]$.

$$q_{mm'nn'} = \frac{1}{4}\sqrt{\pi}\eta s\mathfrak{K}[e^{is\mathfrak{K}(\alpha'_m+\alpha'_n)}]e^{-\alpha_m^2-is\mathfrak{K}(\alpha_m-\alpha_n)-{\alpha_n}^2}\Bigg[e^{\alpha_m^2}\Big(\sqrt{\pi}e^{{\alpha_n}^2}s\mathfrak{K}(\mathrm{Erfc}[\alpha_n] - 2) - 2i{\alpha_n}^2 + 2\alpha_n s\mathfrak{K} + i\Big) - ie^{{\alpha_n}^2+2is\mathfrak{K}(\alpha_m-\alpha_n)}\Bigg(- is\mathfrak{K}\Big(\sqrt{\pi}e^{\alpha_m^2} \times \mathrm{Erfc}[\alpha_m] + 2\alpha_m\Big) + 2\alpha_m^2 - 1\Bigg)\Bigg] + \mathcal{O}(\eta^2)\ ,$$

$$s_{mm'nn'} := \frac{1}{4}\sqrt{\pi}\eta s\mathfrak{K}[e^{is\mathfrak{K}(\alpha'_m+\alpha'_n)}]e^{-\alpha_m^2-s\mathfrak{K}(s\mathfrak{K}+i(\alpha_m+\alpha_n))-{\alpha_n}^2}\Bigg[e^{{\alpha_n}^2}s\mathfrak{K}\Bigg(\sqrt{\pi}e^{{\alpha_m}^2} \times \Big(\mathrm{Erfc}[\alpha_m - is\mathfrak{K}] + \mathrm{Erf}[\alpha_n - is\mathfrak{K}] + (\mathrm{Erfc}[\alpha_n] - 2)e^{s\mathfrak{K}(s\mathfrak{K}+2i\alpha_n)} - 1\Big) - (\sqrt{\pi}e^{{\alpha_m}^2}\mathrm{Erfc}[\alpha_m] + 2\alpha_m)e^{s\mathfrak{K}(s\mathfrak{K}+2i\alpha_m)}\Bigg) + 2(-2i{\alpha_n}^2 + \alpha_n s\mathfrak{K} + i) \times e^{{\alpha_m}^2+s\mathfrak{K}(s\mathfrak{K}+2i\alpha_n)}\Bigg] + \mathcal{O}(\eta^2),$$

$$t_{mm'nn'} = \frac{1}{4}\sqrt{\pi}\eta s\mathfrak{K}e^{is\mathfrak{K}(\alpha'_m+\alpha'_n)}e^{-{\alpha_m}^2-s\mathfrak{K}(s\mathfrak{K}+i(\alpha_m+\alpha_n))-{\alpha_n}^2}\Bigg[s\mathfrak{K}\Big(\sqrt{\pi}e^{{\alpha_m}^2}(\mathrm{Erfc}[\alpha_m] - 2) + 2\alpha_m\Big)e^{{\alpha_n}^2+s\mathfrak{K}(s\mathfrak{K}+2i\alpha_n)} + e^{\alpha_m(\alpha_m+2is\mathfrak{K})}\Bigg(\sqrt{\pi}s\mathfrak{K}e^{\alpha_n(\alpha_n+2is\mathfrak{K})} \times \mathrm{Erf}[\alpha_m + is\mathfrak{K}] - e^{s^2\mathfrak{K}^2}\Big(\sqrt{\pi}e^{{\alpha_n}^2}s\mathfrak{K}\mathrm{Erfc}[\alpha_n] + 4i{\alpha_n}^2 + 2\alpha_n s\mathfrak{K} - 2i\Big)\Bigg)\Bigg] + \mathcal{O}(\eta^2),$$

$$h_{mm'nn'} = \frac{1}{16}\eta e^{is\mathfrak{K}(\alpha'_m+\alpha'_n)}\Bigg\{12\pi\eta(\mathrm{Erf}[\alpha_n]-\mathrm{Erf}[\alpha_m])\left(2\lambda_2+\left(s^2-1\right)\mathfrak{K}^2\right)$$
$$\times e^{is\mathfrak{K}(\alpha_m-\alpha_n)}+4\pi\eta e^{-is\mathfrak{K}(\alpha_m+\alpha_n-is\mathfrak{K})}\mathrm{Erf}[\alpha_m-is\mathfrak{K}]\Big(4\lambda_1+6\lambda_2$$
$$+3\lambda_2 s^4\mathfrak{K}^4+\mathfrak{K}^2\left((4\lambda_1+3)s^2-3\right)\Big)-4\pi\eta e^{-s\mathfrak{K}(s\mathfrak{K}+i(\alpha_m+\alpha_n))}\mathrm{Erf}[\alpha_n-is\mathfrak{K}]$$
$$\times\left(4\lambda_1+6\lambda_2+3\lambda_2 s^4\mathfrak{K}^4+\mathfrak{K}^2\left((4\lambda_1+3)s^2-3\right)\right)+\sqrt{\pi}e^{-{\alpha_m}^2-{\alpha_n}^2}$$
$$\times\Bigg[2e^{-is\mathfrak{K}(\alpha_m+\alpha_n)}\Bigg(ie^{{\alpha_m}^2+2i\alpha_n s\mathfrak{K}}\Big(6{\alpha_n}^2(\lambda_2+8)s\mathfrak{K}+i\alpha_n\Big(8\lambda_1+9\lambda_2$$
$$+6\lambda_2 s^2\mathfrak{K}^2\Big)-s\mathfrak{K}\left(8\lambda_1+3\lambda_2+6\lambda_2 s^2\mathfrak{K}^2\right)\Big)+e^{2i\alpha_m s\mathfrak{K}}\Big(3e^{{\alpha_m}^2}\alpha_n(8\lambda_1$$
$$+3\lambda_2)+e^{{\alpha_n}^2}(3\lambda_2 s\mathfrak{K}(-2i{\alpha_m}^2+2\alpha_m s\mathfrak{K}+2is^2\mathfrak{K}^2+i)-16\alpha_m\lambda_1$$
$$+8i\lambda_1 s\mathfrak{K})\Big)\Bigg)-24ie^{{\alpha_m}^2}{\alpha_n}^3\lambda_2\sin(s\mathfrak{K}(\alpha_m-\alpha_n))\Bigg]\Bigg\}+\mathcal{O}(\eta^2),$$

$$k_{mm'nn'} = \frac{1}{8}\sqrt{\pi}\eta e^{is\mathfrak{K}(\alpha'_m+\alpha'_n)}\Bigg\{e^{-{\alpha_m}^2-{\alpha_n}^2-i(\alpha_m-\alpha_n)s\mathfrak{K}}\Big(-\alpha_m e^{{\alpha_n}^2}\Big(-8\lambda_1$$
$$+\left(-3+2{\alpha_m}^2\right)\lambda_2\Big)+\alpha_n e^{{\alpha_m}^2}\left(-8\lambda_1+\left(-3+2{\alpha_n}^2\right)\lambda_2\right)\Big)$$
$$+e^{-{\alpha_m}^2-{\alpha_n}^2-i(\alpha_m+\alpha_n)s\mathfrak{K}}\Big[e^{\alpha_m(\alpha_m+2is\mathfrak{K})}\Big(8\alpha_n\lambda_1-2{\alpha_n}^3\lambda_2$$
$$+\alpha_n\left(3+2s^2\mathfrak{K}^2\right)\lambda_2+2i{\alpha_n}^2 s\mathfrak{K}(8+\lambda_2)-is\mathfrak{K}\left(8\lambda_1+\lambda_2+2s^2\mathfrak{K}^2\lambda_2\right)\Big)$$
$$+e^{\alpha_n(\alpha_n+2is\mathfrak{K})}\Big(2{\alpha_m}^3\lambda_2-2i{\alpha_m}^2 s\mathfrak{K}\lambda_2+is\mathfrak{K}\left(8\lambda_1+\lambda_2+2s^2\mathfrak{K}^2\lambda_2\right)$$
$$-\alpha_m\left(8\lambda_1+\left(3+2s^2\mathfrak{K}^2\right)\lambda_2\right)\Big)\Big]+2e^{-i(\alpha_m-\alpha_n)s\mathfrak{K}}\sqrt{\pi}\left(\left(s^2-1\right)\mathfrak{K}^2+2\lambda_2\right)$$
$$\times\mathrm{Erf}[\alpha_m]-2e^{-i(\alpha_m-\alpha_n)s\mathfrak{K}}\sqrt{\pi}\left(\left(s^2-1\right)\mathfrak{K}^2+2\lambda_2\right)\mathrm{Erf}[\alpha_n]$$
$$-2e^{is\mathfrak{K}(\alpha_m+\alpha_n+is\mathfrak{K})}\sqrt{\pi}\Big(x^2\left(-1+s^2(1+4\lambda_1)\right)+2\lambda_2+s^4\mathfrak{K}^4\lambda_2\Big)$$
$$\times\mathrm{Erf}[\alpha_m+is\mathfrak{K}]+2e^{is\mathfrak{K}(\alpha_m+\alpha_n+is\mathfrak{K})}\sqrt{\pi}\Big(\mathfrak{K}^2\left(-1+s^2(1+4\lambda_1)\right)$$
$$+2\lambda_2+s^4\mathfrak{K}^4\lambda_2\Big)\mathrm{Erf}[\alpha_n+is\mathfrak{K}]\Bigg\}+\mathcal{O}(\eta^2),$$

$$l_{mm'nn'} = \frac{1}{8}\eta e^{is\Re(\alpha'_m+\alpha'_n)}e^{-{\alpha_n}^2+is\Re(\alpha_n-\alpha_m)}\Bigg[2\pi e^{{\alpha_n}^2}\left(2\lambda_2+\left(s^2-1\right)\mathfrak{K}^2\right)\Big(\mathrm{Erf}[\alpha_n]$$
$$+\mathrm{Erfc}[\alpha_n]e^{2is\Re(\alpha_m-\alpha_n)}\Big)+\sqrt{\pi}\Bigg(\alpha_n\left(\left(2{\alpha_n}^2-3\right)\lambda_2-8\lambda_1\right)e^{2is\Re(\alpha_m-\alpha_n)}$$
$$+2\sqrt{\pi}e^{{\alpha_n}^2}\left(2\lambda_2+\left(s^2-1\right)\mathfrak{K}^2\right)-2{\alpha_n}^3\lambda_2+8\alpha_n\lambda_1+3\alpha_n\lambda_2\Bigg)\Bigg]+\mathcal{O}(\eta^2).$$